Pacific Northwest
NATIONAL LABORATORY

PNNL-31334, Rev. 1
EWG-RPT-033, Rev. 1

Glass Crystallization Constraints for WTP LAW Operations: Assessment of Isothermal Treatments on Crystal Formation

January 2022

Charmayne E Lonergan
Xiaonan Lu
Suzanne M Baird
Sulaiman E Sannoh
John D Vienna

U.S. DEPARTMENT OF ENERGY

Prepared for the U.S. Department of Energy
under Contract DE-AC05-76RL01830

DISCLAIMER

PACIFIC NORTHWEST NATIONAL LABORATORY
operated by
BATTELLE
for the
UNITED STATES DEPARTMENT OF ENERGY
under Contract DE-AC05-76RL01830

Printed in the United States of America

Available to DOE and DOE contractors from the
Office of Scientific and Technical Information,
P.O. Box 62, Oak Ridge, TN 37831-0062;
ph: (865) 576-8401
fax: (865) 576-5728
email: reports@adonis.osti.gov

Available to the public from the National Technical Information Service
5301 Shawnee Rd., Alexandria, VA 22312
ph: (800) 553-NTIS (6847)
email: orders@ntis.gov <https://www.ntis.gov/about>
Online ordering: http://www.ntis.gov

PNNL-31334, Rev. 1
EWG-RPT-033, Rev. 1

Glass Crystallization Constraints for WTP LAW Operations: Assessment of Isothermal Treatments on Crystal Formation

January 2022

Charmayne E Lonergan
Xiaonan Lu
Suzanne M Baird
Sulaiman E Sannoh
John D Vienna

Prepared for
the U.S. Department of Energy
under Contract DE-AC05-76RL01830

Pacific Northwest National Laboratory
Richland, Washington 99354

Executive Summary

Much work has been done to expand the glass composition region available for operation of the Hanford Tank Waste Treatment and Immobilization Plant. This includes the development of updated glass property-composition models as well as constraints. This report supports this effort by suggesting constraints for avoiding excessive, and likely detrimental, crystallization during melter operation while processing advanced low-activity glasses.

The constraints target Cassiterite and ZrO_2-contianing phases (ZCP, e.g., Baddeleyite and Zircon) that can form when melter temperatures drop below 1100 °C. These types of crystals were found to be potentially detrimental during processing as they are denser than low-activity waste glass melts; with densities of 6.95 g/cm^3 for Cassiterite and 5.68 g/cm^3 for Baddeleyite (the most prevalent ZCP). Compared to melt densities of approximately 2.65 g/cm^3. Thus, they have the potential to form during melter idling and settle to the bottom of the melter or inside the melter. If the crystals are present in appreciable amounts, they can result in blockages of the pour-spout riser, which impacts glass pouring and melter operation. Additionally, SnO_2 and ZrO_2 are added to glass formulations to improve glass durability. Their precipitation from the melt may reduce overall glass durability. Using previously acquired results and results from testing during this effort, the following constraints (Table S.1) were determined, and are suggested as options to reduce the risk of forming crystals of the types and concentrations that are likely detrimental to melter operation.

Table S.1. Low-activity waste glass isothermal crystallization constraints.

Constraint	Limit (wt%)
Cassiterite	$SnO_2 < 4.50$
ZCP	$Al_2O_3 + 0.677\ SnO_2 + 0.827\ ZrO_2 < 16.55$

Acknowledgments

The authors gratefully acknowledge the financial support provided by the U.S. Department of Energy Office of River Protection Waste Treatment Plant Project managed by Tom Fletcher, with technical oversight by Albert Kruger.

Eden Rivers performed heat treatments of glasses and a portion of the X-ray Diffraction (XRD) analyses, Joelle Reiser also performed the remainder of XRD analyses, and Dong-Sang Kim (PNNL, retired) helped with the initial constraint formulations.

The authors thank Tongan Jin for the technical review, Matt Wilburn for his editorial review, as well as David MacPherson and Veronica Perez for programmatic support during the conduct of this work.

Acronyms and Abbreviations

DOE	U.S. Department of Energy
LAW	low-activity waste
LIC	LAW isothermal crystallization
MCC	multi-component constraint
mf	mass fraction
NQAP	Nuclear Quality Assurance Program
PNNL	Pacific Northwest National Laboratory
SCC	single-component constraint
VHT	Vapor Hydration Test
VSL	Vitreous State Laboratory
WTP	Hanford Tank Waste Treatment and Immobilization Plant
XRD	X-ray diffraction

Contents

Figures

Tables

1.0 Introduction

Operations of the Hanford Tank Waste Treatment and Immobilization Plant (WTP) will be inextricably tied to process control models, which are the technical backbone of the integrated flowsheet. Key decisions in all unit operations rely on the ability to demonstrate that the waste feed can be effectively processed through the melter and the resulting glass product will meet disposal criteria. The demonstration of effective processing is derived from composition-property predictions and their relation to predefined acceptance criteria. In some instances, there is a lack of reasonable constraint criteria that reduces operational risks while allowing for increased waste loading, especially for crystallization constraints in processing of low-activity waste (LAW). This work contributes to the development of new crystallization constraints for the LAW.

Since the initial issue of this report, an additional glass composition matrix was design, fabricated, and tested for isothermal crystallization. This revision reports the results of this matrix and the resulting change of one of the two crystallinity constraints.

1.1 Operational Constraints

The objective of this task was to identify at least one constraint that allows for reduced risk of operational impacts due to crystallization during LAW melter operations. This is achieved by restricting the formation of crystals that have the potential to form and settle during instances of reduced melter temperatures, e.g., temperatures near 800-1000 °C, or any temperature lower than the planned melting temperature of 1150 °C. Previous work has shown that crystals formed in the glass melt may settle and cause pouring problems due to blockages in the pour-spout riser (Matyáš et al. 2012). This settling is dependent on the crystal's density, particle size, and amount. This is a well-established issue in high-level waste glass melts, as spinel crystals are of great concern, but this is less well-documented in LAW glass melts.

As LAW glass formulations seek to maximize alkali loading while maintaining necessary Vapor Hydration Test (VHT) responses, cassiterite (i.e., SnO_2) is added to the melt to moderate VHT performance. It is important to note that as SnO_2 is added to help reduce VHT response, loss of SnO_2 due to crystallization also has the potential to impact waste form acceptance.

The constraints discussed in this report mainly target high-density crystals (densities greater than 5 g/cm^3) that have shown a tendency to form after isothermal heat treatments of LAW glass melts. For these purposes, Baddeleyite (ZrO_2) and Cassiterite (SnO_2) were the primary crystals of interest. Other crystals that are based on these two oxide minerals are included, but the main crystals discussed in this work are Baddeleyite and Cassiterite.

The proposed constraints are single- or multi-component equations that provide a basis for effectively restricting the accessible glass compositional space for process control models based on crystal formation. The crystal constraints suggested will reduce the risk of melter damage while allowing for enhanced waste loadings. Accompanying the proposed constraints is the data that supported development of the constraints. This data originated from previous work as well as new experimental efforts that occurred as part of this task including one study completed after initial issue of this report.

1.2 Quality Assurance

This work was performed in accordance with the Pacific Northwest National Laboratory (PNNL) Nuclear Quality Assurance Program (NQAP). The NQAP complies with DOE Order 414.1D, *Quality Assurance*, and 10 CFR 830 Subpart A, *Quality Assurance Requirements*. The NQAP uses NQA-1-2012, *Quality Assurance Requirements for Nuclear Facility Application*, as its consensus standard and NQA-1-2012, Subpart 4.2.1, as the basis for its graded approach to quality.

The NQAP works in conjunction with PNNL's laboratory-level Quality Management Program, which is based on the requirements as defined in DOE Order 414.1D, *Quality Assurance*, and 10 CFR 830, *Nuclear Safety Management*, Subpart A, *Quality Assurance Requirements*.

The work of this report was performed to the QA level of applied research with a technology readiness level of 6. This work was performed to support technology development. Data obtained may be used to support design input.

2.0 Data Compilation from Existing Literature

Existing data on LAW glasses that was subjected to isothermal heat treatments was gathered from various LAW glass reports that were previously published by PNNL (Lonergan et al. 2020; Russell et al. 2017, 2021) and the Vitreous State Laboratory (VSL) at the Catholic University of America (Matlack et al. 2001, 2006a,b, 2007a,b; Muller and Pegg 2003a-e; Muller et al. 2006; Rielley et al. 2004). Appendix A provides a summary of the database compiled with glass ID, glass composition, crystallization information, and associated report sources.

Heat treatments performed in this work and at PNNL were performed for at least 24 hours, depending on the heat treatment temperature. Heat treatments performed by VSL were performed for at least 20 hours. These data were combined into one dataset and used in constraint development to capture potential crystallization at a variety of conditions.

3.0 Experimental

This section describes how the glass compositions were designed and tested in two phases of study.

In the first phase (performed before issue of the first version of this report, PNNL-31334, Rev. 0) the objective was to probe Cassiterite crystallization composition boundaries and how the associated heat treatment impacts crystallinity. The descriptions include the matrix design for the LAW isothermal crystallization (LIC) glasses (Section 3.1) and batching and melting of the 10 glasses (Section 3.2).

In the second phases (performed after issue of the first version of this report) the objective was to evaluate glass compositions optimized using the 2020 glass property-composition models (Vienna et al. 2021) and the optimization approach of Lu et al. (2021). The glass compositions and preparation methods are listed in Section 3.3.

Isothermal heat treatments that were completed on the quenched material as well as crystal phase identification and quantification for all samples via X-ray diffraction (XRD) are described in Section 3.4.

3.1 Matrix Design

In the first phase, JMP version 14.0.0 was used to design the matrix of 10 glasses covering a glass composition region based on previous work as well as adjustments to Na_2O and SnO_2 to probe the Cassiterite crystallization composition boundary. The region of interest, based on single-component constraints (SCCs), is given in Table 3.1.

Table 3.1. Single-component constraints used to define the glass composition region of interest.

SCC	Min (wt%)	Max (wt%)
Al_2O_3	3.50	15.53
B_2O_3	6.00	15.09
CaO	2.00	12.35
Cr_2O_3	0.30	1.40
Fe_2O_3	0	1.50
K_2O	0	5.90
Li_2O	0	5.86
MgO	0	10.00
Na_2O	7.50	17.50
SO_3	0.10	2.00
SiO_2	34.90	47.00
SnO_2	2.75	5.00
V_2O_5	0.50	4.00
ZnO	2.00	3.60
ZrO_2	1.00	5.03
Others	0.36	2.69

In addition to the SCCs, two multi-component constraints (MCCs), given in Table 3.2, were used.

Table 3.2. Multi-component constraints used to define the glass composition region of interest (mf = mass fraction).

MCC	Lower	Upper
$Na_2O + 0.66K_2O + 2.07Li_2O$ (mf)	0.150	0.265
Viscosity (η_{1150} °C, Pa.s)	1	10

The JMP design of experiments mixture feature was used to generate five space-filling matrices whose composition bounds were defined according to the constraints given in Table 3.1 and Table 3.2. The options applied in the JMP routine include a mixture design with the Fast Flexible Filling optimality criterion of "MaxPro" with a matrix of individual glass compositions specified. The random number generator seed value was chosen arbitrarily.

To select one matrix of 10 glasses, the dispersion and the relative range for each matrix were calculated and compared. The dispersion value was required to be less than 1.0 and the relative range greater than or equal to 0.85. The final compositions for the matrix of choice are given in Table 3-3.

Table 3-3. Glass IDs and compositions, in mf, for the 10 matrix glasses in the first phase.

	LIC-01	LIC-02	LIC-03	LIC-04	LIC-05	LIC-06	LIC-07	LIC-08	LIC-09	LIC-10
Al_2O_3	0.14616	0.14904	0.03531	0.06006	0.09065	0.06879	0.05059	0.06514	0.14120	0.08398
B_2O_3	0.06558	0.07468	0.13598	0.06666	0.14113	0.12052	0.14012	0.06068	0.11101	0.08645
CaO	0.10384	0.02516	0.05133	0.03181	0.02873	0.05441	0.07547	0.02266	0.03313	0.11754
Cr_2O_3	0.00507	0.01355	0.01064	0.01197	0.00543	0.00753	0.00312	0.00425	0.00675	0.01330
Fe_2O_3	0.00583	0.01019	0.00004	0.00211	0.00512	0.00672	0.01337	0.00841	0.01387	0.00804
K_2O	0.00428	0.02852	0.00626	0.03442	0.05642	0.04584	0.03304	0.01077	0.01218	0.05305
Li_2O	0.05443	0.05841	0.03288	0.01669	0.00160	0.03065	0.00974	0.01405	0.04758	0.03403
MgO	0.07983	0.00096	0.00635	0.08273	0.04869	0.01020	0.01360	0.09985	0.04027	0.00936
Na_2O	0.07653	0.11650	0.16930	0.09466	0.13243	0.07963	0.11831	0.15462	0.09223	0.10524
SO_3	0.00685	0.01877	0.00599	0.01197	0.00220	0.01498	0.01099	0.01603	0.00559	0.00196
SiO_2	0.34906	0.35092	0.40723	0.46427	0.35044	0.44683	0.38982	0.41667	0.35977	0.35992
SnO_2	0.02908	0.03189	0.03342	0.03798	0.04754	0.04460	0.03732	0.03003	0.04405	0.02795
V_2O_5	0.01586	0.02524	0.03708	0.03210	0.02983	0.01050	0.02206	0.00672	0.00844	0.00506
ZnO	0.02366	0.03598	0.03418	0.03057	0.02872	0.02000	0.02218	0.02566	0.03273	0.02437
ZrO_2	0.01592	0.04972	0.01285	0.01191	0.01022	0.02007	0.03516	0.04102	0.04721	0.04410
$Cl^{(a)}$	0.00312	0.00181	0.00367	0.00175	0.00362	0.00325	0.00436	0.00406	0.00069	0.00445
$F^{(a)}$	0.00474	0.00275	0.00557	0.00266	0.00549	0.00493	0.00661	0.00617	0.00105	0.00676
$P_2O_5{}^{(a)}$	0.01015	0.00589	0.01192	0.00569	0.01175	0.01056	0.01415	0.01320	0.00225	0.01445

(a) Indicates the “Others” components, i.e., Cl, F, and P_2O_5.

3.2 Glass Preparation

The glasses were designed according to the steps specified in Section 3.1. Once designed, the glasses were batched using oxides, carbonates, sodium chloride, sodium fluoride, sodium sulfate, and sodium phosphate. The chemicals were mixed together in the appropriate concentrations and homogenized using an Angstrom vibratory mill with an agate mill chamber. The 10 glasses were prepared in batches of 450 g and melted at 1150 °C for 1 h, with the exception of LIC-01, whose temperature was increased after an hour to 1250 °C for 0.5 h. After the first melt was completed, the glasses were ground in a tungsten carbide mill chamber and remelted. The quantity of remelts as well as the chosen temperatures were determined by the glass response upon quenching. Glasses with crystals present upon quenching had an increase in melt temperature for the subsequent melts. Table 3-4 summarizes the melt history of the glasses. Multiple temperatures and times are shown if the temperature was increased during the melt.

Table 3-4. Melt history for 10 matrix glasses.

	1st Melt		2nd Melt		3rd Melt		4th Melt	
Glass ID	Temperature (°C)	Time (h)	Temperature (°C)	Time (h)	Temperature (°C)	Time (h)	Temperature (°C)	Time (h)
LIC-01	1150/1250	1/0.5	1200	1	1200	2	1350/1500	1/1.3
LIC-02	1200	1	1200	1	1200	1	1350/1500	1/1.3
LIC-03	1200	1	1200	1	1200	1	NA	NA
LIC-04	1150	1	1150	1	1200	1	1350	1.3
LIC-05	1150	1	1150	1	1200	1	1350	1
LIC-06	1150	1	1200	1	1200	1	1350	1
LIC-07	1150	1	1150	1	1200	1	NA	NA
LIC-08	1150	1	1200	2	1250	2.3	1350	1
LIC-09	1150/1250	1/1	1350	1	1500	1	1500	1
LIC-10	1150	1	1250	1	1350	1	NA	NA

Images of the quenched glasses after their final melts are shown in Appendix B. Some glasses (LIC-02, LIC-04, and LIC-09) required three or four melts and still did not achieve a homogeneous glass. The modified glasses are discussed in Sections 3.2.1, 3.2.2, and 3.2.3.

3.2.1 LIC-02 Modification

LIC-02 was melted four times and had a sulfate layer and phase separation throughout the various melts. Images of the first melt at 1200 °C and the final melt at 1500 °C are shown in Figure 3-1.

Figure 3-1. Images of LIC-02 after the first melt at 1200 °C (left) and the fourth and final melt at 1500 °C (right).

The first modification of the glass (i.e., LIC-02_mod1) had a decrease in the SO_3 and ZrO_2 concentrations, by 0.3 and 0.9 wt%, respectively, with an equal increase in the SiO_2 concentration (i.e., by 1.2 wt%). These composition changes did not make the glass homogeneous after melting and therefore another modification was pursued. Modification #2, LIC-02_mod2, decreased the amount of Al_2O_3 by 1 wt% and increased "Others" by the same amount relative to the first modification. The glass components that were not varied were kept at their initial concentrations. A summary of composition changes is given in Table 3-5.

Table 3-5. Concentrations for components varied for modifications of LIC-02.

Component Varied	Concentration in LIC-02 (wt%)	Concentration in LIC-02_mod1 (wt%)	Concentration in LIC-02_mod2 (wt%)
Al_2O_3	14.90	14.90	13.90
SO_3	1.88	1.58	1.58
ZrO_2	4.97	4.07	4.07
Others	1.05	1.05	2.05
All other components	See Table 3-3	No change	No change

The final modification (i.e., LIC-02_mod2) did not form a homogeneous melt, as can be seen in Figure 3-2.

Figure 3-2. LIC-02_mod2 quenched glass after third melt at 1500 °C for 1 hour.

The LIC-02 glass, and the associated modifications, were not used in determining the crystallization constraints discussed in this work.

3.2.2 LIC-04 Modification

LIC-04 was melted four times and was inhomogeneous with excess sulfate as well as phase separation visible upon quenching. Images of the first melt at 1150 °C and the fourth/final melt at 1350 °C are shown in Figure 3-3.

Figure 3-3. LIC-04 after the first melt at 1150 °C (left) and the fourth melt at 1350 °C (right).

Only one modification was made for LIC-04: Na_2O was increased by 5 wt% while SiO_2 was decreased by the same amount. All other components remained the same. Table 3-6 provides a summary of the changes.

Table 3-6. Concentrations for components varied for modification of LIC-04.

Component Varied	Concentration in LIC-04 (wt%)	Concentration in LIC-04_mod1 (wt%)
Na_2O	9.47	14.47
SiO_2	46.43	41.43
All other components	See Table 3-3	No change

The modification to LIC-04 worked well to generate a homogeneous glass; Figure 3-4 shows a photo of the modified quenched glass after the third melt at 1500 °C. LIC-04_mod1 was used for further isothermal constraint development.

Figure 3-4. LIC-04_mod1 quenched glass after third melt at 1500 °C for 1 hour.

3.2.3 LIC-09 Modification

LIC-09 was melted four times, and while improvements in homogeneity were noted with each melt, the final quenched glass was still phase separated. The first and fourth melts are shown in Figure 3-5.

Figure 3-5. LIC-09 first melt at 1150 °C (left) and fourth/final melt at 1500 °C (right).

Several modifications were attempted for LIC-09. For the first modification (i.e., LIC-09_mod1), ZrO_2 was decreased by 0.5 wt% and the "Others" component was increased by the same. In the second modification, SiO_2 was increased by 2 wt%, ZnO decreased by 0.5 wt%, SnO_2 decreased by 0.25 wt%, and Al_2O_3 decreased by 1.25 wt%. LIC-09_mod3 maintained the composition changes of mod2 while further decreasing ZrO_2 by 1 wt% and increasing "Others" by 1 wt%. Table 3-7 provides a summary of changes.

Table 3-7. Concentrations for components varied for modifications of LIC-09.

Component Varied	Concentration in LIC-09 (wt%)	Concentration in LIC-09_mod1 (wt%)	Concentration in LIC-09_mod2 (wt%)	Concentration in LIC-09_mod3 (wt%)
Al_2O_3	14.12	14.12	12.87	12.87
SiO_2	35.98	35.98	37.98	37.98
SnO_2	4.41	4.41	4.16	4.16
ZrO_2	4.72	4.22	4.22	3.22
Others	0.40	0.90	0.90	1.90
All other components	See Table 3-3	No change	No change	No change

The final modification, LIC-09_mod3, worked well to produce a homogeneous glass. The crucible and the final quenched glass are shown in Figure 3-6. The final, modified glass was used in the generation of the isothermal crystallization constraints discussed in this work.

Figure 3-6. LIC-09_mod3 final melt crucible (left) and quenched glass (right) after pouring from 1450 °C.

3.3 Algorithm Experimental Verification Glasses

In the second phase of work, Lu[1] developed a test matrix of 17 glasses formulated using models from Vienna et al. (2021) and glass optimization techniques described by Lu et al. (2021). These methods include the application of isothermal crystal constraints from the first version of this report (PNNL-31334, Rev. 0): $SnO_2 < 4.5$ wt% and $ZrO_2 < 0.33 \times Na_2O + 3.70$ (wt%). Glass formulations were generated for each of 54,673 LAW and supplemental LAW batch compositions from the *River Protection Project System Plan Revision 9* (Bernards et al. 2020). From the 54,673 glass compositions 17 were selected that represented the range of expected glass compositions expected from the full Hanford LAW vitrification mission (Table 3-8).

These 17 glass compositions were batched using oxides, carbonates, sodium chloride, sodium fluoride, sodium sulfate, and sodium phosphate to simulate waste components and Kyanite, Boric Acid, Wollastonite, Lithium Carbonate, Silcosil SiO_2, Zincite, Zircon, V_2O_5, and Cassiterite as glass forming chemicals. The chemicals were mixed together in the appropriate concentrations and homogenized using an Angstrom vibratory mill with an agate mill chamber. The 17 glasses were prepared in batches of 500 g and melted at 1150 °C for 1 h. After the first melt was completed, the glasses were ground in a tungsten carbide mill chamber and remelted. A second melt was performed for 1 h at a temperature between 1120 and 1350 °C depending on the presence of crystals in the glass. For seven of the glasses, additional melts were required to fully dissolve all crystals. Details are described in Gervasio et al. (2022).

[1] X. Lu. 2021. *Glass Formulation for Experimental Verification of 2020 ILAW Formulation Algorithm*, EWG-CCP-171, Rev. 0.0.

Table 3-8. Composition of LAW Algorithm Experimental Verification Glasses

Oxide	LAW ALG-01	LAW ALG-02	LAW ALG-03	LAW ALG-04	LAW ALG-05	LAW ALG-06	LAW ALG-07	LAW ALG-08	LAW ALG-09	LAW ALG-10	LAW ALG-11	LAW ALG-12	LAW ALG-13	LAW ALG-14	LAW ALG-15	LAW ALG-16	LAW ALG-17
Al_2O_3	0.03593	0.05442	0.05504	0.08674	0.03588	0.06308	0.05783	0.03596	0.09032	0.08810	0.08737	0.03595	0.03608	0.03597	0.08898	0.08839	0.08886
B_2O_3	0.08497	0.12973	0.06947	0.08709	0.13603	0.11063	0.08285	0.13633	0.08466	0.08673	0.06141	0.12928	0.13586	0.13594	0.08728	0.08275	0.08319
CaO	0.12356	0.09817	0.08377	0.07695	0.12420	0.09054	0.08070	0.12439	0.08098	0.07736	0.07484	0.11134	0.12411	0.12239	0.07752	0.07760	0.07741
Cl	0.00037	0.00066	0.00051	0.00104	0.00060	0.00099	0.00030	0.00042	0.00047	0.00043	0.00150	0.00033	0.00043	0.00066	0.00079	0.00062	0.00438
Cr_2O_3	0.00079	0.00053	0.00079	0.00025	0.00046	0.00065	0.00061	0.00024	0.00189	0.00162	0.00043	0.00050	0.00033	0.00045	0.00056	0.00581	0.00085
F	0.00429	0.00084	0.00281	0.00026	0.00553	0.00064	0.00254	0.00070	0.00299	0.00050	0.00078	0.01005	0.00297	0.00155	0.00037	0.00052	0.00236
Fe_2O_3	0.00121	0.00134	0.00119	0.00103	0.00128	0.00134	0.00104	0.00133	0.00139	0.00126	0.00144	0.00117	0.00116	0.00129	0.00154	0.00129	0.00151
K_2O	0.00230	0.00124	0.00096	0.00364	0.00146	0.00144	0.00093	0.00086	0.00210	0.00070	0.03064	0.00079	0.00071	0.00109	0.00162	0.00074	0.00570
Li_2O	0.02754	0.00000	0.00000	0.00000	0.01684	0.00000	0.00000	0.01677	0.00000	0.00000	0.00000	0.00000	0.01144	0.00818	0.00000	0.00000	0.00000
MgO	0.00182	0.00146	0.00125	0.00115	0.00183	0.00135	0.00120	0.00184	0.00122	0.00117	0.00114	0.00164	0.00182	0.00180	0.00118	0.00117	0.00118
MnO	0.00013	0.00011	0.00009	0.00008	0.00013	0.00010	0.00009	0.00013	0.00009	0.00008	0.00008	0.00012	0.00013	0.00013	0.00008	0.00008	0.00008
Na_2O	0.14901	0.19585	0.22294	0.23333	0.09075	0.20989	0.22820	0.09890	0.22711	0.23382	0.21996	0.17277	0.13473	0.15193	0.23313	0.23342	0.23081
P_2O_5	0.00555	0.00307	0.03114	0.00079	0.00258	0.00224	0.01737	0.00160	0.03520	0.00312	0.00130	0.02178	0.00925	0.00162	0.00316	0.00539	0.00159
SO_3	0.01445	0.01318	0.01012	0.00107	0.01414	0.01203	0.00977	0.01441	0.00291	0.00162	0.00484	0.01385	0.01455	0.01442	0.00838	0.00138	0.00655
SiO_2	0.48703	0.42007	0.38609	0.39843	0.50704	0.39309	0.40345	0.50475	0.35744	0.39912	0.36396	0.43926	0.46539	0.46129	0.39150	0.39847	0.38627
SnO_2	0.00000	0.00000	0.04393	0.04386	0.00000	0.01403	0.04389	0.00000	0.04388	0.04389	0.04395	0.00000	0.00000	0.00000	0.04396	0.04389	0.04391
TiO_2	0.00070	0.00128	0.00117	0.00097	0.00084	0.00137	0.00092	0.00092	0.00164	0.00141	0.00180	0.00079	0.00061	0.00087	0.00197	0.00147	0.00191
UO_3	0.00001	0.00003	0.00004	0.00004	0.00001	0.00004	0.00004	0.00001	0.00004	0.00004	0.00004	0.00001	0.00001	0.00001	0.00004	0.00004	0.00004
V_2O_5	0.03992	0.03989	0.02436	0.00000	0.04001	0.03984	0.00956	0.04011	0.00000	0.00000	0.00000	0.03987	0.03998	0.04001	0.00000	0.00000	0.00000
ZnO	0.00000	0.00000	0.00000	0.00000	0.00000	0.00000	0.00000	0.00000	0.00000	0.00000	0.03861	0.00000	0.00000	0.00000	0.00000	0.00000	0.00000
ZrO_2	0.02042	0.03812	0.06433	0.06328	0.02037	0.05673	0.05872	0.02033	0.06567	0.05904	0.06592	0.02046	0.02041	0.02039	0.05793	0.05697	0.06341

3.4 Isothermal Heat Treatments

Equilibrium crystal fraction at a fixed temperature was measured in Pt-10%Rh crucibles and boats with tight-fitting lids (to minimize volatility) according to the ASTM International standard procedure *Standard Test Method for Determining Liquidus Temperature of Immobilized Waste Glasses and Simulated Waste Glasses* (ASTM C1720). The primary heat treatment times and temperatures were 24 ± 0.5 h at 950 °C, 48 ± 1 h at 850 °C, and 72 ± 2 h at 750 °C, with the times chosen to improve the chances of achieving equilibrium without excessive volatility. Some glasses were tested at other temperatures as well if crystals did not form at the main three temperatures chosen. The samples were then quenched and XRD was performed.

The phases and amounts of crystals formed during heat treatment were analyzed by XRD according to Section 12.4.4 of ASTM C1720. Powdered glass samples were prepared using 5-wt% CeO_2 as an internal standard phase with between 1.5 and 2.5 g of glass powder. Glass and CeO_2 were milled together for 2 min in a 10-cm^3 tungsten carbide disc mill. The powdered samples were loaded into XRD sample holders and scanned at a 0.04° 2θ step size, 4-s dwell time, from 10° to 70° 2θ scan range. XRD spectra were analyzed with TOPAS 4.2 software (Bruker AXS Inc., Madison, Wisconsin) for phase identification and Rietveld refinement to semi-quantify the amounts of crystal phases in some samples with high crystalline content. These results are discussed in Section 4.1.

4.0 Results and Discussion

This section provides the resulting heat treatment data from glasses tested in this effort as well as the Cassiterite and Baddeleyite constraints designed from the LAW data shown in Appendix A. This compiled data included the heat treatment data shown below. The majority of the crystallization information from the LAW glass literature was presented in vol%; therefore, the constraint development uses vol% for representing the amount of crystals present. The conversion from wt% to vol% was completed using the following equation:

$$\frac{V_x}{V_x + V_g} \approx \frac{\rho_g}{\rho_x\left(\frac{1}{mf_x} - 1\right) + \rho_g} \quad 4.1$$

where the V_x is the volume of crystal in a sample, V_g is the volume of glass in a sample, ρ_g is glass density (assumed to be 2.65 g/cm^3 for this study), and ρ_x is crystal density (e.g., 6.95 g/cm^3 for Cassiterite and 5.96 g/cm^3 for Baddeleyite).

4.1 Results for LIC Glasses

The statistically designed glasses were treated as described in Section 3.0 and analyzed after heating to determine the types and amounts of crystals. Table 4.1 provides a summary of the total crystal concentrations, in wt%, and the major phases present, along with the SnO_2 amount, for 750, 850, and 950 °C. Optical images of the samples and XRD data are provided in Appendix C and Appendix D, respectively. Phases presented below indicate best fit possible; certain phases may be unlikely [e.g., a $Li_2Fe_3SbO_8$ phase] but provide space group and cell parameter information. Additionally, totals may vary slightly from sums of phases due to rounding.

Table 4.1. Amount of crystals and phases of crystals, with corresponding amounts, for the LIC matrix glasses. Totals may vary slightly due to rounding.

	750 °C (72 h)		850 °C (48 h)		950 °C (72 h)	
Glass ID	Total Amount (wt%)	Phases (amounts wt%)	Total Amount (wt%)	Phases (amounts wt%)	Total Amount (wt%)	Phases (amounts wt%)
LIC-01	48.15	Diopside (26.29); Nepheline (10.80); Cassiterite (2.44); and 3 others	46.71	Diopside (21.55); Nepheline (7.72); Cassiterite (0.69); and 3 others	9.87	Forsterite (6.28); Hedenbergite (2.06); Cassiterite (1.07); $Li_2Fe_3SbO_8$ (0.46)
LIC-03	0.00	None	0.00	None	0.00	None
LIC-04_mod1	3.07	Diopside (2.38); $Li_2Fe_3SbO_8$ (0.69)	3.32	Diopside (2.75); $Li_2Fe_3SbO_8$ (0.57)	3.02	Cassiterite (1.72); $Li_{0.5}Fe_{2.5}O_4$ (0.67); $Li_2Fe_3SbO_8$ (0.63)
LIC-05	0.00	None	0.30	Cassiterite (0.30)	2.55	Cassiterite (2.55)
LIC-06	0.00	None	0.00	None	0.24	Cassiterite (0.24)
LIC-07	0.68	Baddeleyite (0.68)	1.27	Baddeleyite (1.27)	0.00	None
LIC-08	4.61	Diopside (3.35); Forsterite (1.26)	1.18	Forsterite (1.18)	1.91	Forsterite (1.33); Cassiterite (0.58)
LIC-09_mod3	4.52	Diopside (1.08); Cassiterite (1.05); Forsterite (0.84); and 3 others	3.95	Cassiterite (2.66); Magnesioferrite (0.48); $Li_2Fe_3SbO_8$ (0.40); and 2 others	4.23	Cassiterite (2.96); Magnesioferrite (1.27)
LIC-10	1.50	Baddeleyite (1.50)	0.09	$Li_2Fe_3SbO_8$ (0.09)	0.36	Cassiterite (0.22); $Li_2Fe_3SbO_8$ (0.13)

Only one glass, LIC-03, showed no crystallization at any heat treatment temperature. LIC-06 was another glass very little crystallization, precipitating 0.05 wt% SnO_2 only at 950 °C after 24 h. Overall, all glasses except for LIC-03 had SnO_2 form after at least one heat treatment, which resulted in a successful matrix design effort. The goal of the LIC glass matrix was to gather additional information about Cassiterite formation, and this was achieved. As there were multiple temperatures for heat treatments, the maximum Cassiterite SnO_2 amount formed at a given temperature was used in the constraint design. Many crystals other than baddeleyite and cassiterite formed in these glasses. It should be considered if other constraints would be necessary for WTP operations.

4.2 Results for LAWALG Glasses

Table 4.1 provides a summary of the total crystal concentrations, in wt%, and the major phases present, for 750, 850, 900, and 950 °C. Since these glasses were formulated using the crystal constraints in the previous version of this report, it was expected that no significant Cassiterite or Baddeleyite crystals would form at ≥ 850 °C. However, several glasses formed ZCP phases (e.g., Baddeleyite, Zircon, Parakeldyshite, $Na_4Zr_2(SiO_4)_3$) in quantities larger than 1 vol%: LAWALG-4, -9, -11, -16, and -17.

Table 4.2. Crystal Data for LAWALG Glasses (vol%)

Glass ID	Crystalline Phase	750 °C /72 hrs	850 °C /48 hrs	850 °C /1 week	900 °C /24 hrs	950 °C/24 hrs small crucible	950 °C/24 hrs big crucible
LAWALG-1	Moganite	1.6	1.3	NM	A-OM	A-OM	NM
	Parakeldyshite	0.9	0.7	NM	A-OM	A-OM	NM
	Tridymite2H	0.1	0.3	NM	A-OM	A-OM	NM
	$K_2Ca_2Si_2O_7$	0.2	0.2	NM	A-OM	A-OM	NM
LAWALG-2		Traces	A-OM	NM	A-OM	A-OM	NM
LAWALG-3	Sodium tetrasilicate	1.6	0.8	NM	1.2	NM	NM
	Nasicon	0.9	0.7	NM	0.7	NM	NM
	$K_2Ca_2Si_2O_7$	0.1	0.1	NM	0.2	NM	NM
	Nepheline	1.2	0.9	NM	0.5	NM	NM
LAWALG-4	Parakeldyshite	1.3	0	1.7	NM	0	0
	Na_2CaSiO_4	0.0	0	0.0	NM	0	0
	$Na_4Zr_2(SiO_4)_3$	0	traces	8.9	NM	2.2	1.6
LAWALG-5	Tridymite2H	0.3	traces	NM	A-OM	A-OM	NM
LAWALG-6		A-OM	A-OM	NM	A-OM	A-OM	NM
LAWALG-7		traces	traces	NM	A-OM	A-OM	NM
LAWALG-8		A-OM	A-OM	NM	A-OM	A-OM	NM
LAWALG-9	$Na_4Zr_2(SiO_4)_3$	19.4	16.8	NM	12.3	13.1	NM
	$K_2Ca_2Si_2O_7$	0.5	0.5	NM	0.6	0.6	NM
LAWALG-10		traces	traces	NM	traces	traces	NM
LAWALG-11	Combeite	7.9	14.6	NM	0	0	NM
	Nasicon	4.5	7.8	NM	6.8	11.8	NM
	Nepheline	8.2	14.8	NM	0	0	NM
	Moganite	1.5	2.6	NM	0.7	1.1	NM
	$K_2Ca_2Si_2O_7$	0.8	0.7	NM	0	0	NM
	$Na_2Si_2O_5$	0.2	0.4	NM	0	0	NM
	Na_2SiO_3	0.9	1.5	NM	0	0	NM
	Na_2CaSiO_4	0.1	0	NM	0	0	NM
LAWALG-11 rerun	Combeite	13.7	12.2	NM	0	0	NM
	Nasicon	7.3	12.7	NM	5.7	15.9	NM
	Nepheline	6.6	6.6	NM	0	0	NM
	Moganite	2.8	5.6	NM	0	1.7	NM
	$K_2Ca_2Si_2O_7$	0.7	1.2	NM	0	0.8	NM
	$Na_2Si_2O_5$	0.2	1.3	NM	0	0.2	NM
	Na_2SiO_3	0	5.2	NM	0	0	NM
	Na_2CaSiO_4	0.1	0	NM	0	0	NM
	$ZrSiO_4$	0.1	0.3	NM	0	0	NM
	$Na_4Zr_2(SiO_4)_3$	0	0	NM	1.0	0	NM
LAWALG-12	$Ca_4Na_6(SO_4)_6F_2$	4.1	2.6	NM	3.1	2.4	NM
	Na_2SiO_3	1.1	0.9	NM	0	0	NM
	AlMgOrthosilicate	0.7	0.5	NM	0.3	0.3	NM
	$K_2Ca_2Si_2O_7$	0.3	0.2	NM	0.0	0.0	NM
LAWALG-13	$Ca_4Na_6(SO_4)_6F_2$	1.7	1.7	NM	1.4	NM	NM
LAWALG-14		A-OM	A-OM	NM	A-OM	A-OM	NM
LAWALG-15	Sodium tetrasilicate	traces	2.1	NM	2.2	2.5	NM
LAWALG-16	Parakeldyshite	A-OM	NM	1.7	traces	1.2	NM
	$Na_4Zr_2(SiO_4)_3$	A-OM	NM	3.6	0	2.2	NM
LAWALG-17	combeite	4.0	0	NM	0	0	NM
	Sodium tetrasilicate	2.9	1.4	NM	2.2	2.0	NM
	Na_2CaSiO_4	0	0	NM	0	0	NM
	Na_2SiO_5-gamma	0	1.4	NM	0	0	NM
	Parakeldyshite	0	1.3	NM	0	0	NM

Glass ID	Crystalline Phase	750 °C /72 hrs	850 °C /48 hrs	850 °C /1 week	900 °C /24 hrs	950 °C/24 hrs small crucible	950 °C/24 hrs big crucible
	$ZrSiO_4$	0	0.9	NM	0	0	NM
	$Tridymite_2H$	0	0.1	NM	0.1	0.1	NM
	Nepheline	0	0.2	NM	0.1	0.0	NM
A-OM = Amorphous by OM. traces = crystals not detected by XRD. NM = not measured							

4.3 Cassiterite Constraint

The minimum and maximum amounts of Cassiterite present in the LAW glasses were 0 vol% and 1.5 vol%, respectively, according to the data compiled. The constraint for restricting the formation of Cassiterite was designed by looking at the relationship between the maximum cassiterite formation for a given glass at any heat treatment temperature and the SnO_2 amount in the associated target glass composition. The graph is shown below, Figure 4.1. A boundary region was identified after noting the clustering of data in the bottom right of the plot, as if a right triangle.

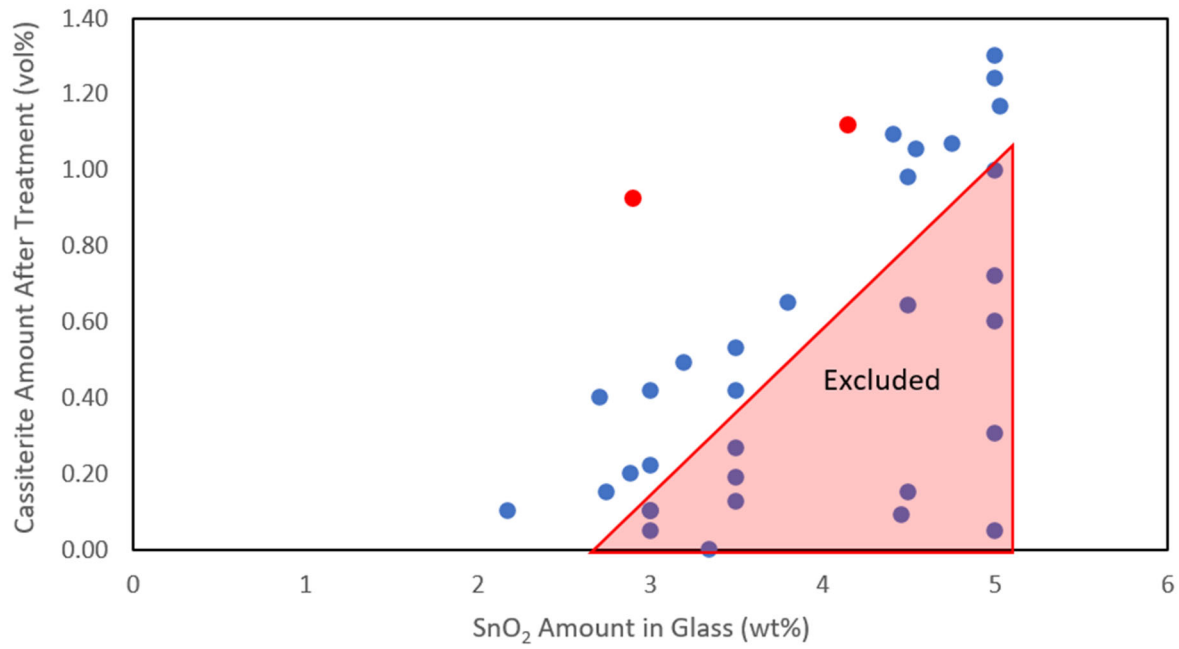

Figure 4.1. SnO_2 amount in glass plotted as a function of Cassiterite formation after heat treatment.

Excluding the data points shown in red and covered by the red triangle, the boundary region was defined by a linear fit shown in Figure 4.2 with the remaining data points.

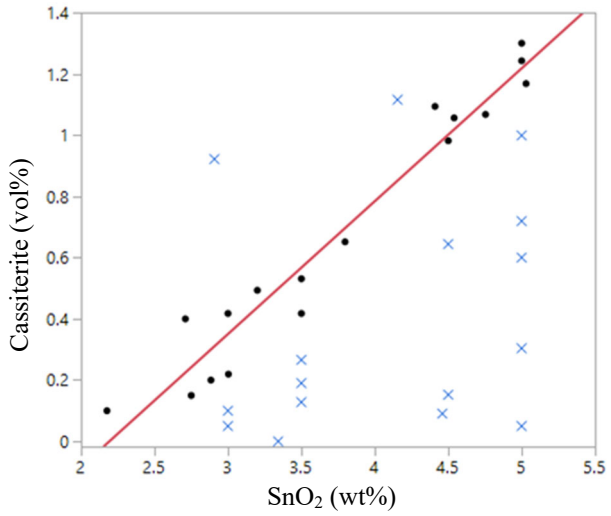

Figure 4.1. SnO_2 amount in glass as a function of Cassiterite amount precipitated after heat treatment.

The resulting equation for the red line in Figure 4.2 is:

$$Cassiterite\ (vol\%) = -0.951145 + 0.4338521\ x\ SnO_2(wt\%) \quad 4.1$$

When equation 4.1 is used to determine the maximum amount of SnO_2 that is allowable for a 1 vol% cassiterite limit, as employed in other crystal constraints (Kot et al. 2001; Piepel et al. 2008; Vienna et al. 2014), the limit for SnO_2 in glass is 4.50 wt%. Tables summarizing the data used may be found in Appendix A.

The suggested constraint, which restricts the amount of SnO_2 in the glass is the following equation.

$$SnO_2 \leq 4.50\ (wt\%) \quad 4.2$$

Since no LAWALG glasses (formulated to contain ≤ 4.5 wt% SnO_2) formed Cassiterite, this constraint was not updated.

4.4 ZCP Constraint

The previous version (PNNL-31334, Rev. 0) of Baddeleyite constraint ($ZrO_2 \leq 0.33\ Na_2O + 3.7$ wt%) was successful in avoiding formation of Baddeleyite. However, it was not successful in avoiding the formation of other zirconium-containing phases (ZCP) in the LAWALG glasses. In this revised version of the report (PNNL-31334, Rev. 1), a constraint is developed to avoid excessive (e.g., ≥ 1 vol%) of combined ZCP. The combined database of isothermally heat-treated glasses (Appendix A) was evaluated. A partition model was found to best separate the glasses between the P (= pass or < 1.0 vol% ZCP) and F (= fail or ≥ 1.0 vol% ZCP) as shown in Figure 4.3. The most effective single term in dividing between P and F compositions is normalized alumina (in wt%, $NAlSnZr = Al_2O_3 + 0.677\ SnO_2 + 0.827\ ZrO_2$). The ratios of the oxides are in direct proportion to molecular weight differences from Al_2O_3 making it generally the equivalent mass of Al_2O_3 if Al_2O_3, ZrO_2, and SnO_2 have similar molar effects on crystallinity.

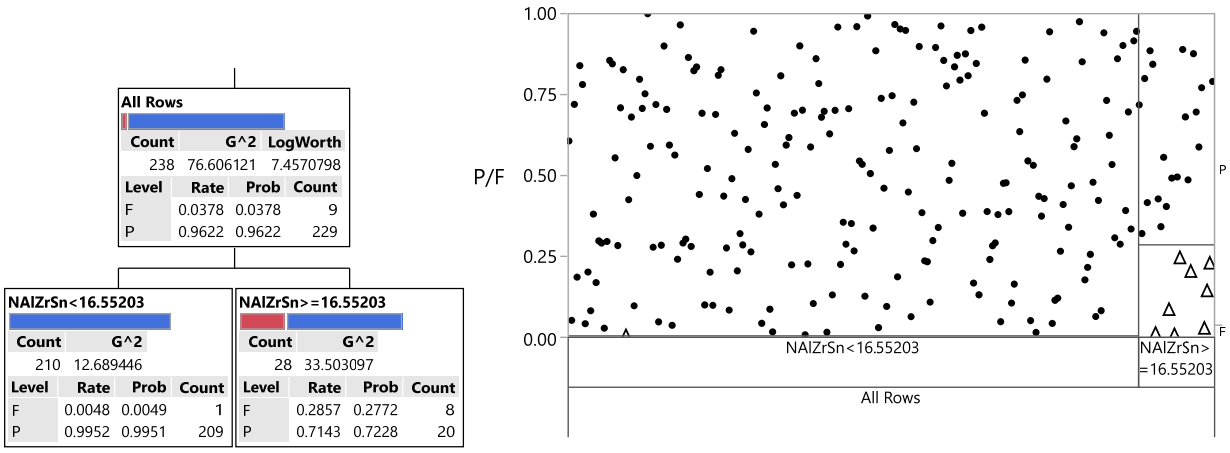

Figure 4.3. Partition model for ZCP (in wt%). Circles pass the constrain (e.g., ZCP ≤ 1 vol%) while triangles fail the constraint.

Of 238 LAW glasses with isothermal crystallization data, 21 are predicted incorrectly – one false positive and 20 false negatives. These glasses are listed in Table 4.3. The false negative glass (New-OL-14844) formed 1.13 vol% baddeleyite despite a NAlZrSn of 8.90 wt%. However, this glass would not be formulated by current methods (Lu et al. 2021) due to Li_2O > 4.3 wt%. Of the 20 false negative glasses, 12 were found to have unacceptable crystallinity due to other phases and/or would be excluded from formulation by current methods due to composition constraints (primarily Li_2O > 4.3 wt% and SnO_2 > 4.5 wt%). Practically, only 7 of 238 test glasses would have be misclassified by implementing this constrain as part of current formulation methods; and all of those would be false negatives (or conservative).

Table 4.3. Summary of incorrectly predicted glasses

Glass ID	NAlZrSn, wt%	ZCP, vol%	Other Phases, vol%	SnO_2, wt%	Li_2O, wt%	Comments
LAWA197	16.79	0	few, fine particles	0.00	0.00	
New-OL-45748	17.25	0	1.28 Cassiterite	**5.00**	**5.00**	Unacceptable SnO_2, excluded due to composition
New-OL-65959Mod	16.91	0	1.01 Cassiterite	4.50	**5.00**	Unacceptable SnO_2, excluded due to composition
LORPM29S4-W	17.53	0	unknown phase	**5.10**	**5.10**	Excluded due to composition
LORPM23	19.56	0	0.2 Cassiterite	2.88	**5.00**	Excluded due to composition
LORPM24	17.22	0	0.1 unknown	2.18	0.00	
LORPM29	17.28	0	1 Cassiterite + Spinel	**5.00**	**5.00**	Unacceptable SnO_2, excluded due to composition
LORPM31	19.32	0	0.6 Cassiterite + Spinel	**5.00**	4.35	Excluded due to composition
LIC-01	17.92	0	0.93 Cassiterite	2.91	**5.44**	Borderline SnO_2, excluded due to composition
LIC-09_mod3	18.37	0	1 Cassiterite	4.16	**4.76**	Unacceptable SnO_2, excluded due to composition
New-OL-8445	17.81	0.94	1.8 Fluoroapatite	0.00	2.01	Borderline ZCP, additional phases
ORPLG1	16.98	0	~0.2 Cr_2O_3	2.97	0.00	
ORPLG2	16.87	0	~0.2 Cr_2O_3	2.94	0.00	
ORPLG3	16.76	0	~0.2 Cr_2O_3	2.91	0.00	

ORPLG5	16.76	0	~0.2 Cr_2O_3	2.91	0.00	
ORPLB1	17.25	0	~0.2 Cr_2O_3	1.08	0.00	
LAW-ORP-LD1(M)	18.02	0	8.5 Hauyne, Nosean, Spinel	0.00	0.00	Unacceptable other phases
New-OL-62909Mod	19.91	0.63	1.13 SnO_2; 1.5 Wadalite	4.41	2.50	
LAWALG-10	16.69	0	trace unknown crystal	4.39	0.00	
LAWALG-15	16.70	0	2.2 $Na_2Si_4O_9$	4.40	0.00	Borderline other phases
New-OL-14844	**8.90**	1.13	none	0.00	**5.00**	Excluded due to composition

The suggested ZCP constraint is therefore:

$$Al_2O_3 + 0.677\ SnO_2 + 0.827\ ZrO_2 \leq 16.55\ wt\% \quad 4.3$$

5.0 Summary

Crystallization data from various LAW glass reports were compiled to determine crystallization constraints. These constraints were pursued as ways to mitigate crystal formation that might be detrimental to WTP LAW vitrification operations. Primary crystals of concern were Cassiterite and ZCP (primarily Baddeleyite, Zircon, Parakeldyshite, and Sodium Zirconium Silicate) as these crystals are frequently formed and have densities significantly above glass melts, which may settle in the melter causing operation problems. Also, their addition to glass serves the role of improving glass durability, which may not happen if they crystallize out of the glass. After a preliminary assessment of compiled data, 10 glasses in phase one were designed to crystallize Cassiterite upon isothermal heat treatments. Of the 10 glasses designed in this effort, only one (LIC-03) did not precipitate Cassiterite after any heat treatment. One glass (LIC-02) was modified twice but did not produce a homogeneous glass upon quenching.

A second study was performed to experimentally verify the formulation methods described by Lu et al. (2021) which generated 5 glasses out of 17 that crystallized > 1 vol% of ZCP.

The constraints resulting from this effort are proposed to restrict the amount of cassiterite and ZCP formed in glass to less than 1 vol% by restricting the concentrations of ZrO_2, SnO_2, and Al_2O_3 in glass. The suggested constraints, given in Table 5-1, will allow for less risk when processing enhanced waste glass formulations while allowing for access to higher waste loadings for LAW glasses.

Table 5-1. Low-activity waste glass isothermal crystallization constraints.

Constraint	Limit (wt%)
Cassiterite	$SnO_2 \leq 4.50$
ZCP	$Al_2O_3 + 0.677\ SnO_2 + 0.827\ ZrO_2 \leq 16.55$

6.0 References

10 CFR 830 Subpart A, *Quality Assurance Requirements*. U.S. Code of Federal Regulations.

ASTM C1720, *Standard Test Method for Determining Liquidus Temperature of Immobilized Waste Glasses and Simulated Waste Glasses.* ASTM International, West Conshohocken, PA.

Bernards, JK, GA Hersi, TM Hohl, RT Jasper, PD Mahoney, NK Pak, SD Reaksecker, AJ Schubick, EB West, LM Bergmann, GR Golcar, AN Praga, SN Tilanus, and TW Crawford. 2020. *River Protection Project System Plan*, ORP-11242, Rev. 9, U.S. Department of Energy, Office of River Protection, Richland, WA.

DOE Order 414.1D, *Quality Assurance.* U.S. Department of Energy, Washington, DC.

Gervasio, V, JD Vienna, SK Cooley, SM Baird, DL Bellofatto, BE Westman, DS Kim, X Lu, JB Lang, DA Cutforth, EL Rivers, and NA Lumetta. 2022. *Experimental Verification of the Preliminary Enhanced LAW Glass Formulation Algorithm*, EWG-RPT-036, PNNL-DRAFT, Pacific Northwest National Laboratory, Richland, WA.

Kot WK and IL Pegg. 2001. *Glass Formulation and Testing with RPP-WTP HLW Simulants*. VSL-01R2540-2, Vitreous State Laboratory, The Catholic University of America, Washington, DC.

Lonergan CE, JL George, D Cutforth, T Jin, P Cholsaipant, SE Sannoh, CH Skidmore, BA Stanfill, SK Cooley, RL Russell, and JD Vienna. 2020. *Enhanced Hanford Low-Activity Waste Glass Property Data Development: Phase 3*. PNNL-29847, Pacific Northwest National Laboratory, Richland, WA.

Lu, X., D.S. Kim, and J.D. Vienna. 2021. "Impacts of Constraints and Uncertainties on Projected Amount of Hanford Low-Activity Waste Glasses," *Nuclear Engineering and Design*, **385:**111543, DOI: 10.1016/j.nucengdes.2021.111543.

Matlack KS, I Joseph, W Gong, IS Muller, and IL Pegg. 2007a. *Enhanced LAW Glass Formulation Testing*. VSL-07R1130-1, Vitreous State Laboratory, The Catholic University of America, Washington, DC.

Matlack KS, IS Muller, W Gong, and IL Pegg. 2006a. *DuraMelter 100 Tests To Support LAW Glass Formulation Correlation Development*. VSL-06R6480-1, Vitreous State Laboratory, The Catholic University of America, Washington, DC.

Matlack KS, IS Muller, W Gong, and IL Pegg. 2007b. *Small Scale Melter Testing of LAW Salt Phase Separation*. VSL-07R7480-1, Rev. 0, Vitreous State Laboratory, The Catholic University of America, Washington, DC.

Matlack KS, S Morgan, and IL Pegg. 2001. *Melter Tests with LAW Envelope A and C Simulants To Support Enhanced Sulfate Incorporation*. VSL-01R3501-2, Rev. 0, Vitreous State Laboratory, The Catholic University of America, Washington, DC.

Matlack KS, W Gong, IS Muller, I Joseph, and IL Pegg. 2006b. *LAW Envelope A and B Glass Formulations Testing To Increase Waste Loading*. VSL-06R6900-1, Rev. 0, Vitreous State Laboratory, The Catholic University of America, Washington, DC.

Matyas, J, AR Huckleberry, CP Rodriguez, JB Lang, AT Owen, and AA Kruger. 2012. *HLW Glass Studies: Development of Crystal-Tolerant HLW Glasses.* PNNL-21308, Pacific Northwest National Laboratory, Richland, WA.

Muller IS and IL Pegg. 2003a. *Baseline LAW Glass Formulation Testing*. VSL-03R3460-1, Vitreous State Laboratory, The Catholic University of America, Washington, DC.

Muller IS and IL Pegg. 2003b. *LAW Glass Formulation To Support Melter Runs with Simulants*. , VSL-03R3460-2, Vitreous State Laboratory, The Catholic University of America, Washington, DC.

Muller IS and IL Pegg. 2003c. *LAW Glass Formulation To Support AZ-102 Actual Waste Testing*. VSL-03R3470-1, Rev.0, Vitreous State Laboratory, The Catholic University of America, Washington, DC.

Muller IS and IL Pegg. 2003d. *LAW Glass Formulation To Support AZ-101 Actual Waste Testing*. VSL-03R3470-3, Vitreous State Laboratory, The Catholic University of America, Washington, DC.

Muller IS and IL Pegg. 2003e. *LAW Glass Formulation To Support AP-101 Actual Waste Testing*. VSL-03R3470-2, Vitreous State Laboratory, The Catholic University of America, Washington, DC .

Muller IS, I Joseph, and IL Pegg. 2006. *Preparation and Testing of Law High Phosphorus and High-Chromium Glasses*. VSL-06R6480-2, Rev. 0, Vitreous State Laboratory, The Catholic University of America, Washington, DC.

NQA-1-2012, *Quality Assurance Requirements for Nuclear Facility Application*. American Society of Mechanical Engineers, New York, NY.

Piepel GF, SK Cooley, A Heredia-Langner, SM Landmesser, WK Kot, H Gan, and IL Pegg. 2008. *IHLW PCT, Spinel T1%, Electrical Conductivity, and Viscosity Model Development*. VSL-07R1240-4, Rev.0, Vitreous State Laboratory, The Catholic University of America, Washington, DC.

Rielley E, IS Muller, and IL Pegg. 2004. *Preparation and Testing of LAW Matrix Glasses To Support WTP Property-Composition Model Development*. VSL-04R4480-1, Rev.0, Vitreous State Laboratory, The Catholic University of America, Washington, DC.

Russell RL, BP McCarthy, SK Cooley, EA Cordova, SE Sannoh, V Gervasio, MJ Schweiger, JB Lang, CH Skidmore, CE Lonergan, BA Stanfill, JM Meline, and JD Vienna. 2021. *Enhanced Hanford Low-Activity Waste Glass Property Data Development: Phase 2*. PNNL-28838, Rev. 2, Pacific Northwest National Laboratory, Richland, WA.

Russell RL, T Jin, BP McCarthy, LP Darnell, DE Rinehart, CC Bonham, V Gervasio, JM Mayer, CL Arendt, JB Lang, MJ Schweiger, and JD Vienna. 2017. *Enhanced Hanford Low-Activity Waste Glass Property Data Development: Phase 1*. PNNL-26630, Pacific Northwest National Laboratory, Richland, WA.

Vienna, J.D., A. Heredia-Langner, S.K. Cooley, A.E. Holmes, D.S. Kim, and N.A. Lumetta. 2021. *Glass Property-Composition Models for Support of Hanford WTP LAW Facility Operation,* PNNL-30932, Rev. 1, Pacific Northwest National Laboratory, Richland, WA.

Appendix A – Summary of Data Used in Constraint Development

This appendix contains the glass IDs, sources, compositions, maximum total vol% of ZCP at any heat treatment temperatures and relevant phase description for glasses considered in the development of the ZCP constraint.

Table A.1. Glass IDs, sources, compositions (wt%, unnormalized), maximum total vol% of Zr-containing phases at any heat treatment temperatures and relevant phase description for glasses considered in the development of the ZCP constraint.

Source	Glass ID	Al_2O_3	B_2O_3	CaO	Cl	Cr_2O_3	F	Fe_2O_3	K_2O	Li_2O	MgO	Na_2O	P_2O_5	SO_3	SiO_2	SnO_2	TiO_2	V_2O_5	ZnO	ZrO_2	Others	ZCP, vol%	Cassiterite, vol%	Relevant phase description
VSL-03R3460-2, Rev. 0	B1-AZ101	6.17	10.01	6.76	0.02	0.03	0.08	5.27	0.18	4.30	2.98	5.47	0.04	0.65	48.51	0.00	1.40	0.00	4.84	3.16	0.15	0.00	0.00	Secondary phases observed on crucible contact, less than 1% total sample volume.
VSL-03R3470-1, Rev. 0	LAWB53	6.10	10.03	6.75	0.01	0.11	0.06	5.34	0.23	5.86	3.00	5.00	0.01	0.81	48.92	0.00	1.41	0.00	3.19	3.19	0.00	0.00	0.00	Dark greenish brown homogenous glass. SEM revealed <0.3 vol.% crystals.
VSL-03R3460-1, Rev. 0	LAWB90	6.18	10.03	6.78	0.01	0.04	0.06	5.29	0.19	3.61	2.97	6.87	0.04	0.65	47.90	0.00	1.39	0.00	4.84	3.16	0.10	0.00	0.00	Amber brown glass. Some crystals (less than 1 vol%) formed along crucible contact interface.
VSL-03R3460-1, Rev. 0	LAWB91	6.18	10.03	6.78	0.01	0.04	0.06	5.29	0.19	2.92	2.97	8.72	0.04	0.65	46.74	0.00	1.39	0.00	4.84	3.16	0.10	0.00	0.00	Amber brown glass. Some crystals (less than 1 vol%) along crucible contact interface.
VSL-03R3460-1, Rev. 0	LAWB92	6.18	10.03	6.78	0.01	0.04	0.06	5.29	0.19	2.22	2.97	10.11	0.04	0.65	46.05	0.00	1.39	0.00	4.84	3.16	0.10	0.00	0.00	Amber brown glass. Some crystals (less than 1 vol%) along crucible contact interface.
VSL-03R3460-1, Rev. 0	LAWB93	6.18	10.03	6.78	0.01	0.04	0.06	5.29	0.19	4.66	2.97	4.78	0.04	0.65	48.94	0.00	1.39	0.00	4.84	3.16	0.10	0.00	0.00	Amber brown glass. Some crystals (less than 1 vol%) along crucible contact interface.
VSL-03R3460-1, Rev. 0	LAWB95	6.18	10.03	6.78	0.01	0.04	0.06	5.29	0.19	5.77	2.97	3.38	0.04	0.65	49.64	0.00	1.39	0.00	4.84	3.16	0.10	0.00	0.00	Amber brown glass. Some crystals (less than 1 vol%) along crucible contact interface.
VSL-06R6900-1, Rev. 0	LAWA187	10.65	12.79	6.48	0.65	0.52	0.00	0.91	0.51	0.00	0.91	23.00	0.00	0.75	34.86	1.00	0.00	0.98	3.00	3.00	0.00	0.00	0.00	<1 vol% crystals of 1-10 micron size
VSL-03R3460-1, Rev. 0	LAWB94	6.18	10.03	6.78	0.01	0.04	0.06	5.29	0.19	5.36	2.97	2.46	0.04	0.65	50.17	0.00	1.39	0.00	4.84	3.16	0.10	0.00	0.00	Amber brown glass. Crystals (less than 5 vol%) along crucible contact interface.
VSL-04R4480-1, Rev. 0	LAWM6	9.00	10.61	10.00	0.02	0.01	0.01	8.00	4.00	0.00	5.00	9.00	0.01	0.34	40.00	0.00	3.00	0.00	1.00	0.00	0.00	0.00	0.00	Optically clear, brown glass. SEM revealed secondary phases ~ 5 vol%.
VSL-06R6900-1, Rev. 0	LAWA190	12.15	11.29	5.98	0.65	0.52	0.00	0.91	0.51	0.00	0.91	23.00	0.00	0.75	34.86	0.00	0.00	0.98	3.00	4.50	0.00	0.00	0.00	moderate optical clarity; 0.5-2 vol% reddish particulates
VSL-06R6900-1, Rev. 0	LAWA193	12.15	11.29	5.48	0.65	0.52	0.00	0.91	0.51	0.00	0.91	23.00	0.00	0.75	35.86	0.00	0.00	0.98	3.00	4.00	0.00	0.00	0.00	0.5-2 vol% reddish particulates
VSL-06R6900-1, Rev. 0	LAWA179	10.85	9.26	7.98	0.71	0.02	0.00	0.91	0.56	0.00	0.91	25.00	0.00	0.75	35.32	0.00	0.00	0.94	2.35	4.45	0.00	0.00	0.00	green clear glass
VSL-06R6900-1, Rev. 0	LAWA180	10.85	7.76	7.98	0.71	0.02	0.00	0.91	0.56	0.00	0.91	25.00	0.00	0.75	35.32	0.00	0.00	0.94	2.35	5.95	0.00	0.00	0.00	<1% vol% crystals
VSL-06R6900-1, Rev. 0	LAWA181	12.36	9.26	7.98	0.71	0.02	0.00	0.91	0.56	0.00	0.91	25.00	0.00	0.75	35.32	0.00	0.00	0.94	2.35	2.95	0.00	0.00	0.00	few crystals
VSL-06R6900-1, Rev. 0	LAWA182	13.85	7.76	7.98	0.71	0.02	0.00	0.91	0.56	0.00	0.91	25.00	0.00	0.75	35.32	0.00	0.00	0.94	2.35	2.95	0.00	0.00	0.00	few crystals

Source	Glass ID	Al_2O_3	B_2O_3	CaO	Cl	Cr_2O_3	F	Fe_2O_3	K_2O	Li_2O	MgO	Na_2O	P_2O_5	SO_3	SiO_2	SnO_2	TiO_2	V_2O_5	ZnO	ZrO_2	Others	ZCP, vol%	Cassiterite, vol%	Relevant phase description
VSL-06R6900-1, Rev. 0	LAWA197	11.85	7.76	5.48	0.71	0.53	0.00	0.91	0.56	0.00	0.91	25.00	0.00	0.75	36.32	0.00	0.00	0.94	2.35	5.95	0.00	0.00	0.00	clear green glass with fine particulates
VSL-06R6900-1, Rev. 0	LAWA189	10.65	11.29	7.49	0.65	0.52	0.00	0.91	0.51	0.00	0.91	23.00	0.00	0.75	34.86	0.00	0.00	0.98	3.00	4.50	0.00	0.00	0.00	~ 0.1 vol.% of a Cr-Zn-Mg-Al Spinel
VSL-03R3470-1, Rev. 0	B01CC5	6.10	10.03	6.75	0.01	0.11	0.06	5.34	0.23	5.86	3.00	5.00	0.01	0.81	48.92	0.00	1.41	0.00	3.19	3.19	0.00	0.00	0.00	Increased amounts of swirls of crystals growing from the Quartz crucible and reaching as much as 4.2 vol.% in this area.
VSL-06R6900-1, Rev. 0	LAWA192	12.15	11.29	5.98	0.65	0.02	0.00	0.91	0.51	0.00	0.91	23.00	0.00	0.75	35.86	0.00	0.00	0.98	3.00	4.00	0.00	0.00	0.00	0.5-2 vol%
EWG-RPT-012-Rev 0/PNNL-26630	New-IL-5253	6.25	11.75	2.75	0.12	0.08	0.18	1.25	0.20	3.50	2.50	15.00	0.38	1.30	39.75	3.50	0.00	3.00	4.00	4.50	0.00	0.00	0.27	Cassiterite
EWG-RPT-012-Rev 0/PNNL-26630	New-IL-5255	6.25	11.75	2.75	0.12	0.08	0.18	1.25	0.20	3.50	2.50	18.00	0.38	1.30	36.75	3.50	0.00	3.00	4.00	4.50	0.00	0.00	0.19	Cassiterite
EWG-RPT-012-Rev 0/PNNL-26630	New-IL-94020	11.50	8.00	3.53	0.12	0.08	0.18	1.25	0.20	3.50	2.50	15.00	0.38	1.02	43.25	3.50	0.00	0.50	4.00	1.50	0.00	0.00	0.54	Cassiterite
EWG-RPT-012-Rev 0/PNNL-26630	New-IL-166697	11.25	10.22	2.75	0.31	0.21	0.47	1.25	1.00	3.50	0.50	17.49	1.01	1.29	36.75	3.50	0.00	3.00	4.00	1.50	0.00	0.00	0.42	Cassiterite
EWG-RPT-012-Rev 0/PNNL-26630	New-IL-166731	11.50	9.31	2.75	0.31	0.21	0.47	0.50	0.20	3.50	2.50	18.02	1.01	1.27	36.75	3.20	0.00	3.00	4.00	1.50	0.00	0.00	0.50	Cassiterite
EWG-RPT-012-Rev 0/PNNL-26630	New-OL-45748	13.85	6.00	12.24	0.47	0.31	0.71	1.50	0.00	5.00	0.00	11.40	1.51	0.10	34.00	5.00	0.00	2.91	5.00	0.00	0.00	0.00	1.28	Cassiterite
EWG-RPT-012-Rev 0/PNNL-26630	New-OL-54017	3.50	6.00	11.17	0.06	0.04	0.09	1.50	0.00	0.00	3.50	15.00	0.20	0.10	47.00	5.00	0.00	1.85	5.00	0.00	0.00	0.00	0.31	Cassiterite
EWG-RPT-012-Rev 0/PNNL-26630	New-OL-62380	3.50	13.75	12.24	0.11	0.08	0.17	1.50	1.50	0.00	0.00	14.01	0.37	0.10	34.00	4.50	0.00	2.66	5.00	6.50	0.00	0.00	0.15	Cassiterite
EWG-RPT-012-Rev 0/PNNL-26630	New-OL-65959Mod	13.85	13.05	0.00	0.06	0.04	0.09	0.00	0.00	5.00	3.50	16.50	0.20	0.10	34.50	4.50	0.00	3.60	5.00	0.00	0.00	0.00	1.01	Cassiterite
EWG-RPT-012-Rev 0/PNNL-26630	New-OL-80309	3.50	13.75	0.00	0.06	0.04	0.09	1.50	1.50	5.00	3.50	15.10	0.20	1.75	34.00	4.50	0.00	4.00	5.00	6.50	0.00	0.00	0.66	Cassiterite
EWG-RPT-012-Rev 0/PNNL-26630	New-OL-90780	13.85	13.75	0.00	0.47	0.31	0.71	0.00	1.50	5.00	3.50	15.51	1.51	1.64	34.25	3.00	0.00	4.00	1.00	0.00	0.00	0.00	0.42	Cassiterite
EWG-RPT-012-Rev 0/PNNL-26630	New-OL-127708Mod	10.94	13.75	0.30	0.06	0.04	0.09	1.50	1.50	2.01	3.50	12.50	0.20	0.61	47.00	5.00	0.00	0.00	1.00	0.00	0.00	0.00	0.73	Cassiterite
EWG-RPT-021 Rev.	LP2-OL-18	6.00	6.00	8.72	0.47	0.60	0.71	0.00	0.00	0.00	1.35	21.00	1.52	1.14	34.90	3.50	0.00	4.00	3.60	6.50	0.00	0.00	0.13	Cassiterite - 0.336; Calcium Sodium Tin - 0.287; Halite - 0.313

Source	Glass ID	Al_2O_3	B_2O_3	CaO	Cl	Cr_2O_3	F	Fe_2O_3	K_2O	Li_2O	MgO	Na_2O	P_2O_5	SO_3	SiO_2	SnO_2	TiO_2	V_2O_5	ZnO	ZrO_2	Others	ZCP, vol%	Cassiterite, vol%	Relevant phase description
1/PNNL-28838 Rev 1																								
EWG-RPT-012-Rev 0/PNNL-26630	New-OL-116208Mod	3.53	6.05	12.35	0.47	0.31	0.72	1.51	0.00	5.05	3.53	16.34	1.52	0.93	34.31	4.54	0.00	1.26	1.01	6.56	0.00	0.00	1.09	Nasicon - 6.8
EWG-RPT-012-Rev 0/PNNL-26630	New-OL-108249Mod	12.03	6.04	10.07	0.47	0.31	0.71	1.51	1.51	5.03	0.00	15.61	1.52	0.89	34.23	5.03	0.00	0.00	5.03	0.00	0.00	0.00	1.21	Nosean and Hauyne - 4.6
VSL-18R4360-1, Rev. 0	LORPM3S4-W	4.20	7.30	1.80	0.70	0.30	0.27	7.20	1.00	0.00	2.50	22.90	0.40	4.00	37.30	5.00	3.00	2.50	1.70	1.60	0.08	0.00	some	these glasses were after sulfate solubility
VSL-18R4360-1, Rev. 0	LORPM5S4-W	10.90	6.10	4.30	0.80	0.30	0.30	8.10	0.60	5.00	0.00	8.40	0.50	4.00	48.50	5.00	0.00	0.00	1.00	0.00	0.08	0.00	some	these glasses were after sulfate solubility
VSL-18R4360-1, Rev. 0	LORPM6S4-W	3.50	13.70	12.30	0.80	0.30	0.30	0.30	0.80	0.00	4.10	13.20	0.50	4.00	35.00	5.00	0.00	0.00	5.00	5.10	0.08	0.00	some	these glasses were after sulfate solubility
VSL-18R4360-1, Rev. 0	LORPM15S4-W	5.60	7.60	5.90	0.10	0.10	0.05	6.50	1.30	4.00	3.50	10.10	0.10	4.00	40.60	3.60	0.90	3.20	1.80	5.00	0.00	0.00	some	these glasses were after sulfate solubility
VSL-18R4360-1, Rev. 0	LORPM16R1S4-W	11.80	12.30	2.50	0.80	0.30	0.30	2.60	2.50	4.00	2.00	10.70	0.50	4.00	38.60	2.90	0.90	0.80	4.00	2.30	0.08	0.00	some	these glasses were after sulfate solubility
VSL-18R4360-1, Rev. 0	LORPM18S4	5.60	7.60	2.50	0.00	0.00	0.01	1.80	1.30	3.40	3.20	10.60	0.00	4.00	48.00	4.00	2.40	3.20	1.80	4.60	0.00	0.00	some	these glasses were after sulfate solubility
VSL-18R4360-1, Rev. 0	LORPM26S4-W	10.10	6.10	10.10	0.80	0.30	0.30	7.30	5.40	0.00	0.00	11.00	0.50	4.00	35.30	5.00	2.60	0.00	5.00	0.00	0.08	0.00	some	these glasses were after sulfate solubility
VSL-18R4360-1, Rev. 0	LORPM29S4-W	9.50	10.00	0.00	0.80	0.30	0.30	0.30	5.90	5.10	4.70	8.90	0.50	4.00	35.40	5.10	3.00	0.00	4.60	5.50	0.08	0.00	some	these glasses were after sulfate solubility
VSL-18R4360-1, Rev. 0	LORPM30S4	3.50	6.00	12.30	0.20	0.10	0.06	8.00	5.90	4.40	3.00	5.00	0.10	4.00	35.00	5.00	0.50	4.00	1.00	6.00	0.02	0.00	some	these glasses were after sulfate solubility
VSL-09R1510-2, Rev. 0	ORPLA25	9.17	8.39	3.45	0.73	0.49	0.00	0.00	0.58	0.00	0.00	26.00	0.00	0.20	39.10	3.00	0.00	0.00	2.89	6.00	0.00	0.1	0.10	Mostly clear glass. ~0.1 vol% Na-Zr silicate +Sn crystal
VSL-14R3050-1, Rev. 0	LORPM23	12.61	7.07	1.81	0.02	0.01	0.01	6.86	0.11	5.00	4.33	8.81	0.01	0.10	36.69	2.88	2.68	4.00	1.00	6.00	0.00	0.00	0.20	Tin oxide subhedral clusters were observed in LORPM23 (0.2 vol%),
VSL-14R3050-1, Rev. 0	LORPM24	11.38	6.00	0.00	0.02	0.01	0.01	7.10	5.88	0.00	3.85	13.48	0.01	0.28	35.98	2.18	0.00	4.00	4.57	5.25	0.00	0.00	0.10	
VSL-14R3050-1, Rev. 0	LORPM26	10.05	6.00	10.04	0.80	0.32	0.30	7.20	5.31	0.00	0.00	10.92	0.50	0.91	35.00	5.00	2.58	0.00	5.00	0.00	0.08	0.00	1.30	
VSL-14R3050-1, Rev. 0	LORPM29	9.39	9.92	0.00	0.80	0.32	0.30	0.30	5.88	5.00	4.64	8.86	0.50	1.00	35.00	5.00	3.00	0.00	4.60	5.42	0.08	0.00	1.00	Less 1 vol% tin oxide crystals; Trace amounts of a Cr-Zn-Fe Spinel (0.1 – 0.2 vol%) were observed in LORPM29 and LORPM31.
VSL-14R3050-1, Rev. 0	LORPM31	10.94	10.13	0.00	0.80	0.32	0.30	6.38	0.11	4.35	0.63	9.46	0.50	1.00	35.00	5.00	0.00	4.00	5.00	6.00	0.08	0.00	0.60	Tin oxide subhedral clusters 0.6 vol%; Trace amounts of a Cr-Zn-Fe Spinel (0.1 – 0.2 vol%) were observed in LORPM29 and LORPM31.
NA	LIC-01	14.62	6.56	10.38	0.31	0.51	0.47	0.58	0.43	5.44	7.98	7.65	1.01	0.69	34.91	2.91	0.00	1.59	2.37	1.59	0.00	0.00	0.94	
NA	LIC-03	3.53	13.60	5.13	0.37	1.06	0.56	0.00	0.63	3.29	0.63	16.93	1.19	0.60	40.72	3.34	0.00	3.71	3.42	1.29	0.00	0.00	0.00	

Source	Glass ID	Al_2O_3	B_2O_3	CaO	Cl	Cr_2O_3	F	Fe_2O_3	K_2O	Li_2O	MgO	Na_2O	P_2O_5	SO_3	SiO_2	SnO_2	TiO_2	V_2O_5	ZnO	ZrO_2	Others	ZCP, vol%	Cassiterite, vol%	Relevant phase description
NA	LIC-04_mod1	6.01	6.67	3.18	0.18	1.20	0.27	0.21	3.44	1.67	8.27	14.47	0.57	1.20	41.43	3.80	0.00	3.21	3.06	1.19	0.00	0.00	0.66	
NA	LIC-05	9.06	14.11	2.87	0.36	0.54	0.55	0.51	5.64	0.16	4.87	13.24	1.17	0.22	35.04	4.75	0.00	2.98	2.87	1.02	0.00	0.00	1.10	
NA	LIC-06	6.88	12.05	5.44	0.33	0.75	0.49	0.67	4.58	3.06	1.02	7.96	1.06	1.50	44.68	4.46	0.00	1.05	2.00	2.01	0.00	0.00	0.09	
NA	LIC-07	5.06	14.01	7.55	0.44	0.31	0.66	1.34	3.30	0.97	1.36	11.83	1.41	1.10	38.98	3.73	0.00	2.21	2.22	3.52	0.00	0.60	0.00	ZrO_2
NA	LIC-08	6.51	6.07	2.27	0.41	0.43	0.62	0.84	1.08	1.41	9.99	15.46	1.32	1.60	41.67	3.00	0.00	0.67	2.57	4.10	0.00	0.00	0.22	
NA	LIC-09_mod3	12.87	11.10	3.31	0.33	0.68	0.50	1.39	1.22	4.76	4.03	9.22	1.07	0.56	37.98	4.16	0.00	0.84	2.77	3.22	0.00	0.00	1.15	
NA	LIC-10	8.40	8.64	11.75	0.44	1.33	0.68	0.80	5.30	3.40	0.94	10.52	1.45	0.20	35.99	2.79	0.00	0.51	2.44	4.41	0.00	0.70	0.00	ZrO_2
EWG-RPT-012-Rev 0/PNNL-26630	New-OL-14844	3.50	6.15	12.24	0.47	0.31	0.71	0.00	1.50	5.00	3.50	15.51	1.51	0.10	34.00	0.00	0.00	4.00	5.00	6.50	0.00	1.13	0.00	Baddeleyite/ZrO_2
EWG-RPT-012-Rev 0/PNNL-26630	New-OL-8788Mod	12.35	6.00	0.05	0.47	0.31	0.71	1.50	1.50	2.50	3.50	13.00	1.51	0.10	46.00	0.00	0.00	0.00	5.00	5.50	0.00	1.04	0.00	Baddeleyite/ZrO_2 - 2.2; Iron Oxide - 1
EWG-RPT-012-Rev 0/PNNL-26630	New-OL-8445	12.41	13.75	12.24	0.47	0.31	0.71	0.00	1.50	2.01	3.50	10.00	1.51	0.10	34.00	0.00	0.00	0.00	1.00	6.50	0.00	0.94	0.00	Baddeleyite/ZrO_2 - 2; Fluorapatite - 1.5
EWG-RPT-021 Rev. 1/PNNL-28838 Rev 1	LP2-IL-01	7.50	8.00	7.62	0.17	0.53	0.26	0.20	2.00	0.00	0.30	23.68	0.56	0.80	37.98	0.50	0.00	2.00	2.40	5.50	0.00	0.14	0.00	Nasicon - 0.67; Baddeleyite - 0.29
EWG-RPT-021 Rev. 1/PNNL-28838 Rev 1	LP2-IL-02	7.50	8.13	2.00	0.17	0.38	0.26	0.58	2.00	0.00	1.00	23.68	0.56	0.80	41.81	2.50	0.00	0.50	2.63	5.50	0.00	0.14	0.00	Nasicon - 1.2; Baddeleyite - 0.29
EWG-RPT-021 Rev. 1/PNNL-28838 Rev 1	LP2-IL-03	8.73	8.73	2.00	0.35	0.53	0.53	0.20	0.76	0.00	0.30	24.50	1.13	0.20	40.36	2.50	0.00	0.50	3.20	5.50	0.00	0.28	0.00	Nasicon - 1.96; Baddeleyite - 0.59
VSL-00R3501-1, Rev. 0	LAWBS1-G-36F	6.16	12.09	4.70	0.01	0.09	0.10	5.15	0.32	2.96	2.91	7.90	3.40	1.03	46.91	0.00	0.00	0.00	3.09	3.09	0.10	0.10	0.00	Zircon
VSL-13R2940-1, Rev. 0	LORPM2R1	12.88	6.52	10.59	0.80	0.32	0.30	0.30	5.25	2.66	4.61	6.82	0.50	0.19	35.00	2.16	0.28	3.73	1.00	6.00	0.08	1.50	0.00	1.5 vol% ZrO_2 in clusters.
VSL-13R2940-1, Rev. 0	LORPM13	13.85	13.73	0.00	0.02	0.01	0.01	8.00	0.11	0.50	0.00	13.31	0.01	1.00	37.06	1.39	0.00	4.00	1.00	6.00	0.00	2.10	0.00	2.1 vol% ZrO_2 crystals in clusters.
VSL-06R6480-2, Rev. 0	LAWCrP9	6.10	10.00	6.98	0.14	0.43	0.07	5.50	0.09	4.30	2.93	5.40	2.51	0.73	46.91	0.00	1.40	0.00	3.50	3.00	0.03	0.00	0.00	Mixture of small Cr-rich ZnFeTi Spinels (about 1/3) and Chloro-apatite (about 2/3) - total ~0.7 vol.% crystals.
VSL-09R1510-2, Rev. 0	ORPLG1	10.04	8.90	2.23	0.20	0.60	0.08	0.30	5.06	0.00	0.96	18.50	0.13	0.36	41.27	2.97	0.00	0.00	2.45	5.93	0.02	0.00	0.00	Mostly clear glass. ~0.2 vol% tiny Cr oxide crystals
VSL-09R1510-2, Rev. 0	ORPLG2	9.99	8.82	2.20	0.21	0.60	0.08	0.29	5.20	0.00	0.96	19.00	0.13	0.37	40.89	2.94	0.00	0.00	2.43	5.88	0.02	0.00	0.00	Mostly clear glass. ~0.2 vol% tiny Cr oxide crystals
VSL-09R1510-2, Rev. 0	ORPLG3	9.95	8.74	2.18	0.21	0.60	0.08	0.29	5.34	0.00	0.95	19.50	0.13	0.38	40.50	2.91	0.00	0.00	2.40	5.82	0.02	0.00	0.00	Mostly clear glass. ~0.2 vol% tiny Cr oxide crystals

Source	Glass ID	Al_2O_3	B_2O_3	CaO	Cl	Cr_2O_3	F	Fe_2O_3	K_2O	Li_2O	MgO	Na_2O	P_2O_5	SO_3	SiO_2	SnO_2	TiO_2	V_2O_5	ZnO	ZrO_2	Others	ZCP, vol%	Cassiterite, vol%	Relevant phase description
VSL-09R1510-2, Rev. 0	ORPLG4	9.95	8.74	2.18	0.21	0.60	0.08	0.29	5.34	0.00	0.95	19.50	0.13	0.38	40.50	4.80	0.00	0.00	2.40	3.93	0.02	0.00	0.00	Mostly clear glass. ~0.2 vol% tiny Cr oxide crystals
VSL-09R1510-2, Rev. 0	ORPLG5	9.95	8.74	2.77	0.21	0.60	0.08	0.00	5.34	0.00	0.00	19.50	0.13	0.38	40.79	2.91	0.00	0.00	2.77	5.82	0.02	0.00	0.00	Mostly clear glass. ~0.2 vol% tiny Cr oxide crystals
VSL-09R1510-2, Rev. 0	ORPLG6	6.77	8.70	2.75	0.22	0.60	0.09	0.29	5.40	0.00	0.98	19.75	0.14	0.38	41.75	2.90	0.00	0.00	3.48	5.80	0.02	0.00	0.00	Mostly clear glass. ~0.2 vol% tiny Cr oxide crystals
VSL-09R1510-2, Rev. 0	ORPLG7	6.77	8.65	2.74	0.22	0.59	0.09	0.29	5.47	0.00	0.97	20.00	0.14	0.39	41.55	2.88	0.00	0.00	3.46	5.77	0.02	0.00	0.00	Mostly clear glass. ~0.2-0.3 vol% tiny Cr oxide crystals
VSL-09R1510-2, Rev. 0	ORPLG8	6.75	8.57	2.71	0.23	0.59	0.09	0.29	5.61	0.00	0.96	20.50	0.14	0.40	41.15	2.86	0.00	0.00	3.43	5.71	0.02	0.00	0.00	Mostly clear glass. ~0.2-0.3 vol% tiny Cr oxide crystals
VSL-09R1510-2, Rev. 0	ORPLG9	6.74	8.49	2.69	0.23	0.59	0.09	0.28	5.75	0.00	0.95	21.00	0.14	0.41	40.75	2.83	0.00	0.00	3.39	5.66	0.02	0.00	0.00	Mostly clear glass. ~0.2-0.3 vol% tiny Cr oxide crystals
VSL-09R1510-2, Rev. 0	ORPLF1	10.03	9.75	10.00	0.01	0.55	0.07	0.31	0.41	3.75	1.01	10.00	0.03	1.61	43.35	0.88	0.00	1.25	3.00	4.00	0.00	0.00	0.00	Mostly clear glass. ~0.2 vol% Cr oxide crystals + Zn and Sn
VSL-09R1510-2, Rev. 0	ORPLF2	9.89	9.61	9.86	0.01	0.55	0.08	0.30	0.45	3.70	0.99	11.00	0.03	1.77	42.74	0.86	0.00	1.24	2.96	3.94	0.00	0.00	0.00	Mostly clear glass. ~0.2 vol% Cr oxide crystals + Zn and Sn
VSL-09R1510-2, Rev. 0	ORPLF3	9.76	9.48	9.72	0.01	0.56	0.08	0.30	0.50	3.65	0.98	12.00	0.04	1.93	42.14	0.85	0.00	1.22	2.91	3.88	0.00	0.00	0.00	Mostly clear glass. ~0.3 vol% Cr oxide crystals + Zn and Sn
VSL-09R1510-2, Rev. 0	ORPLF4	8.60	9.50	9.72	0.01	0.56	0.08	0.30	0.50	3.50	0.98	12.00	0.04	1.93	42.14	0.85	0.00	2.50	2.91	3.88	0.00	0.00	0.00	Mostly clear glass. <0.1 vol% Cr oxide crystals + Zn and Sn
VSL-10R1790-1, Rev. 0	ORPLG17	5.52	8.26	2.73	0.23	0.59	0.09	0.29	5.64	0.00	2.05	20.61	0.14	0.40	41.38	3.23	0.00	0.00	2.73	6.10	0.02	0.00	0.00	Mostly clear glass ~0.6 vol% small Cr-rich crystals with Zn and few large NaZr silicate crystals with Sn
VSL-10R1790-1, Rev. 0	ORPLG18	5.52	8.04	2.73	0.23	0.59	0.09	0.29	5.64	0.00	1.97	20.61	0.14	0.40	42.24	2.73	0.00	0.00	2.73	6.03	0.02	0.00	0.00	Mostly clear glass ~0.3 vol% small Cr-rich crystals with Zn and few large NaZr silicate crystals with Sn
VSL-10R1790-1, Rev. 0	ORPLG19	5.51	7.96	2.70	0.23	0.59	0.09	0.28	5.78	0.00	1.95	21.12	0.14	0.41	41.83	2.70	0.00	0.00	2.70	5.97	0.02	0.00	0.00	Mostly clear glass ~0.7 vol% small Cr-rich crystals with Zn and few large NaZr silicate crystals with Sn
VSL-10R1790-1, Rev. 0	ORPLG20	6.04	8.00	2.71	0.23	0.59	0.09	0.29	5.61	0.00	0.96	20.50	0.14	0.40	42.01	3.71	0.00	0.00	2.71	6.00	0.02	0.00	0.00	Mostly clear glass ~0.3 vol% small Cr-rich crystals with Zn and few large NaZr silicate crystals with Sn
VSL-10R1790-1, Rev. 0	ORPLG21	6.04	8.00	2.71	0.23	0.59	0.09	0.29	5.61	0.00	0.96	20.50	0.14	0.40	43.01	2.71	0.00	0.00	2.71	6.00	0.02	0.00	0.00	Mostly clear glass ~0.4 vol% small Cr-rich crystals with Zn, few large NaZr silicate crystals with Sn and Cr-rich crystal cluster
VSL-10R1790-1, Rev. 0	ORPLG22	6.04	8.00	2.71	0.23	0.59	0.09	0.29	5.61	0.00	0.46	20.50	0.14	0.40	42.01	3.46	0.00	0.00	2.71	6.75	0.02	0.00	0.00	Mostly clear glass ~0.4 vol% small Cr-rich crystals with Zn, few large NaZr silicate crystals with Sn and Cr-rich crystal cluster
VSL-10R1790-1, Rev. 0	ORPLG23	6.04	8.00	2.71	0.23	0.59	0.09	0.29	5.61	0.00	0.46	20.50	0.14	0.40	42.51	3.21	0.00	0.00	2.71	6.50	0.02	0.00	0.00	Mostly clear glass ~0.3 vol% small Cr-rich crystals with Zn few large NaZr silicate crystals with Sn
VSL-10R1790-1, Rev. 0	ORPLG24	6.03	7.92	2.69	0.23	0.59	0.09	0.28	5.75	0.00	0.94	21.00	0.14	0.41	41.60	3.69	0.00	0.00	2.69	5.94	0.02	0.00	0.00	Mostly clear glass ~0.3 vol% small Cr-rich crystals with Zn few large NaZr silicate crystals with Sn

Source	Glass ID	Al_2O_3	B_2O_3	CaO	Cl	Cr_2O_3	F	Fe_2O_3	K_2O	Li_2O	MgO	Na_2O	P_2O_5	SO_3	SiO_2	SnO_2	TiO_2	V_2O_5	ZnO	ZrO_2	Others	ZCP, vol%	Cassiterite, vol%	Relevant phase description
VSL-10R1790-1, Rev. 0	ORPLG25	6.03	7.92	2.69	0.23	0.59	0.09	0.28	5.75	0.00	0.94	21.00	0.14	0.41	42.60	2.69	0.00	0.00	2.69	5.94	0.02	0.00	0.00	Mostly clear glass ~0.3 vol% small Cr-rich crystals with Zn few large NaZr silicate crystals with Sn
VSL-10R1790-1, Rev. 0	ORPLG26	6.03	7.92	2.69	0.23	0.59	0.09	0.28	5.75	0.00	0.44	21.00	0.14	0.41	41.60	3.44	0.00	0.00	2.69	6.69	0.02	0.00	0.00	Foamy region observed ~0.3 vol% small Cr-rich crystals with Zn few large NaZr silicate crystals with Sn
VSL-07R1130-1, Rev. 0	ORPLD1	10.16	12.05	8.02	0.33	0.50	0.17	1.00	0.16	0.00	1.00	21.00	0.29	0.96	37.17	0.00	0.00	1.00	3.00	3.00	0.18	0.00	0.00	Mostly clear glass. ~ 0.1 to 0.2 vol% of small Cr+Zn crystals
VSL-09R1510-2, Rev. 0	ORPLG10	6.72	8.40	2.66	0.24	0.59	0.09	0.28	5.88	0.00	0.94	21.50	0.15	0.42	40.35	2.80	0.00	0.00	3.36	5.60	0.02	0.00	0.00	Mostly clear glass. ~0.2 vol% tiny Cr oxide & NaZrSn silicate crystals
VSL-09R1510-2, Rev. 0	ORPLG11	6.75	8.57	3.96	0.23	0.59	0.09	0.00	5.61	0.00	0.00	20.50	0.14	0.40	41.15	2.86	0.00	0.00	3.43	5.71	0.02	0.00	0.00	Mostly clear glass. ~0.2 vol% tiny Cr oxide & NaZrSn silicate crystals
VSL-09R1510-2, Rev. 0	ORPLG12	6.75	8.57	2.71	0.23	0.59	0.09	0.29	5.61	0.00	0.96	20.50	2.00	0.40	41.15	2.86	0.00	0.00	3.43	3.86	0.02	0.00	0.00	Mostly clear glass. ~0.1 vol% tiny Cr oxide crystals
VSL-10R1790-1, Rev. 0	ORPLG16	5.52	8.26	2.73	0.23	0.59	0.09	0.29	5.64	0.00	2.05	20.61	0.14	0.40	41.38	2.87	0.00	0.00	3.45	5.74	0.02	0.00	0.00	Mostly clear glass ~0.2 vol% small Cr oxide crystals
VSL-09R1510-2, Rev. 0	ORPLF5	9.62	9.34	9.58	0.01	0.56	0.09	0.29	0.54	3.59	0.97	13.00	0.04	2.09	41.54	0.84	0.00	1.20	2.87	3.83	0.00	0.00	0.00	Clear glass. <<0.1 vol% Cr-Zn oxide crystals
VSL-09R1510-2, Rev. 0	ORPLF6	8.48	9.36	9.58	0.01	0.56	0.09	0.29	0.54	3.45	0.97	13.00	0.04	2.09	41.54	0.84	0.00	2.47	2.87	3.83	0.00	0.00	0.00	Clear glass. <<0.1 vol% Cr-Zn oxide crystals
VSL-09R1510-2, Rev. 0	ORPLF7	8.60	9.50	9.72	0.01	0.56	0.08	0.30	0.50	4.35	0.98	12.00	0.04	1.93	42.14	0.00	0.00	2.50	2.91	3.88	0.00	0.00	0.00	Mostly clear glass. ~0.1 vol% Cr-Zn oxide crystals
VSL-09R1510-2, Rev. 0	ORPLF8	8.60	8.85	9.72	0.01	0.56	0.08	0.30	0.50	5.00	0.98	12.00	0.04	1.93	42.14	0.00	0.00	2.50	2.91	3.88	0.00	0.00	0.00	Mostly clear glass. <0.1 vol% Cr-Zn oxide crystals
VSL-09R1510-2, Rev. 0	ORPLF10	8.60	9.50	10.57	0.01	0.56	0.08	0.30	0.50	3.50	0.98	12.00	0.04	1.93	42.14	0.00	0.00	2.50	2.91	3.88	0.00	0.00	0.00	~0.1-0.2 vol% Cr-Zn oxide crystals
VSL-09R1510-2, Rev. 0	ORPLF12	8.60	9.50	9.72	0.01	0.56	0.09	0.30	0.50	3.50	0.98	12.00	0.04	1.93	42.14	0.00	0.00	2.75	2.91	4.49	0.00	0.00	0.00	~0.1-0.2 vol.% Cr-Zn oxide crystals
VSL-07R1130-1, Rev. 0	ORPLB1	12.00	7.30	1.10	0.11	0.52	0.49	1.10	0.12	0.00	1.10	25.00	0.23	0.52	37.98	1.08	0.00	2.00	3.65	5.44	0.25	0.00	0.00	0.1 to 0.2 vol% of Cr-rich Spinel with Zn, Al, and Sn.
VSL-07R1130-1, Rev. 0	ORPLB2	10.00	7.30	1.10	0.11	0.52	0.49	1.10	0.12	0.00	1.10	25.00	0.23	0.52	39.98	1.08	0.00	2.00	3.65	5.44	0.25	0.00	0.00	0.1 to 0.2 vol% of Cr-rich Spinel with Zn, Al, and Sn.
VSL-08R1410-1, Rev. 0	LAWM43	7.00	8.68	5.00	0.80	0.32	0.30	5.00	0.30	2.50	2.50	12.00	0.50	0.42	45.00	0.00	2.00	0.00	4.60	3.00	0.08	0.00	0.00	0.1 vol% Spinel
VSL-08R1410-1, Rev. 0	LAWM25R1	8.00	12.00	2.00	0.80	0.32	0.30	3.68	2.00	3.00	3.50	10.00	0.50	0.40	49.92	0.00	0.50	0.00	2.00	1.00	0.08	0.00	0.00	0.1 vol% Spinel
VSL-08R1410-1, Rev. 0	LAWM41	7.00	8.00	7.00	0.80	0.32	0.30	5.00	0.30	1.00	2.50	14.00	0.50	0.37	45.00	0.00	1.00	0.00	4.60	2.23	0.08	0.00	0.00	0.1 vol% Spinel
VSL-08R1410-1, Rev. 0	LAWM39	7.00	9.05	5.00	0.80	0.32	0.30	3.00	0.10	2.50	2.50	14.00	0.50	0.35	48.00	0.00	1.00	0.00	3.50	2.00	0.08	0.00	0.00	0.1 vol% Spinel
VSL-08R1410-1, Rev. 0	LAWCrP6	6.10	10.00	6.94	0.14	0.63	0.07	5.50	0.09	4.17	2.55	8.00	2.51	0.65	44.74	0.00	1.40	0.00	3.50	3.00	0.03	0.00	0.00	0.7 vol% Spinel

Source	Glass ID	Al_2O_3	B_2O_3	CaO	Cl	Cr_2O_3	F	Fe_2O_3	K_2O	Li_2O	MgO	Na_2O	P_2O_5	SO_3	SiO_2	SnO_2	TiO_2	V_2O_5	ZnO	ZrO_2	Others	ZCP, vol%	Cassiterite, vol%	Relevant phase description
VSL-08R1410-1, Rev. 0	LAWCrP5	6.10	10.00	5.81	0.14	0.59	0.07	5.50	0.09	2.64	1.49	14.38	1.33	0.51	43.45	0.00	1.40	0.00	3.50	3.00	0.03	0.00	0.00	0.3 vol% Spinel
VSL-08R1410-1, Rev. 0	LAWM8	9.00	13.00	6.43	0.80	0.32	0.30	0.00	0.00	2.08	5.00	5.00	0.50	1.00	44.49	0.00	3.00	0.00	5.00	4.00	0.08	0.00	0.00	0.1 vol% Spinel
VSL-06R6480-2, Rev. 0	LAWCrP2	6.10	10.00	2.11	0.19	0.59	0.10	5.50	0.27	0.00	1.48	21.00	1.33	0.34	43.07	0.00	1.40	0.00	3.50	3.00	0.00	0.00	0.00	Large number of small Cr-rich Spinels estimated at ~0.4 vol.%.
VSL-06R6480-2, Rev. 0	LAWCrP2R	6.10	10.00	2.11	0.19	0.59	0.10	5.50	0.27	0.00	1.48	21.00	1.33	0.34	43.07	0.00	1.40	0.00	3.50	3.00	0.00	0.00	0.00	Few Cr-rich Spinels < 0.1 vol.%.
VSL-06R6480-2, Rev. 0	LAWCrP5	6.10	10.00	5.81	0.14	0.59	0.07	5.50	0.09	2.64	1.49	14.38	1.33	0.51	43.45	0.00	1.40	0.00	3.50	3.00	0.03	0.00	0.00	Few small (5 to 20 µm) Cr-rich ZnFeTi Spinels distributed uniformly throughout the sample ~0.3 vol.%.
VSL-06R6480-2, Rev. 0	LAWCrP6	6.10	10.00	6.94	0.14	0.63	0.07	5.50	0.09	4.17	2.55	8.00	2.51	0.65	44.74	0.00	1.40	0.00	3.50	3.00	0.03	0.00	0.00	Few small (~1 to 10 µm) Cr-rich ZnFeTi Spinels throughout the sample with heavy crystallization along the crucible contact surfaces ~0.7 vol.%.
VSL-06R6480-2, Rev. 0	LAWCrP7	6.10	10.00	6.98	0.14	0.63	0.07	5.50	0.09	4.30	2.93	5.40	2.51	0.73	46.71	0.00	1.40	0.00	3.50	3.00	0.03	0.00	0.00	Cr-rich ZnFeTi Spinels and some apatite ~0.7 vol.%.
VSL-06R6480-2, Rev. 0	LAWCrP8	6.10	10.00	6.94	0.14	0.43	0.07	5.50	0.09	4.17	2.55	8.00	2.51	0.65	44.94	0.00	1.40	0.00	3.50	3.00	0.03	0.00	0.00	Few small Cr-rich ZnFeTi Spinels ~0.1 vol.%.
VSL-06R6480-2, Rev. 0	LAWCrP10	6.10	10.00	6.98	0.14	0.33	0.07	5.50	0.09	4.30	2.93	5.40	1.33	0.73	48.19	0.00	1.40	0.00	3.50	3.00	0.03	0.00	0.00	Few small Cr-rich ZnFeTi Spinels ~0.2 vol%.
VSL-06R6480-2, Rev. 0	LAWE3Cr1	6.10	10.00	2.02	0.20	1.20	0.08	5.50	4.99	0.00	1.48	18.21	0.12	0.35	41.83	0.00	1.40	0.00	3.50	3.00	0.02	0.00	0.00	About 0.3 vol.% of Cr-rich Spinels with Zn and Fe. Remaining glass shows ~1 wt% Cr_2O_3.
VSL-06R6480-2, Rev. 0	LAWE3Cr2	6.10	10.00	2.02	0.20	1.40	0.08	5.50	4.99	0.00	1.48	18.21	0.12	0.35	41.63	0.00	1.40	0.00	3.50	3.00	0.02	0.00	0.00	About 0.3 vol.% of very fine Cr-rich Spinels with Zn, Fe and Ti. Remaining glass shows ~1 wt% Cr_2O_3.
VSL-06R6480-2, Rev. 0	LAWE4HCr1	5.97	9.79	2.46	0.20	1.20	0.08	5.38	0.54	0.00	1.45	21.27	0.12	0.41	43.38	0.00	1.37	0.00	3.43	2.94	0.02	0.00	0.00	About 0.4 vol.% of Cr-rich Spinels with Zn, Fe and Ti. Remaining glass shows ~1 wt% Cr_2O_3.
VSL-06R6480-2, Rev. 0	LAWE4HCr2	5.97	9.79	2.46	0.20	1.40	0.08	5.38	0.54	0.00	1.45	21.27	0.12	0.41	43.18	0.00	1.37	0.00	3.43	2.94	0.02	0.00	0.00	About 0.6 vol.% of very fine Cr-rich Spinels with Zn, Fe and Ti. Remaining glass shows ~1 wt% Cr_2O_3.
VSL-06R6480-2, Rev. 0	LAWE7HCr1	6.02	9.87	6.31	0.20	1.20	0.08	5.43	0.54	3.17	1.49	13.53	0.12	0.59	43.63	0.00	1.38	0.00	3.46	2.96	0.02	0.00	0.00	About 0.5 vol.% of Cr-rich Spinels with Zn, Fe and Ti. Remaining glass shows ~0.4 wt% Cr_2O_3.
VSL-06R6480-2, Rev. 0	LAWE7HCr2	6.02	9.87	6.31	0.20	1.40	0.08	5.43	0.54	3.17	1.49	13.53	0.12	0.59	43.43	0.00	1.38	0.00	3.46	2.96	0.02	0.00	0.00	About 0.4 vol.% of Cr-rich Spinels with Zn, Fe and Ti. Remaining glass shows ~0.6 wt% Cr_2O_3.
VSL-06R6480-2, Rev. 0	LAWE9HCr1	6.05	9.92	6.86	0.20	0.60	0.08	5.45	0.54	4.08	2.36	8.93	0.12	0.69	46.27	0.00	1.39	0.00	3.47	2.97	0.02	0.00	0.00	About 0.4 vol.% of Cr-rich Spinels with Zn, Fe and Ti. Remaining glass shows ~0.3 wt% Cr_2O_3.
VSL-06R6480-2, Rev. 0	LAWE9HCr2	6.05	9.92	6.86	0.20	0.45	0.08	5.45	0.54	4.08	2.36	8.93	0.12	0.69	46.42	0.00	1.39	0.00	3.47	2.97	0.02	0.00	0.00	About 0.2 vol.% of small Cr-rich Spinels with Zn, Fe and Ti, mostly at the crucible contact.
VSL-06R6480-2, Rev. 0	LAWE10HCr1	6.07	9.95	6.96	0.20	1.20	0.08	5.48	0.54	4.26	2.94	5.72	0.12	0.80	47.80	0.00	1.39	0.00	3.48	2.99	0.02	0.00	0.00	About 0.8 vol.% of Cr-rich Spinels with Zn, Fe and Ti.

Source	Glass ID	Al_2O_3	B_2O_3	CaO	Cl	Cr_2O_3	F	Fe_2O_3	K_2O	Li_2O	MgO	Na_2O	P_2O_5	SO_3	SiO_2	SnO_2	TiO_2	V_2O_5	ZnO	ZrO_2	Others	ZCP, vol%	Cassiterite, vol%	Relevant phase description
																								Remaining glass shows no detectable Cr_2O_3.
VSL-06R6480-2, Rev. 0	LAWE10HCr2	6.07	9.95	6.96	0.20	0.60	0.08	5.48	0.54	4.26	2.94	5.72	0.12	0.80	48.40	0.00	1.39	0.00	3.48	2.99	0.02	0.00	0.00	About 0.4 vol.% of Cr-rich Spinels with Zn, Fe and Ti. Remaining glass shows no detectable Cr_2O_3.
VSL-06R6480-2, Rev. 0	LAWE10HCr3	6.07	9.95	6.96	0.20	0.35	0.08	5.48	0.54	4.26	2.94	5.72	0.12	0.80	48.65	0.00	1.39	0.00	3.48	2.99	0.02	0.00	0.00	About 0.2 vol.% of Cr-rich Spinels with Zn, Fe and Ti. Remaining glass shows ~0.1 wt% Cr_2O_3.
VSL-06R6480-2, Rev. 0	LAWE10HCr4	6.07	9.95	6.96	0.20	0.25	0.08	5.48	0.54	4.26	2.94	5.72	0.12	0.80	48.75	0.00	1.39	0.00	3.48	2.99	0.02	0.00	0.00	Clear homogeneous glass with a few Cr-rich Spinels with Zn, Fe and Ti only at the crucible contact surface. Remaining glass shows ~0.2 wt% Cr_2O_3.
VSL-06R6480-2, Rev. 0	LAWCrP3	6.10	10.00	2.76	0.12	0.33	0.11	5.50	0.13	0.00	1.48	19.34	2.38	0.39	43.45	0.00	1.40	0.00	3.50	3.00	0.00	0.00	0.00	CrZnFeMgAl Spinels and NaCaPhosphates estimated at ~0.5 vol.%.
VSL-06R6480-2, Rev. 0	LAWCrP4	6.10	10.00	2.11	0.19	0.59	0.10	5.50	0.27	0.00	1.48	21.00	2.38	0.34	42.03	0.00	1.40	0.00	3.50	3.00	0.00	0.00	0.00	CrZnFeMgAl Spinels and NaCaPhosphates estimated at ~0.3 vol.%.
VSL-09R1510-2, Rev. 0	ORPLD4	10.18	12.07	8.03	0.33	0.50	0.17	0.30	0.16	0.00	1.00	21.00	0.29	0.96	37.92	0.00	0.00	1.00	3.01	3.01	0.05	0.00	0.00	Mostly clear glass. ~ 0.1 vol% of small Cr+Zn crystals
VSL-07R7480-1, Rev. 0	FWV-G-35B	6.03	9.88	6.91	0.43	0.08	0.52	5.44	0.54	4.23	2.92	5.72	0.12	0.79	48.57	0.00	1.38	0.00	3.46	2.97	0.02	0.00	0.00	Mostly clear glass; a few Cr-rich Spinels containing Fe, Ni and Zn, < 0.1 vol.%
VSL-07R7480-1, Rev. 0	FWV-G-108B	5.78	9.48	2.38	1.00	0.08	1.20	5.21	0.53	0.00	1.40	21.27	0.12	0.40	43.63	0.00	1.33	0.00	3.33	2.85	0.02	0.00	0.00	Mostly clear glass; one Cr-rich Spinel containing Fe, Al and Mg, estimated < 0.1 vol.%
VSL-07R7480-1, Rev. 0	FWV-G-138B	5.86	9.60	2.41	0.32	0.63	0.38	5.27	0.54	0.00	1.42	21.27	0.12	0.41	44.16	0.00	1.34	0.00	3.37	2.88	0.02	0.00	0.00	Mostly clear glass; a few Cr Fe-Ni spinels containing trace Zn, estimated < 0.1 vol.%
VSL-08R1410-1, Rev. 0	LAWE9HCr1	6.05	9.92	6.86	0.20	0.60	0.08	5.45	0.54	4.08	2.36	8.93	0.12	0.69	46.27	0.00	1.39	0.00	3.47	2.97	0.02	0.00	0.00	0.4 vol% Spinel
VSL-08R1410-1, Rev. 0	LAWE9HCr2	6.05	9.92	6.86	0.20	0.45	0.08	5.45	0.54	4.08	2.36	8.93	0.12	0.69	46.42	0.00	1.39	0.00	3.47	2.97	0.02	0.00	0.00	0.2 vol% Spinel
VSL-08R1410-1, Rev. 0	LAWCrP11	6.10	10.00	6.37	0.14	0.61	0.07	5.50	0.09	3.40	2.02	11.19	1.92	0.58	44.10	0.00	1.40	0.00	3.50	3.00	0.02	0.00	0.00	0.3 ± 0.2 vol.% Cr-rich Spinel with Fe and Zn
VSL-08R1410-1, Rev. 0	LAWCrP12	6.10	10.00	6.09	0.14	0.60	0.07	5.50	0.09	3.02	1.75	12.78	1.63	0.54	43.77	0.00	1.40	0.00	3.50	3.00	0.03	0.00	0.00	0.3 ± 0.2 vol.% Cr-rich Spinel with Fe and Zn
VSL-08R1410-1, Rev. 0	LAWE10HCr1	6.07	9.95	6.96	0.20	1.20	0.08	5.48	0.54	4.26	2.94	5.72	0.12	0.80	47.80	0.00	1.39	0.00	3.48	2.99	0.02	0.00	0.00	0.8 vol% Spinel
VSL-08R1410-1, Rev. 0	LAWE10HCr2	6.07	9.95	6.96	0.20	0.60	0.08	5.48	0.54	4.26	2.94	5.72	0.12	0.80	48.40	0.00	1.39	0.00	3.48	2.99	0.02	0.00	0.00	0.4 vol% Spinel
VSL-08R1410-1, Rev. 0	LAWE10HCr3	6.07	9.95	6.96	0.20	0.35	0.08	5.48	0.54	4.26	2.94	5.72	0.12	0.80	48.65	0.00	1.39	0.00	3.48	2.99	0.02	0.00	0.00	0.2 vol% Spinel
VSL-08R1410-1, Rev. 0	LAWCrP6	6.10	10.00	6.94	0.14	0.63	0.07	5.50	0.09	4.17	2.55	8.00	2.51	0.65	44.74	0.00	1.40	0.00	3.50	3.00	0.03	0.00	0.00	0.2 vol% Spinel
VSL-08R1410-1, Rev. 0	LAWCrP7	6.10	10.00	6.98	0.14	0.63	0.07	5.50	0.09	4.30	2.93	5.40	2.51	0.73	46.71	0.00	1.40	0.00	3.50	3.00	0.03	0.00	0.00	0.2 vol% Spinel
VSL-06R6480-2, Rev. 0	LAWCrP4R	6.10	10.00	2.11	0.19	0.59	0.10	5.50	0.27	0.00	1.48	21.00	2.38	0.34	42.03	0.00	1.40	0.00	3.50	3.00	0.00	0.00	0.00	Few Cr-rich Spinels ~0.1 vol.%.

Source	Glass ID	Al_2O_3	B_2O_3	CaO	Cl	Cr_2O_3	F	Fe_2O_3	K_2O	Li_2O	MgO	Na_2O	P_2O_5	SO_3	SiO_2	SnO_2	TiO_2	V_2O_5	ZnO	ZrO_2	Others	ZCP, vol%	Cassiterite, vol%	Relevant phase description
VSL-04R4480-1, Rev. 0	LAWM8	9.00	13.00	6.43	0.80	0.32	0.30	0.00	0.00	2.08	5.00	5.00	0.50	1.00	44.49	0.00	3.00	0.00	5.00	4.00	0.08	0.00	0.00	Optical microscopy showed a light brown glass with secondary phases. SEM revealed much less than 0.1% volume of Ti, Cr, Fe, Ni, Zn Spinel at the Pt/Au crucible contact.
VSL-03R3460-2, Rev. 0	LAWB83	6.18	10.03	6.78	0.01	0.04	0.06	5.29	0.19	4.31	2.97	5.47	0.04	0.65	48.60	0.00	1.39	0.00	4.84	3.16	0.10	0.00	0.00	Amber brown glass. Augite formation along crucible contact interface.
VSL-06R6480-1, Rev. 0	BWV-G-32B	6.06	9.94	6.95	0.20	0.08	0.08	5.47	0.54	4.26	2.94	5.71	0.12	0.80	48.88	0.00	1.39	0.00	3.48	2.99	0.13	0.00	0.00	~0.4 vol.% of small augite crystals at crucible contact
VSL-03R3470-3, Rev. 0	LAWB83	6.18	10.03	6.78	0.01	0.04	0.06	5.29	0.19	4.31	2.97	5.47	0.04	0.65	48.60	0.00	1.39	0.00	4.84	3.16	0.10	0.00	0.00	Amber brown glass. Minor augite formation along crucible contact interface (- 0.2 vol.%).
VSL-04R4480-1, Rev. 0	LAWM7	5.43	6.94	10.00	0.02	0.01	0.01	8.00	0.00	2.58	5.00	5.00	0.01	1.00	52.00	0.00	3.00	0.00	1.00	0.00	0.00	0.00	0.00	Medium brown opaque glass. Appears to have cooled in a non-uniform manner. Secondary phase optically appears as fibrous or acicular bundles with a greenish, waxy look ~ 22 vol%. EDS analysis suggests augite as likely match, despite unusual morphology.
VSL-06R6480-1, Rev. 0	LAWE10H	6.07	9.95	6.96	0.20	0.08	0.08	5.48	0.54	4.26	2.94	5.72	0.12	0.80	48.92	0.00	1.39	0.00	3.48	2.99	0.02	0.00	0.00	~0.6 vol.% of large augite crystals
VSL-03R3460-1, Rev. 0	LAWB73	6.17	9.91	9.31	0.00	0.10	0.07	1.90	0.26	5.03	2.96	5.47	0.01	1.28	48.35	0.00	1.39	0.00	4.65	3.15	0.00	0.00	0.00	Lime green glass; contained very small amount (less than 0.1 vol%) of Augite - Aegirine crystals at the crucible interface after heat treatment at 850°C and about 2.6 vol% crystals after heat treatment at 700°C.
VSL-03R3460-1, Rev. 0	LAWB82	6.15	10.08	7.12	0.01	0.05	0.08	9.50	0.23	4.26	1.48	6.62	0.05	0.78	45.44	0.00	0.00	0.00	5.00	3.15	0.10	0.00	0.00	Amber brown glass. Significant Augite/Aegirine formation along crucible interface; some crystal clusters observed in the bulk glass along with a small amount of Spinel crystals.
VSL-08R1410-1, Rev. 0	LAWM2	3.50	6.00	10.00	0.80	0.32	0.30	8.00	0.00	4.50	5.00	5.00	0.50	1.00	47.00	0.00	3.00	0.00	5.00	0.00	0.08	0.00	0.00	18 vol% Augite-Aegirine forming along 0.1 vol% Spinel
VSL-08R1410-1, Rev. 0	LAWM7	5.43	6.94	10.00	0.02	0.01	0.01	8.00	0.00	2.58	5.00	5.00	0.01	1.00	52.00	0.00	3.00	0.00	1.00	0.00	0.00	0.00	0.00	22 vol% Augite-Aegirine forming along 0.1 vol% Spinel
VSL-03R3460-1, Rev. 0	LAWB67	6.17	9.91	5.17	0.00	0.10	0.07	5.28	0.26	4.29	2.96	5.47	3.01	1.28	48.35	0.00	1.39	0.00	3.15	3.15	0.00	0.00	0.00	Amber brown glass. Augite and Apatite were detected.
VSL-03R3460-1, Rev. 0	LAWB68	6.17	8.41	8.17	0.00	0.10	0.07	5.28	0.26	4.29	2.96	5.47	0.01	1.28	48.35	0.00	1.39	0.00	4.65	3.15	0.00	0.00	0.00	Amber brown glass. Augite observed near crucible interface and meniscus.
VSL-04R4480-1, Rev. 0	LAWM2	3.50	6.00	10.00	0.80	0.32	0.30	8.00	0.00	4.50	5.00	5.00	0.50	1.00	47.00	0.00	3.00	0.00	5.00	0.00	0.08	0.00	0.00	Optical microscopy observations showed light amber brown glass with secondary phases. SEM analysis revealed » 18 vol. % of what appears to be Augite crystals throughout the glass. Additionally about six Cr Fe Zn Mg Ti spinel crystals (<0.5%) were observed.
VSL-01R3560-2, Rev. 0	LAWB31	6.16	12.09	4.03	0.01	0.09	0.10	7.17	0.32	2.96	2.24	7.90	2.72	1.03	46.91	0.00	0.00	0.00	3.09	3.09	0.10	0.00	0.00	Positive identification of the particular phosphate could not be made. The Ca:P ratio from EDS and the weak XRD pattern

Source	Glass ID	Al_2O_3	B_2O_3	CaO	Cl	Cr_2O_3	F	Fe_2O_3	K_2O	Li_2O	MgO	Na_2O	P_2O_5	SO_3	SiO_2	SnO_2	TiO_2	V_2O_5	ZnO	ZrO_2	Others	ZCP, vol%	Cassiterite, vol%	Relevant phase description
																								obtained could agree either with $CaJ(PO_4)_2$ or Apatite $(Ca_5(PO_4)_3(OH,F,Cl))$.
VSL-01R3560-2, Rev. 0	LAWB32	6.16	15.09	4.03	0.01	0.09	0.10	4.17	0.32	2.96	2.24	7.90	2.72	1.03	46.91	0.00	0.00	0.00	3.09	3.09	0.10	0.00	0.00	Positive identification of the particular phosphate could not be made. The Ca:P ratio from EDS and the weak XRD pattern obtained could agree either with $Ca_3(PO_4)_2$ or Apatite $(Ca_5(PO_4)$-$(OH,F,Cl))$.
VSL-01R3560-2, Rev. 0	LAWB33	6.16	12.09	4.03	0.01	0.09	0.10	5.15	0.32	2.96	2.24	7.90	4.74	1.03	46.91	0.00	0.00	0.00	3.09	3.09	0.10	0.00	0.00	Ca $(PO_4)_2$ or apatite $(Ca_5(PO_4)_3(OH,F,Cl))$
VSL-01R3560-2, Rev. 0	LAWB34S	6.16	12.09	6.05	0.01	0.09	0.10	5.15	0.32	2.96	2.24	7.90	2.72	2.50	46.91	0.00	0.00	0.00	3.09	3.09	0.10	0.00	0.00	Positive identification of the particular phosphate could not be made. The Ca:P ratio from EDS and the weak XRD pattern obtained could agree either with Ca $(PO_4)_2$ or Apatite $(Ca_5(PO_4)_3(OH,F,Cl))$.
VSL-01R3560-2, Rev. 0	LAWB35S	6.16	12.09	4.03	0.01	0.09	0.10	5.15	0.32	2.96	4.26	7.90	2.72	2.50	46.91	0.00	0.00	0.00	3.09	3.09	0.10	0.00	0.00	Positive identification of the particular phosphate could not be made. The Ca:P ratio from EDS and the weak XRD pattern obtained could agree either with Ca $(PO_4)_2$ or Apatite $(Ca_5(PO_4)_3(OH,F,Cl))$.
VSL-01R3560-2, Rev. 0	LAWB36S	6.16	12.09	4.03	0.01	0.09	0.10	5.15	0.32	3.85	2.24	7.90	4.74	2.50	43.33	0.00	0.00	2.69	3.09	3.09	0.10	0.00	0.00	Positive identification of the particular phosphate could not be made. The Ca:P ratio from EDS and the weak XRD pattern obtained could agree either with Ca $(PO_4)_2$ or Apatite $(Ca_5(PO_4)_3(OH,F,Cl))$.
VSL-01R3560-2, Rev. 0	LAWB37	6.16	12.09	4.70	0.01	0.09	0.10	5.15	0.32	2.96	2.91	7.90	3.40	1.03	46.91	0.00	0.00	0.00	3.09	3.09	0.10	0.00	0.00	Positive identification of the particular phosphate could not be made. The Ca:P ratio from EDS and the weak XRD pattern obtained could agree either with Ca $(PO_4)_2$ or Apatite $(Ca_5(PO_4)_3(OH,F,Cl))$.
VSL-01R3560-2, Rev. 0	LAWB38	6.16	12.09	4.75	0.01	0.09	0.10	5.15	0.32	3.81	2.24	7.90	3.17	1.03	46.91	0.00	0.00	0.00	3.09	3.09	0.10	0.00	0.00	Positive identification of the particular phosphate could not be made. The Ca:P ratio from EDS and the weak XRD pattern obtained could agree either with Ca $(PO_4)_2$ or Apatite $(Ca_5(PO_4)_3(OH,F,Cl))$.
VSL-01R3560-2, Rev. 0	LAWB43	6.07	11.92	4.63	0.01	0.09	0.10	10.33	0.31	0.00	2.87	7.79	0.04	4.44	46.23	0.00	0.00	0.00	4.02	3.05	0.00	0.00	0.00	Positive identification of the particular phosphate could not be made. The Ca:P ratio from EDS and the weak XRD pattern obtained could agree either with Ca $(PO_4)_2$ or Apatite $(Ca_5(PO_4)_3(OH,F,Cl))$.
EWG-RPT-012-Rev 0/PNNL-26630	New-OL-57284	3.50	13.75	2.98	0.47	0.31	0.71	0.00	1.50	0.00	0.00	14.01	1.51	0.10	47.00	0.00	0.00	4.00	5.00	5.16	0.00	0.00	0.00	Fluorapatite
VSL-01R3560-2, Rev. 0	LAWB52S	6.09	10.02	6.74	0.01	0.11	0.06	6.74	0.23	5.85	3.00	5.00	0.01	1.50	48.88	0.00	0.00	0.00	3.18	3.18	0.10	0.00	0.00	~ 0.2 vol. % of a Ca-Fe-Mg Silicate

Source	Glass ID	Al_2O_3	B_2O_3	CaO	Cl	Cr_2O_3	F	Fe_2O_3	K_2O	Li_2O	MgO	Na_2O	P_2O_5	SO_3	SiO_2	SnO_2	TiO_2	V_2O_5	ZnO	ZrO_2	Others	ZCP, vol%	Cassiterite, vol%	Relevant phase description
VSL-01R3560-2, Rev. 0	LAWB53S	6.09	10.02	6.74	0.01	0.11	0.06	5.34	0.23	5.85	3.00	5.00	0.01	1.50	48.88	0.00	1.40	0.00	3.18	3.18	0.10	0.00	0.00	~ 0.3 vol. % of a Ca-Fe-Mg Silicate
VSL-01R3560-2, Rev. 0	LAWC4C	0.00	0.00	0.00	0.00	0.00	0.00	0.00	0.00	0.00	0.00	0.00	0.00	0.00	0.00	0.00	0.00	0.00	0.00	0.00	0.00	0.00	0.00	~ 0.3 vol. % of a Ca-Fe-Mg Silicate
EWG-RPT-021 Rev. 1/PNNL-28838 Rev 1	LP2-IL-11	9.00	8.00	3.08	0.35	0.38	0.53	1.00	2.00	0.00	0.30	22.00	1.13	0.20	38.85	2.50	0.00	2.00	3.20	5.50	0.00	0.00	0.00	Nasicon
EWG-RPT-021 Rev. 1/PNNL-28838 Rev 1	LP2-OL-04-1	10.50	6.00	7.84	0.06	0.60	0.10	1.50	5.75	0.00	1.35	21.00	0.20	0.10	34.90	0.00	0.00	0.00	3.60	6.50	0.00	0.00	0.00	Nasicon
EWG-RPT-021 Rev. 1/PNNL-28838 Rev 1	LP2-OL-22	7.00	6.00	11.00	0.06	0.30	0.10	1.50	0.00	0.00	0.00	21.00	0.20	0.10	36.74	3.50	0.00	4.00	2.00	6.50	0.00	0.00	0.00	Nasicon
PNNL-29847, Rev. 0.0	LAWPH3-09	7.82	8.60	9.23	0.26	0.31	0.39	0.84	5.50	0.00	0.21	21.29	0.84	0.96	35.51	0.24	0.00	0.64	2.29	5.09	0.00	0.00	0.00	nasicon
PNNL-29847, Rev. 0.0	LAWPH3-15	7.30	9.43	8.67	0.11	0.43	0.16	1.25	4.14	0.00	0.01	21.71	0.34	0.39	35.34	1.69	0.00	1.60	2.94	4.50	0.00	0.00	0.00	nasicon
PNNL-29847, Rev. 0.0	LAWPH3-16	6.11	6.92	7.42	0.19	0.43	0.29	0.33	4.08	0.00	0.79	23.20	0.63	0.17	36.56	0.12	0.00	3.62	3.43	5.71	0.00	0.00	0.00	Nasicon - 0.54; Grossular - 1.46; Combeite - 1.38
EWG-RPT-012-Rev 0/PNNL-26630	New-OL-15493	3.50	6.00	12.24	0.06	0.04	0.09	0.00	1.50	0.00	3.50	25.51	0.20	0.10	39.25	3.00	0.00	4.00	1.00	0.00	0.00	0.00	0.00	Combeite High
VSL-06R6900-1, Rev. 0	LAWA195	10.85	7.76	6.48	0.71	0.53	0.00	0.91	0.56	0.00	0.91	25.00	0.00	0.75	35.32	1.00	0.00	0.94	2.35	5.95	0.00	0.00	0.00	~ 3.6 vol.% of a Cr-Sodalite and a Sn-Sodium Zirconium Silicate
EWG-RPT-021 Rev. 1/PNNL-28838 Rev 1	LP2-OL-24	12.50	6.00	7.25	0.06	0.30	0.10	1.50	0.00	0.00	1.35	25.20	0.20	0.10	34.90	0.00	0.00	4.00	3.60	2.95	0.00	0.00	0.00	Hauyne - 1.22; Lazurite 1C - 0.033; Aluminum Phosphate - 2.22
EWG-RPT-012-Rev 1/PNNL-26630	LAW-ORP-LD1(M)	15.53	12.04	8.01	0.33	0.50	0.17	1.00	0.16	0.00	1.00	20.98	0.29	1.06	37.14	0.00	0.00	1.00	3.00	3.00	0.18	0.00	0.00	Hauyne, Nosean, $FeNi_2O_4$
EWG-RPT-021 Rev. 1/PNNL-28838 Rev 1	LP2-OL-05	12.50	6.00	11.00	0.47	0.30	0.71	1.50	0.00	0.00	0.00	21.00	1.52	0.98	39.08	0.00	0.00	0.00	2.00	2.95	0.00	0.00	0.00	Lazurite 1C
EWG-RPT-021 Rev. 1/PNNL-28838 Rev 1	LP2-OL-10 MOD	12.52	6.01	11.02	0.47	0.30	0.71	1.50	0.00	0.00	0.00	21.04	1.52	0.80	39.15	0.00	0.00	0.00	2.00	2.96	0.00	0.00	0.00	Lazurite 1C
EWG-RPT-021 Rev. 1/PNNL-28838 Rev 1	LP2-OL-20	6.00	6.00	8.05	0.06	0.30	0.10	0.00	0.00	0.00	0.00	26.00	0.20	0.10	46.64	0.00	0.00	0.00	3.60	2.95	0.00	0.00	0.00	Mullite (Al, Si, O) - 0.544; Lazurite - 0.224; Zircon - 0.131; Zirconium Aluminum - 0.292; Silicon - 1.18
VSL-06R6480-2, Rev. 0	LAWCrP3R	6.10	10.00	2.76	0.12	0.33	0.11	5.50	0.13	0.00	1.48	19.34	2.38	0.39	43.45	0.00	1.40	0.00	3.50	3.00	0.00	0.00	0.00	NaCaPhosphate crystals ~0.2 vol.%
EWG-RPT-021 Rev. 1/PNNL-28838 Rev 1	LP2-OL-13	6.00	6.00	11.00	0.47	0.30	0.71	0.00	5.75	0.00	0.00	22.21	1.52	0.10	35.41	0.00	0.00	4.00	3.60	2.95	0.00	0.00	0.00	Nasicon - 1.72; Quartz low - 0.261
EWG-RPT-021 Rev.	LP2-OL-03 MOD2	10.74	6.11	10.91	0.06	0.61	0.10	0.00	0.00	0.00	1.37	26.46	0.21	0.75	35.52	2.78	0.00	0.00	2.04	2.34	0.00	0.00	0.00	Nasicon - 2.02; Combeite high - 5.29; Lazurite 4A - 4.25; Tin Fluoride - 0.11

Source	Glass ID	Al_2O_3	B_2O_3	CaO	Cl	Cr_2O_3	F	Fe_2O_3	K_2O	Li_2O	MgO	Na_2O	P_2O_5	SO_3	SiO_2	SnO_2	TiO_2	V_2O_5	ZnO	ZrO_2	Others	ZCP, vol%	Cassiterite, vol%	Relevant phase description
1/PNNL-28838 Rev 1																								
EWG-RPT-021 Rev. 1/PNNL-28838 Rev 1	LP2-OL-08 MOD	6.12	6.12	10.88	0.06	0.61	0.10	1.53	0.00	0.00	0.00	26.52	0.21	0.82	35.60	0.00	0.00	4.08	2.04	5.31	0.00	0.00	0.00	Nasicon - 6.56; Combeite high - 10.9
VSL-07R1130-1, Rev. 0	ORPLE8	7.60	9.45	10.05	0.02	0.10	0.20	1.05	0.55	3.00	1.05	16.00	0.12	1.25	41.41	0.00	0.00	1.25	3.22	3.54	0.15	0.00	0.00	Clear glass. ~ 0.2 vol% Sodalite (Na-Al silicate sulfate) at platinum crucible interface.
VSL-07R1130-1, Rev. 0	ORPLE9	7.60	9.05	9.65	0.02	0.50	0.20	1.05	0.55	3.00	1.05	16.00	0.12	1.25	41.41	0.00	0.00	1.25	3.22	3.94	0.15	0.00	0.00	Clear glass. ~ 0.1 vol% Sodalite (Na-Al silicate sulfate) at platinum crucible interface.
VSL-07R1130-1, Rev. 0	ORPLE10	8.80	10.46	9.25	0.02	0.10	0.20	0.24	0.55	3.00	1.05	16.00	0.12	1.25	40.81	0.00	0.00	1.25	3.22	3.54	0.15	0.00	0.00	Clear glass. ~ 0.2 vol% Sodalite (Na-Al silicate sulfate) at platinum crucible interface.
VSL-09R1510-2, Rev. 0	ORPLD5	10.18	10.03	8.03	0.33	0.50	0.17	0.30	0.16	0.00	1.00	21.00	0.29	0.96	37.92	0.00	0.00	2.00	3.01	4.05	0.05	0.00	0.00	Mostly clear glass ~0.3 vol% Large sodalite (Na,Ca,Al Silicate with S &Cr)
VSL-09R1510-2, Rev. 0	ORPLD6	10.12	9.87	7.91	0.35	0.50	0.18	0.30	0.17	0.00	0.99	22.00	0.30	1.01	37.33	0.00	0.00	1.97	2.97	3.99	0.05	0.00	0.00	Mostly clear glass ~0.3 vol% Large Sodalite (Na,Ca,Al Silicate with S &Cr)
VSL-09R1510-2, Rev. 0	ORPLD7	10.08	9.87	7.91	0.35	0.50	0.18	0.30	0.17	0.00	0.99	22.00	0.30	1.01	37.33	1.00	0.00	1.00	2.97	3.99	0.05	0.00	0.00	Mostly clear glass ~0.2 vol% Large Sodalite (Na,Ca,Al silicate with S &Cr)
VSL-09R1510-2, Rev. 0	ORPLD8	10.03	9.50	7.35	0.36	0.50	0.19	0.29	0.18	0.00	0.97	23.00	0.31	1.06	36.74	1.00	0.00	1.46	2.99	4.02	0.06	0.00	0.00	Mostly clear glass ~0.3 vol% Large Sodalite (Na,Ca,Al silicate with S &Cr)
VSL-10R1790-1, Rev. 0	ORPLA27	10.33	12.20	6.18	0.64	0.50	0.00	0.86	0.51	0.00	4.00	23.00	0.00	0.95	33.23	0.96	0.00	0.93	2.86	2.86	0.00	0.00	0.00	~2.7 vol% large Sodalite crystals with Mg, Sn, Zn, & Fe, Sodalite formula $(Na, Ca)_8(AlSiO_4)_6(SO_4)_2$
VSL-10R1790-1, Rev. 0	ORPLA28	10.10	11.64	5.90	0.64	0.48	0.00	0.82	0.51	0.00	7.00	23.00	0.00	0.95	31.71	0.91	0.00	0.89	2.72	2.72	0.00	0.00	0.00	~3.8 vol% large Sodalite crystals with Mg, Sn, Zn, & Fe
VSL-10R1790-1, Rev. 0	ORPLA29	9.87	11.08	5.62	0.64	0.45	0.00	0.78	0.51	0.00	10.00	23.00	0.00	0.95	30.19	0.87	0.00	0.84	2.59	2.59	0.00	0.00	0.00	~2.5 vol% large Sodalite crystals with Mg, Sn, Zn, & Fe
VSL-10R1790-1, Rev. 0	ORPLA30	9.56	11.73	5.43	0.64	0.52	0.00	0.90	0.51	0.00	4.00	23.00	0.00	0.95	34.80	1.00	0.00	0.97	2.99	2.99	0.00	0.00	0.00	~0.3 vol% small Sodalite crystals with Mg, Sn, Zn, & Fe
VSL-10R1790-1, Rev. 0	ORPLA31	8.65	10.68	4.39	0.64	0.52	0.00	0.90	0.51	0.00	7.00	23.00	0.00	0.95	34.80	1.00	0.00	0.97	2.99	2.99	0.00	0.00	0.00	~0.4 vol% Sodalite crystals with Mg, Sn, Zn, & Fe
VSL-10R1790-1, Rev. 0	ORPLA32	7.73	9.64	3.34	0.64	0.52	0.00	0.90	0.51	0.00	10.00	23.00	0.00	0.95	34.80	1.00	0.00	0.97	2.99	2.99	0.00	0.00	0.00	~0.3 vol% Sodalite crystals with Mg, Sn, Zn, & Fe
VSL-06R6900-1, Rev. 0	LAWA191	12.15	11.29	7.49	0.65	0.52	0.00	0.91	0.51	0.00	0.91	23.00	0.00	0.75	34.86	0.00	0.00	0.98	3.00	3.00	0.00	0.00	0.00	~1.5 vol.% Sodalite crystals along crucible contact and some Cr-Zn-Al-Mg Spinel
VSL-07R7480-1, Rev. 0	FWV-G-63B	6.01	9.86	6.30	0.20	0.08	0.19	5.42	0.54	3.17	1.49	13.53	0.12	0.59	44.69	0.00	1.38	0.00	3.46	2.96	0.02	0.00	0.00	Mostly clear glass; a few Fe_2O_3 crystals observed, estimated < 0.1 vol.%
EWG-RPT-012-Rev 0/PNNL-26630	New-OL-62909Mod	12.35	8.90	12.24	0.47	0.31	0.71	0.00	0.00	2.50	3.50	13.00	1.51	0.10	33.50	4.41	0.00	0.00	1.00	5.50	0.00	1.4	2.9	Cassiterite - 2.9; Baddeleyite/ZrO_2 - 1.4; SiO_2 and Wadalite - 1.7
VSL-07R1130-1, Rev. 0	ORPLA15	9.46	8.65	3.34	0.68	0.50	0.00	0.93	0.54	0.00	0.93	24.00	0.00	0.18	39.50	2.75	0.00	0.00	2.45	5.95	0.15	0.25	0.00	0.2 – 0.3 vol% of Na-Zr-silicate crystals + Sn crystal
VSL-09R1510-2, Rev. 0	ORPLA21	6.91	8.64	3.28	0.71	0.50	0.00	0.29	0.56	0.00	0.91	25.00	0.00	0.19	41.72	2.71	0.00	0.00	2.71	5.88	0.00	0.8	0.00	~0.8 vol% large Na-Zr silicate +Sn crystal

Source	Glass ID	Al_2O_3	B_2O_3	CaO	Cl	Cr_2O_3	F	Fe_2O_3	K_2O	Li_2O	MgO	Na_2O	P_2O_5	SO_3	SiO_2	SnO_2	TiO_2	V_2O_5	ZnO	ZrO_2	Others	ZCP, vol%	Cassiterite, vol%	Relevant phase description
VSL-09R1510-2, Rev. 0	ORPLA22	9.46	8.80	3.55	0.68	0.50	0.00	0.00	0.54	0.00	0.00	24.00	0.00	0.18	40.29	3.00	0.00	0.00	3.00	6.00	0.00	0.2	0.2	~0.2 vol% large Na-Zr silicate +Sn crystal
VSL-09R1510-2, Rev. 0	ORPLA23	9.46	8.80	3.55	0.68	0.50	0.00	0.00	0.54	0.00	0.00	24.00	0.00	0.18	40.29	5.00	0.00	0.00	3.00	4.00	0.00	0.05	0.05	Mostly clear glass. ~0.1 vol% large Na-Zr silicate +Sn crystal
VSL-09R1510-2, Rev. 0	ORPLA24	9.34	8.55	3.52	0.71	0.50	0.00	0.00	0.56	0.00	0.00	25.00	0.00	0.19	39.70	3.00	0.00	0.00	2.94	6.00	0.00	0.05	0.05	Mostly clear glass. ~0.1 vol% Na-Zr silicate +Sn crystal
VSL-10R1790-1, Rev. 0	ORPLG13	6.54	8.28	2.62	0.22	0.57	0.09	0.28	5.47	0.00	4.04	20.00	0.14	0.39	39.76	2.76	0.00	0.00	3.31	5.52	0.02	0.4	0.4	Opaque green glass ~0.4 vol% large NaZr silicate with Sn and a few Cr-rich crystals
VSL-10R1790-1, Rev. 0	ORPLG14	6.53	8.20	2.60	0.23	0.57	0.09	0.27	5.61	0.00	4.00	20.50	0.14	0.40	39.38	2.73	0.00	0.00	3.28	5.47	0.02	0.4	0.00	Opaque green glass ~0.4 vol% large NaZr silicate with Sn and a few Cr-rich crystals
VSL-10R1790-1, Rev. 0	ORPLG15	6.51	8.12	2.57	0.23	0.57	0.09	0.27	5.75	0.00	3.96	21.00	0.14	0.41	39.00	2.71	0.00	0.00	3.25	5.41	0.02	0.4	0.00	Opaque green glass ~0.4 vol% large NaZr silicate with Sn and a few Cr-rich crystals
VSL-10R1790-1, Rev. 0	ORPLG27	6.03	7.92	2.69	0.23	0.59	0.09	0.28	5.75	0.00	0.44	21.00	0.14	0.41	42.10	3.19	0.00	0.00	2.69	6.44	0.02	0.5	0.00	Mostly clear glass ~0.5 vol% several NaZr silicate crystals with Sn
VSL-07R1130-1, Rev. 0	ORPLC1	9.50	6.06	3.00	0.66	0.50	0.01	1.00	0.58	0.00	1.00	25.00	0.20	0.55	38.32	2.00	1.00	3.00	3.00	4.50	0.15	0.00	0.00	~ 0.1 to 0.3 vol% Sodalite (Na,Al-silicate sulfate) and Cr crystals
VSL-01R3560-2, Rev. 0	LAWB44	6.07	11.92	4.63	0.01	0.09	0.10	13.20	0.31	0.00	0.00	7.79	0.04	4.44	46.23	0.00	0.00	0.00	4.02	3.05	0.00	0.00	0.00	Presence of spinel, Ca-Mg-Fe silicate (Augite) and Sircon. In total ~12.3 vol%
VSL-01R3560-2, Rev. 0	LAWB51S	6.09	12.54	6.74	0.01	0.11	0.06	5.34	0.23	4.73	3.00	5.00	0.01	1.50	48.88	0.00	0.00	0.00	3.18	3.18	0.10	0.00	0.00	~0.2wt% Ca-Mg-Fe silicate (Augite)
VSL-01R3560-2, Rev. 0	LAWB34	6.16	12.09	6.05	0.01	0.09	0.10	5.15	0.32	2.96	2.24	7.90	2.72	1.03	46.91	0.00	0.00	0.00	3.09	3.09	0.10	0.00	0.00	Trace amount of crystals
EWG-RPT-036, Rev. 0	LAWALG-01	3.59	8.50	12.36	0.04	0.08	0.43	0.12	0.23	2.75	0.18	14.90	0.56	1.45	48.70	0.00	0.07	3.99	0.00	2.04	0.00	0.85	0.00	maximum total 2.8 vol% of Moganite, Parakeldyshite, Tridymite2H and $K_2Ca_2Si_2O_7$
EWG-RPT-036, Rev. 0	LAWALG-02	5.44	12.97	9.82	0.07	0.05	0.08	0.13	0.12	0.00	0.15	19.59	0.31	1.32	42.01	0.00	0.13	3.99	0.00	3.81	0.00	0.00	0.00	amorphous
EWG-RPT-036, Rev. 0	LAWALG-03	5.50	6.95	8.38	0.05	0.08	0.28	0.12	0.10	0.00	0.13	22.29	3.11	1.01	38.61	4.39	0.12	2.44	0.00	6.43	0.00	0.92	0.00	maximum total 3.9 vol% of Sodium tetrasilicate, Nasicon, Nepheline and $K_2Ca_2Si_2O_7$
EWG-RPT-036, Rev. 0	LAWALG-04	8.67	8.71	7.70	0.10	0.03	0.03	0.10	0.36	0.00	0.12	23.33	0.08	0.11	39.84	4.39	0.10	0.00	0.00	6.33	0.00	10.63	0.00	maximum total 10.7 vol% of Parakeldyshite, Na_2CaSiO_4 and $Na_4Zr_2(SiO_4)_3$
EWG-RPT-036, Rev. 0	LAWALG-05	3.59	13.60	12.42	0.06	0.05	0.55	0.13	0.15	1.68	0.18	9.08	0.26	1.41	50.70	0.00	0.08	4.00	0.00	2.04	0.00	0.00	0.00	0.3 vol% of Tridymite2H
EWG-RPT-036, Rev. 0	LAWALG-06	6.31	11.06	9.05	0.10	0.07	0.06	0.13	0.14	0.00	0.14	20.99	0.22	1.20	39.31	1.40	0.14	3.98	0.00	5.67	0.00	0.00	0.00	Amorphous
EWG-RPT-036, Rev. 0	LAWALG-07	5.78	8.29	8.07	0.03	0.06	0.25	0.10	0.09	0.00	0.12	22.82	1.74	0.98	40.35	4.39	0.09	0.96	0.00	5.87	0.00	0.00	0.00	crystals not detected by XRD
EWG-RPT-036, Rev. 0	LAWALG-08	3.60	13.63	12.44	0.04	0.02	0.07	0.13	0.09	1.68	0.18	9.89	0.16	1.44	50.48	0.00	0.09	4.01	0.00	2.03	0.00	0.00	0.00	Amorphous
EWG-RPT-036, Rev. 0	LAWALG-09	9.03	8.47	8.10	0.05	0.19	0.30	0.14	0.21	0.00	0.12	22.71	3.52	0.29	35.74	4.39	0.16	0.00	0.00	6.57	0.00	19.44	0.00	maximum total 19.4 vol% of $Na_4Zr_2(SiO_4)_3$ and $K_2Ca_2Si_2O_7$
EWG-RPT-036, Rev. 0	LAWALG-10	8.81	8.67	7.74	0.04	0.16	0.05	0.13	0.07	0.00	0.12	23.38	0.31	0.16	39.91	4.39	0.14	0.00	0.00	5.90	0.01	0.00	0.00	crystals not detected by XRD
EWG-RPT-036, Rev. 0	LAWALG-11	8.74	6.14	7.48	0.15	0.04	0.08	0.14	3.06	0.00	0.11	22.00	0.13	0.48	36.40	4.40	0.18	0.00	3.86	6.59	0.01	15.89	0.00	maximum total 45.1 vol% of combeite, Nasicon, Nepheline, Moganite, $K_2Ca_2Si_2O_7$, $Na_2Si_2O_5$, Na_2CaSiO_4, Na_2SiO_3 and Zircon
EWG-RPT-036, Rev. 0	LAWALG-12	3.60	12.93	11.13	0.03	0.05	1.01	0.12	0.08	0.00	0.16	17.28	2.18	1.39	43.93	0.00	0.08	3.99	0.00	2.05	0.02	0.00	0.00	maximum total 6.2 vol% of $Ca_4Na_6(SO_4)_6F_2$, Na_2SiO_3,

Source	Glass ID	Al_2O_3	B_2O_3	CaO	Cl	Cr_2O_3	F	Fe_2O_3	K_2O	Li_2O	MgO	Na_2O	P_2O_5	SO_3	SiO_2	SnO_2	TiO_2	V_2O_5	ZnO	ZrO_2	Others	ZCP, vol%	Cassiterite, vol%	Relevant phase description
																								$K_2Ca_2Si_2O_7$ and Al Mg Orthosilicate
EWG-RPT-036, Rev. 0	LAWALG-13	3.61	13.59	12.41	0.04	0.03	0.30	0.12	0.07	1.14	0.18	13.47	0.93	1.46	46.54	0.00	0.06	4.00	0.00	2.04	0.02	0.00	0.00	1.7 vol% of $Ca_4Na_6(SO_4)_6F_2$
EWG-RPT-036, Rev. 0	LAWALG-14	3.60	13.59	12.24	0.07	0.05	0.16	0.13	0.11	0.82	0.18	15.19	0.16	1.44	46.13	0.00	0.09	4.00	0.00	2.04	0.01	0.00	0.00	amorphous
EWG-RPT-036, Rev. 0	LAWALG-15	8.90	8.73	7.75	0.08	0.06	0.04	0.15	0.16	0.00	0.12	23.31	0.32	0.84	39.15	4.40	0.20	0.00	0.00	5.79	0.01	0.00	0.00	maximum 2.5 vol% of Sodium tetrasilicate
EWG-RPT-036, Rev. 0	LAWALG-16	8.84	8.28	7.76	0.06	0.58	0.05	0.13	0.07	0.00	0.12	23.34	0.54	0.14	39.85	4.39	0.15	0.00	0.00	5.70	0.01	5.37	0.00	maximum total 5.4 vol% of Parakeldyshite and $Na_4Zr_2(SiO_4)_3$
EWG-RPT-036, Rev. 0	LAWALG-17	8.89	8.32	7.74	0.44	0.09	0.24	0.15	0.57	0.00	0.12	23.08	0.16	0.66	38.63	4.39	0.19	0.00	0.00	6.34	0.01	2.16	0.00	total 5.3 vol% of Sodium tetrasilicate, Na_2SiO_5-gamma, Parakeldyshite, Zircon, Tridymite2H and Nepheline

Appendix B – Images of As-Melted LIC Glasses

This appendix shows images of the 10 low-activity waste isothermal crystallization (LIC) glasses studied during this effort after their final melts.

Figure B.1. LIC-01 final melt.

Figure B.2. LIC-02-MOD2 final melt.

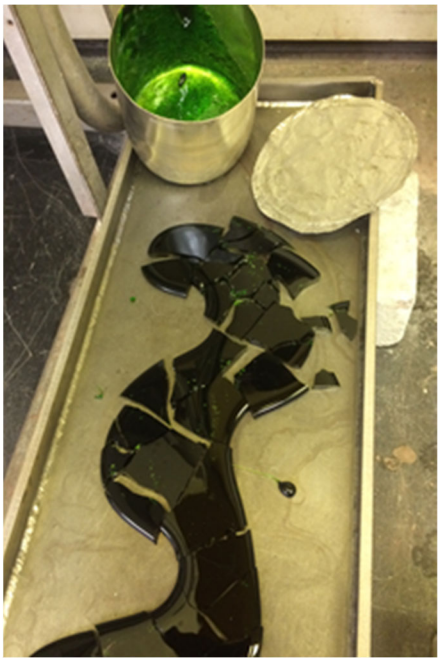

Figure B.3. LIC-03 final melt.

Figure B.4. LIC-04-MOD1 final melt.

Figure B.5. LIC-05 final melt.

Figure B.6. LIC-06 final melt.

Figure B.7. LIC-07 final melt.

Figure B.8. LIC-08 final melt.

Figure B.9. LIC-09-MOD3 final melt.

Figure B.10. LIC-10 final melt.

Appendix C – Images of LIC Glasses after Heat Treatment

This appendix contains images of the glasses in this study after isothermal heat treatment at various temperatures for the indicated times.

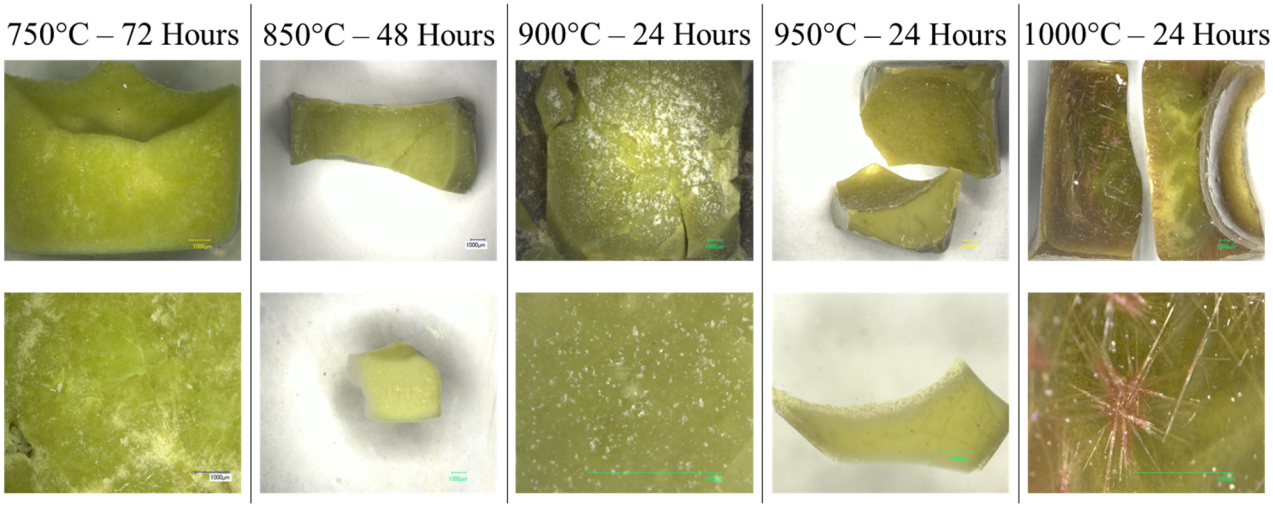

Figure C.1. Optical images of heat-treated of LIC-01 glasses.

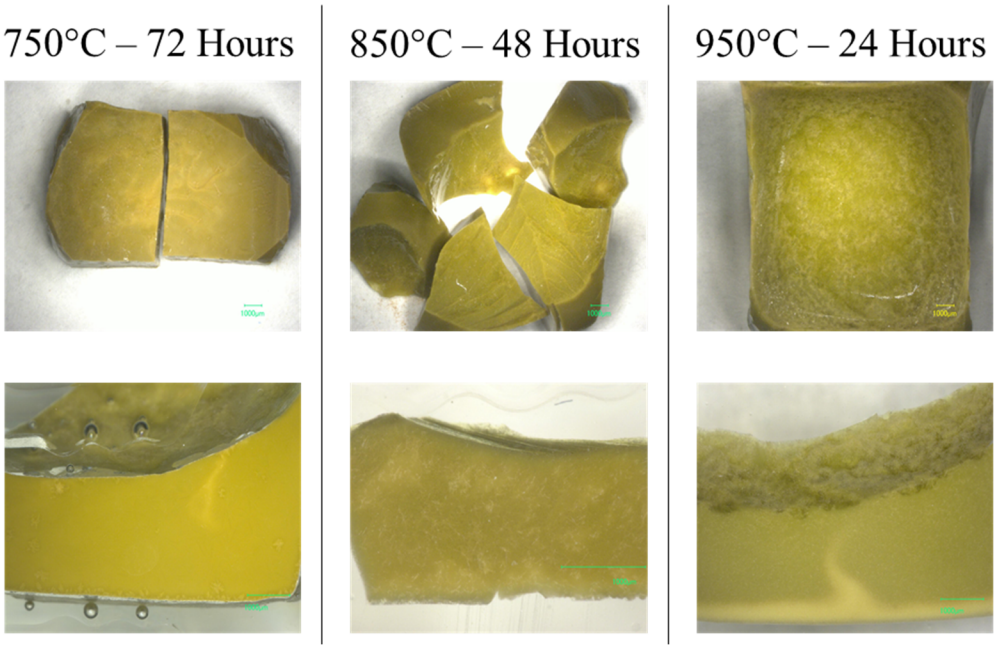

Figure C.2. Optical images of heat-treated LIC-02 second modification glasses

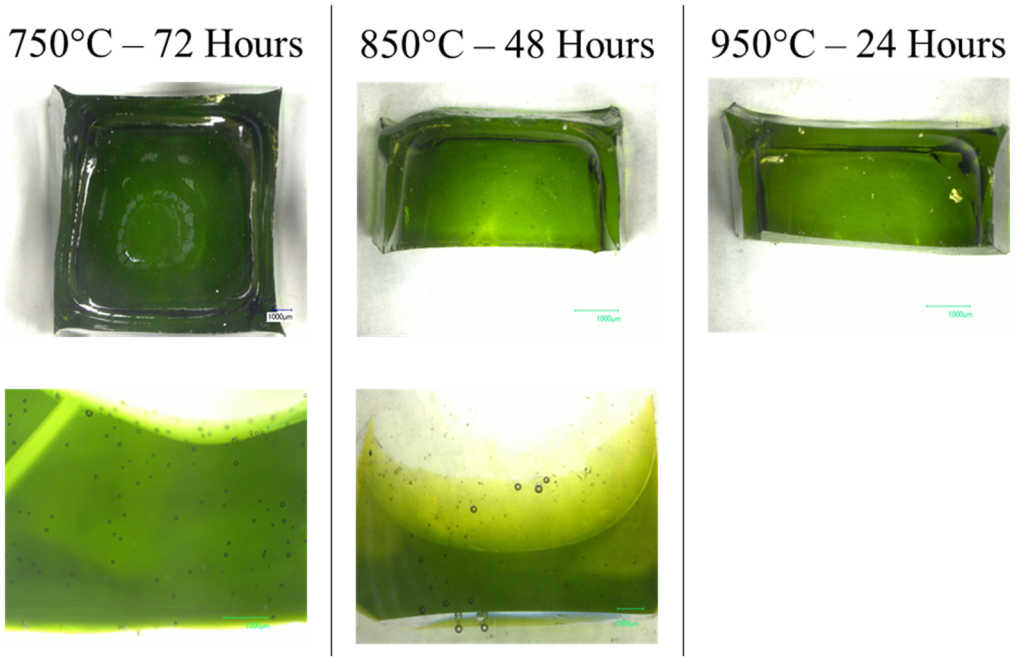

Figure C.3. Optical images of heat-treated LIC-03 glasses.

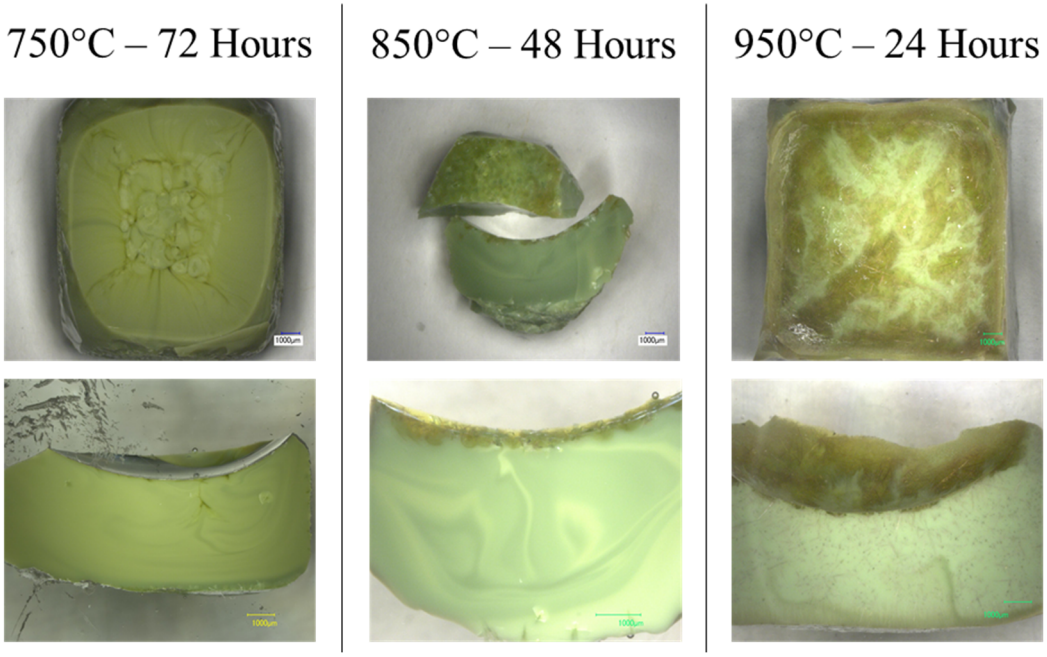

Figure C.4. Optical images of heat-treated LIC-04 first modification glasses.

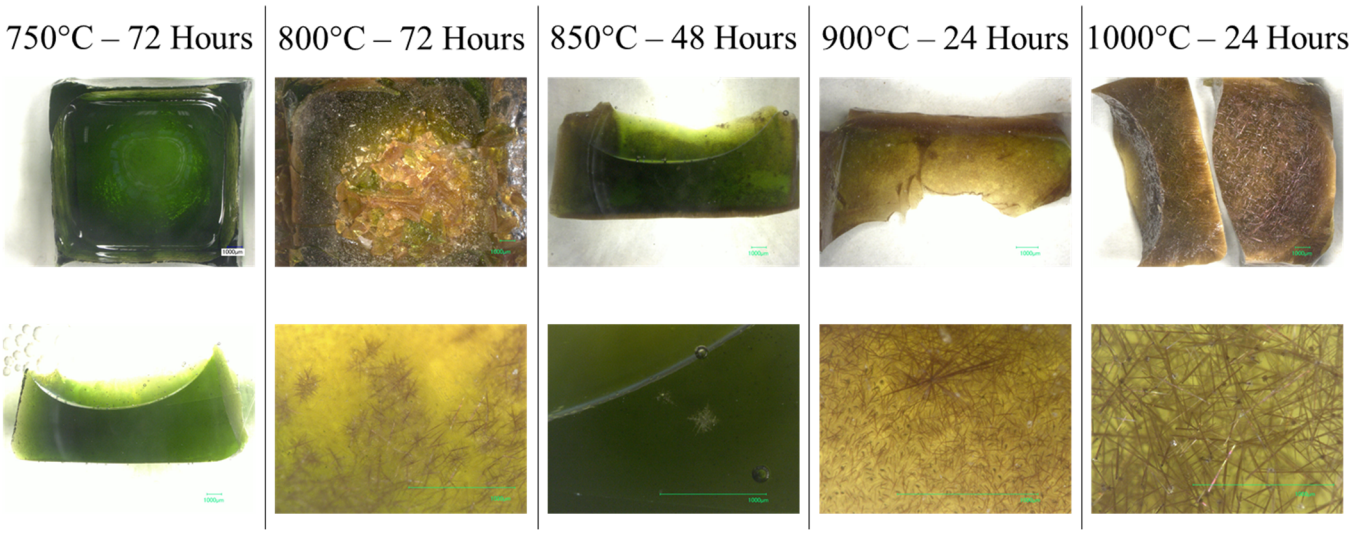

Figure C.5. Optical images of heat-treated LIC-05 glasses.

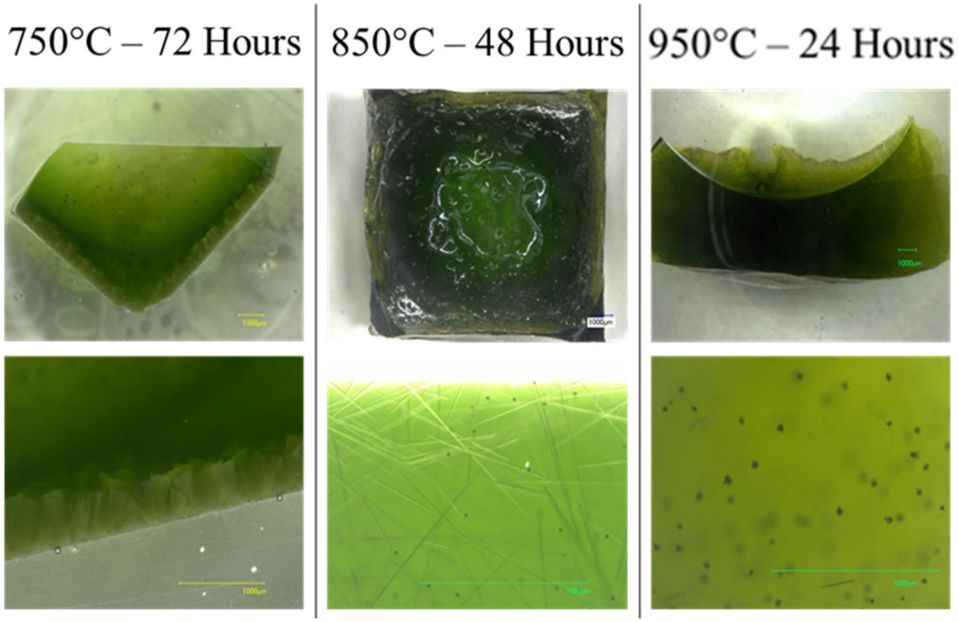

Figure C.6. Optical images of heat-treated LIC-06 glasses.

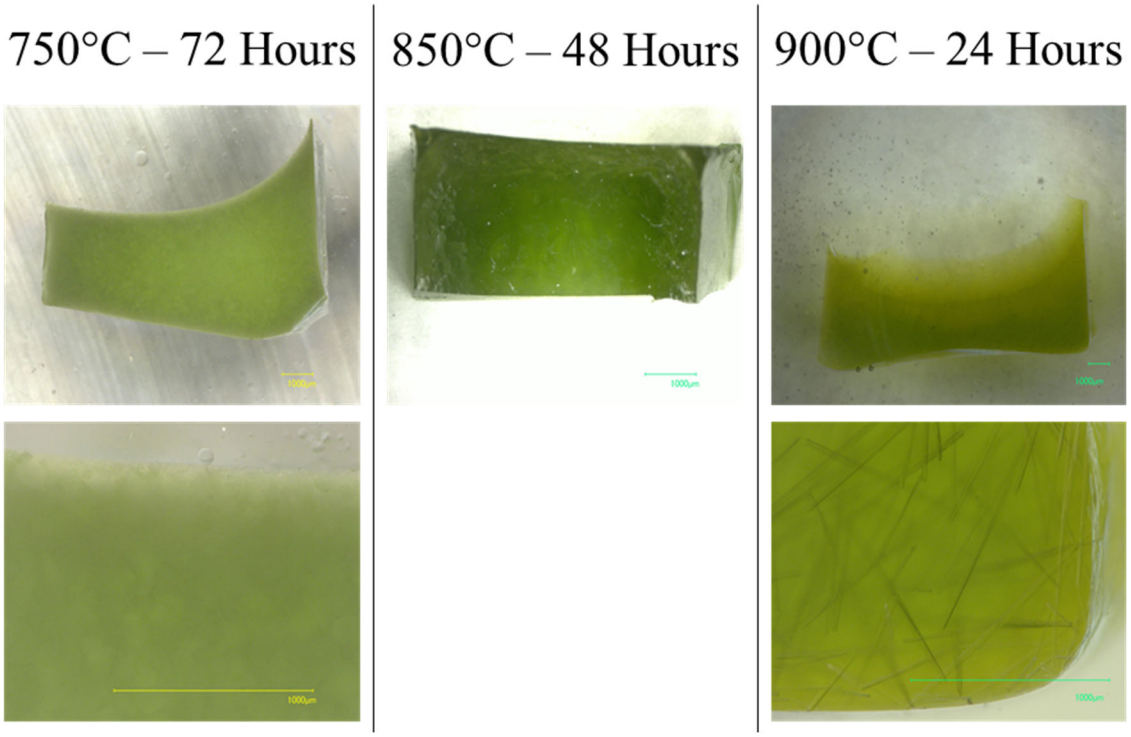

Figure C.7. Optical images of heat-treated LIC-07 glasses.

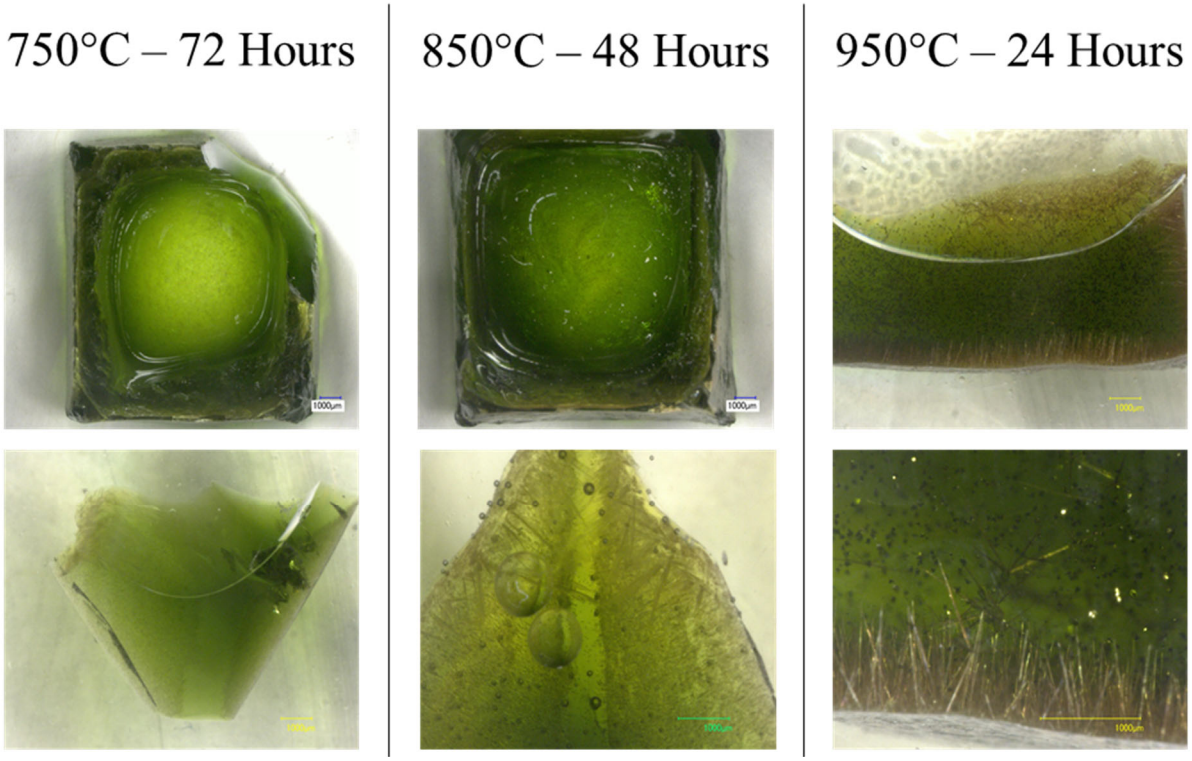

Figure C.8. Optical images of heat-treated LIC-08 glasses.

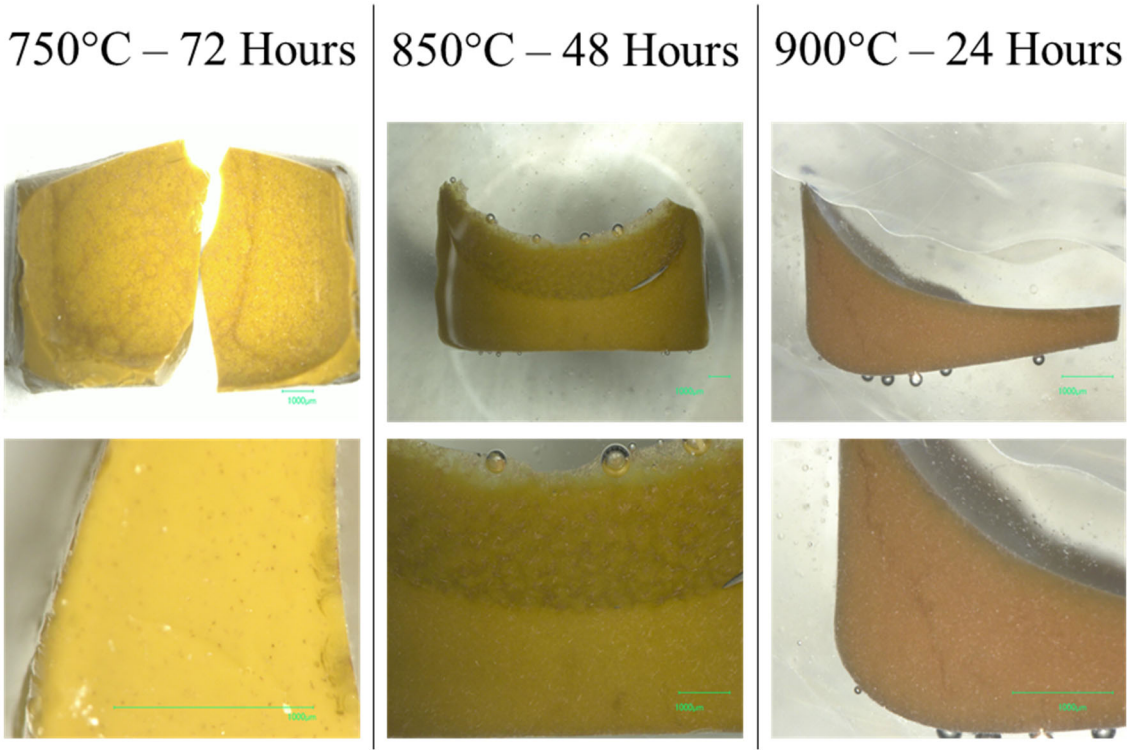

Figure C.9. Optical images of heat-treated LIC-09 third modification glasses.

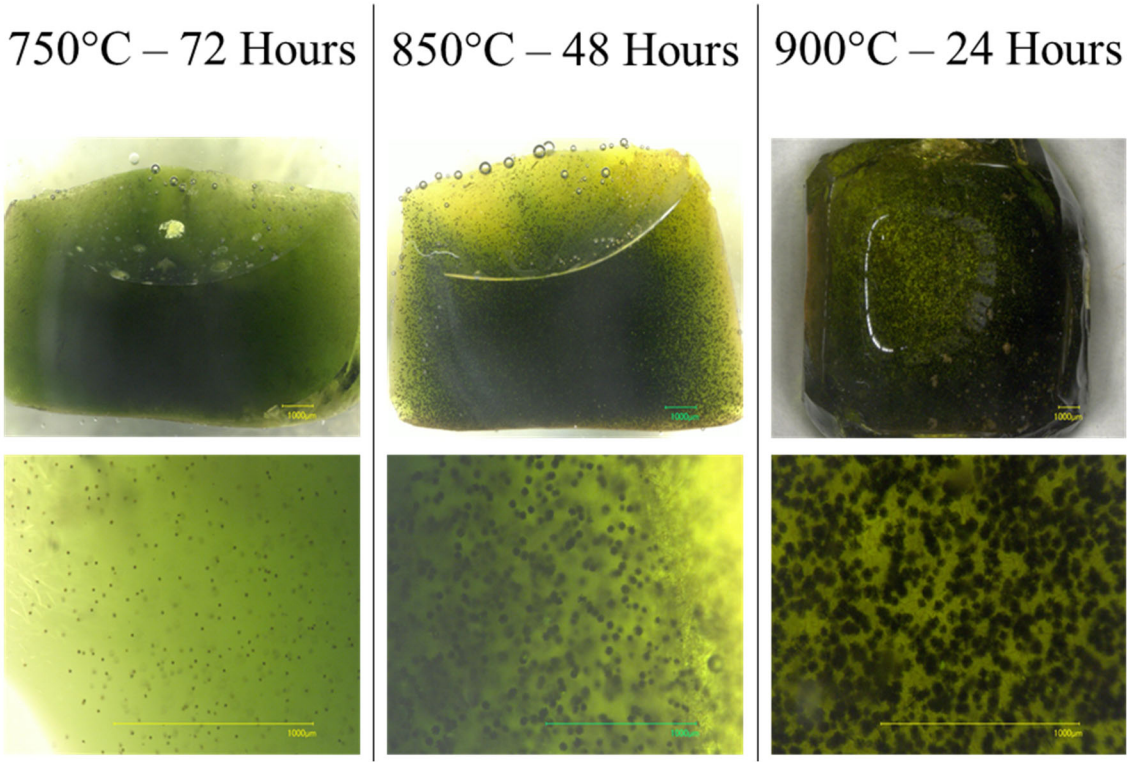

Figure C.10. Optical images of heat-treated LIC-10 glasses.

Appendix D – X-Ray Diffraction Data for LIC Glasses

This appendix contains X-ray diffraction (XRD) data for the low-activity waste isothermal crystallization (LIC) glasses after quench and upon various isothermal heat treatments. The diffractograms as well as the corresponding tables with phase identification and quantification are shown for each of the 10 glasses. CeO_2 was used as the internal standard for all samples.

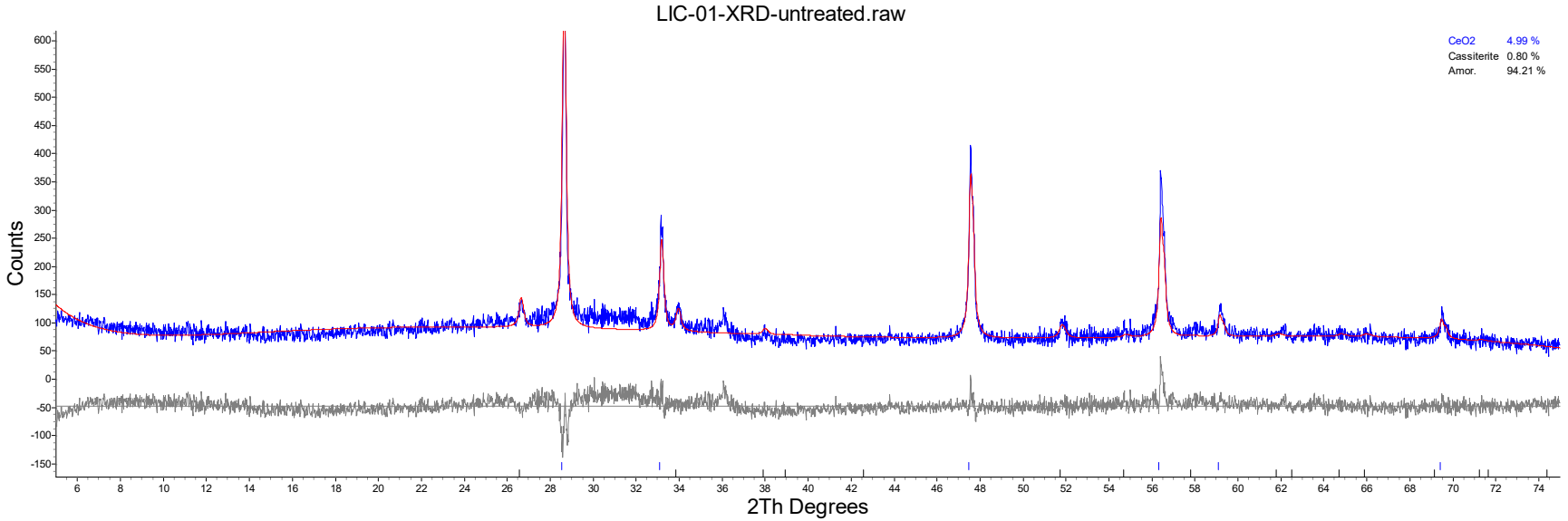

Figure D.1. XRD data for LIC-01 final melt.

Table D.1. XRD data for LIC-01 final melt.

Phase Name	Wt% of Spike	Wt% in Spiked Sample	Wt% in Original Sample
CeO_2	4.99	4.99	0
Cassiterite	0	0.80	0.84

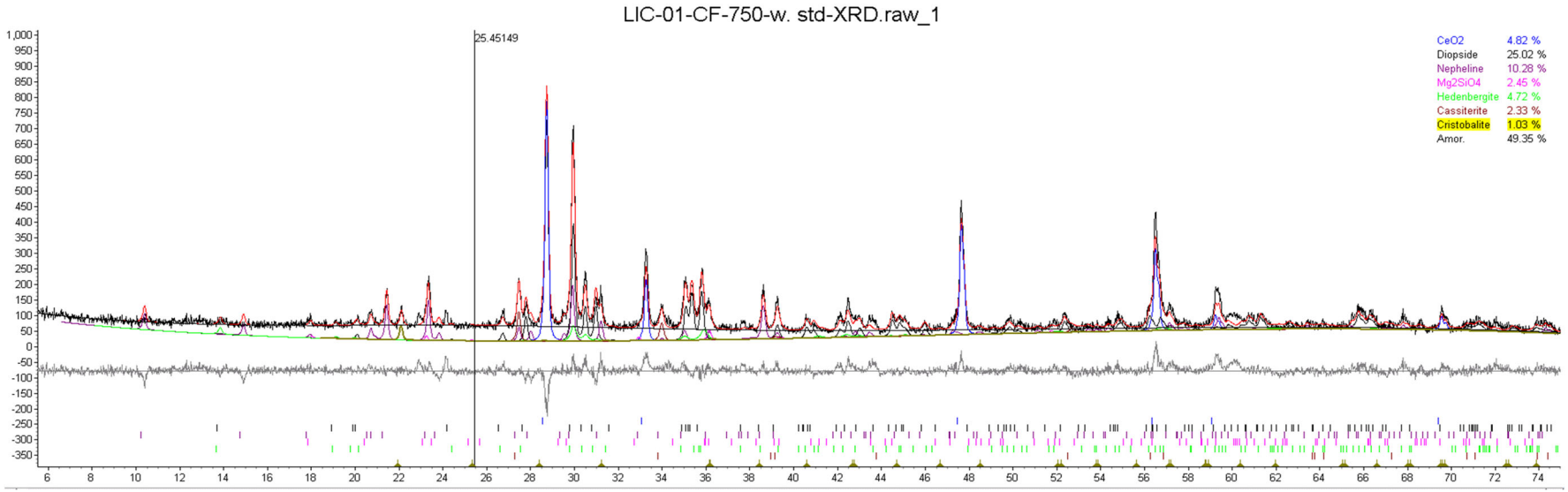

Figure D.2. XRD data for LIC-01-CF-750.

Table D.2. XRD data for LIC-01-CF-750

Phase Name	Wt% of Spike	Wt% in Spiked Sample	Wt% in Original Sample
CeO_2	4.82	4.82	0.00
Diopside	0	25.02	26.29
Nepheline	0	10.28	10.80
Mg_2SiO_4 (Forsterite)	0	2.45	2.57
Hedenbergite	0	4.73	4.96
Cassiterite	0	2.33	2.44
Cristobalite	0	1.03	1.08

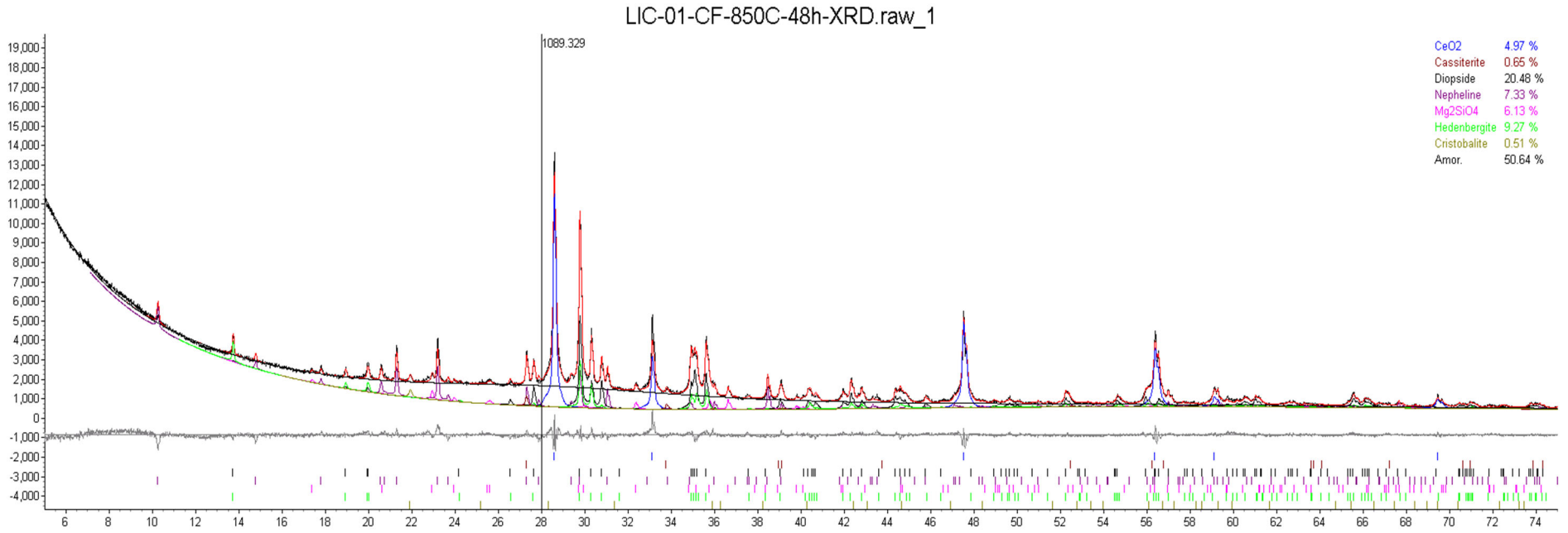

Figure D.3. XRD data for LIC-01-CF-850C-48hr.

Table D.3. XRD data for LIC-01-CF-850C-48hr.

Phase Name	Wt% of Spike	Wt% in Spiked Sample	Wt% in Original Sample
CeO_2	4.97	4.97	0.00
Diopside	0	20.48	21.55
Nepheline	0	7.33	7.72
Mg_2SiO_4	0	6.13	6.45
Hedenbergite	0	9.27	9.76
Cassiterite	0	0.65	0.69
Cristobalite	0	0.52	0.54

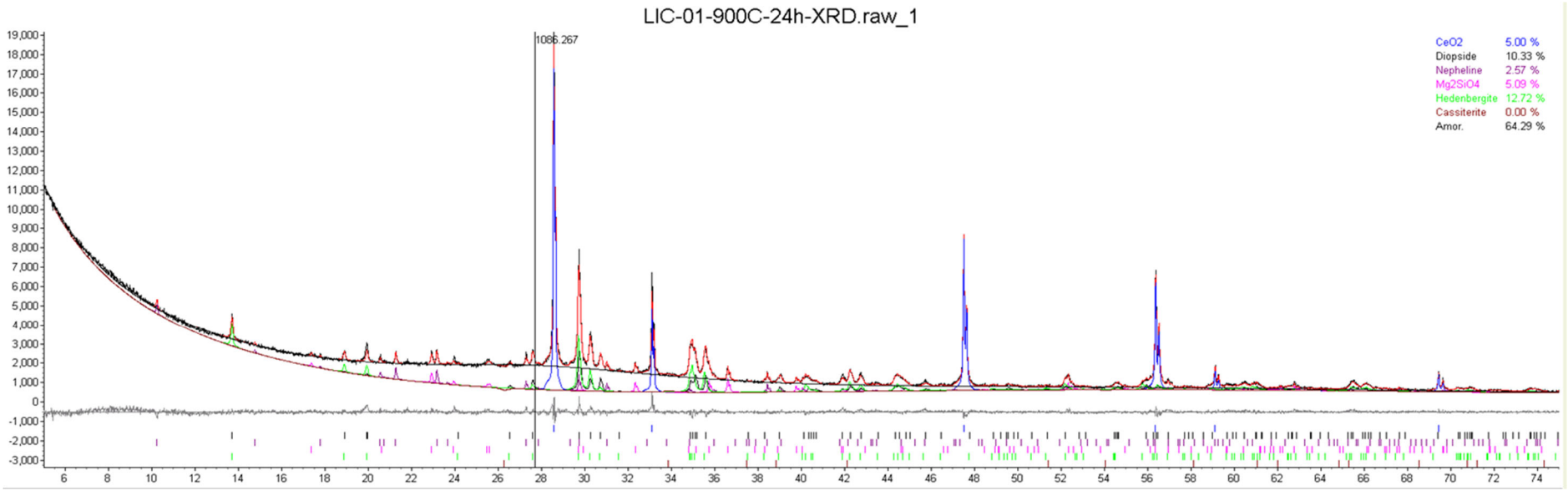

Figure D.4. XRD data for LIC-01-900C-24hr.

Table D.4. XRD data for LIC-01-900C-24hr.

Phase Name	Wt% of Spike	Wt% in Spiked Sample	Wt% in Original Sample
CeO_2	5.00	5.00	0
Diopside	0	10.33	10.87
Nepheline	0	2.57	2.71
Mg_2SiO_4	0	5.09	5.36
Hedenbergite	0	12.72	13.39
Cassiterite	0	0.01	0.01

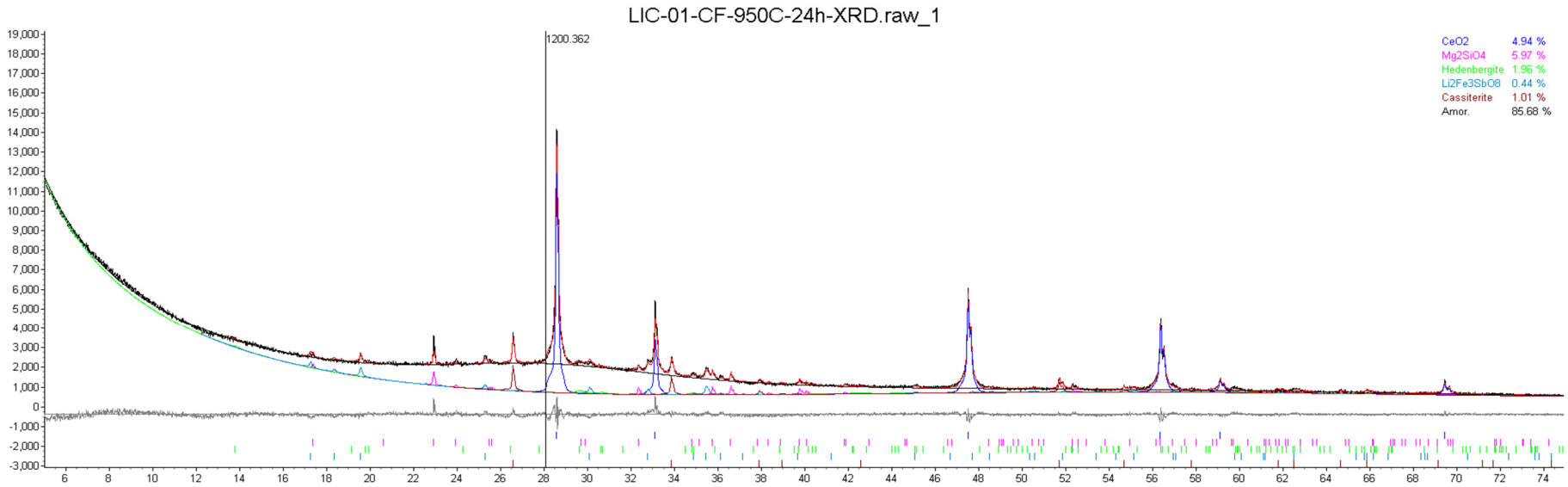

Figure D.5. XRD data for LIC-01-CF-950C-24hr.

Table D.5. XRD data for LIC-01-CF-950C-24hr.

Phase Name	Wt% of Spiked	Wt% in Spiked Sample	Wt% in Original Sample
CeO_2	4.94	4.94	0.00
Mg_2SiO_4	0	5.97	6.28
Hedenbergite	0	1.96	2.06
$Li_2Fe_3SbO_8$	0	0.44	0.46
Cassiterite	0	1.01	1.07

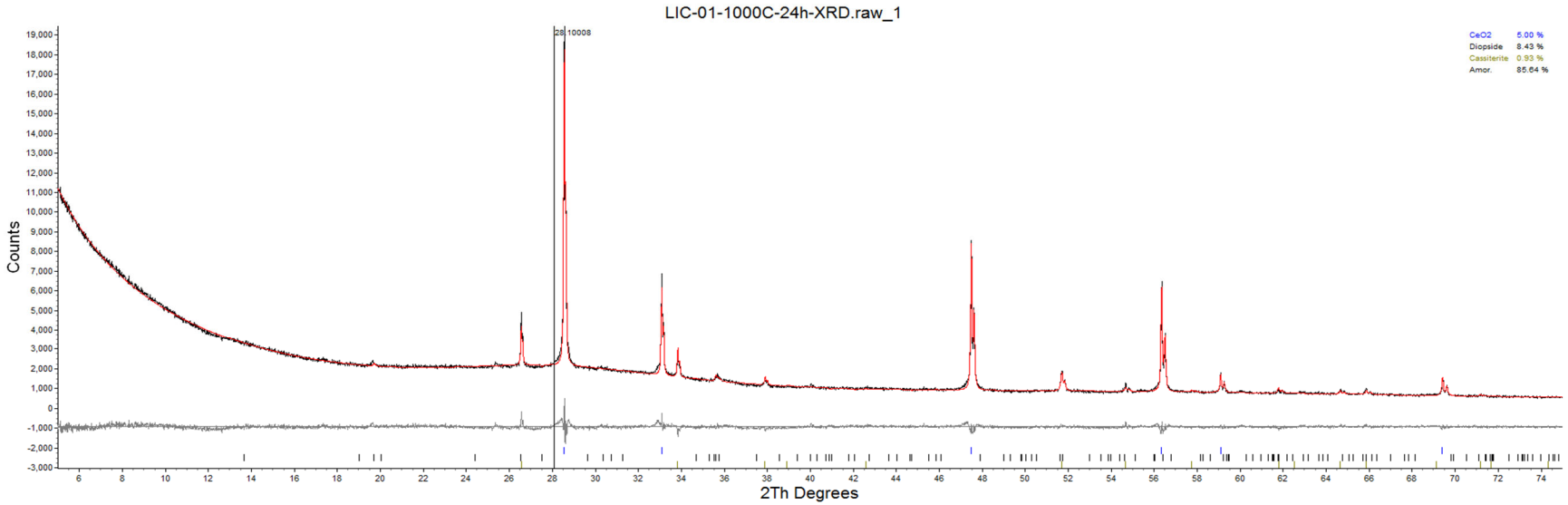

Figure D.6. XRD data for LIC-01-1000C-24hr.

Table D.6. XRD data for LIC-01-1000C-24hr.

Phase Name	Wt% of Spike	Wt% in Spiked Sample	Wt% in Original Sample
CeO_2	5.00	5.00	0
$Li_2Fe_3SbO_8$	0	0.35	0.36
Cassiterite	0	1.44	1.52

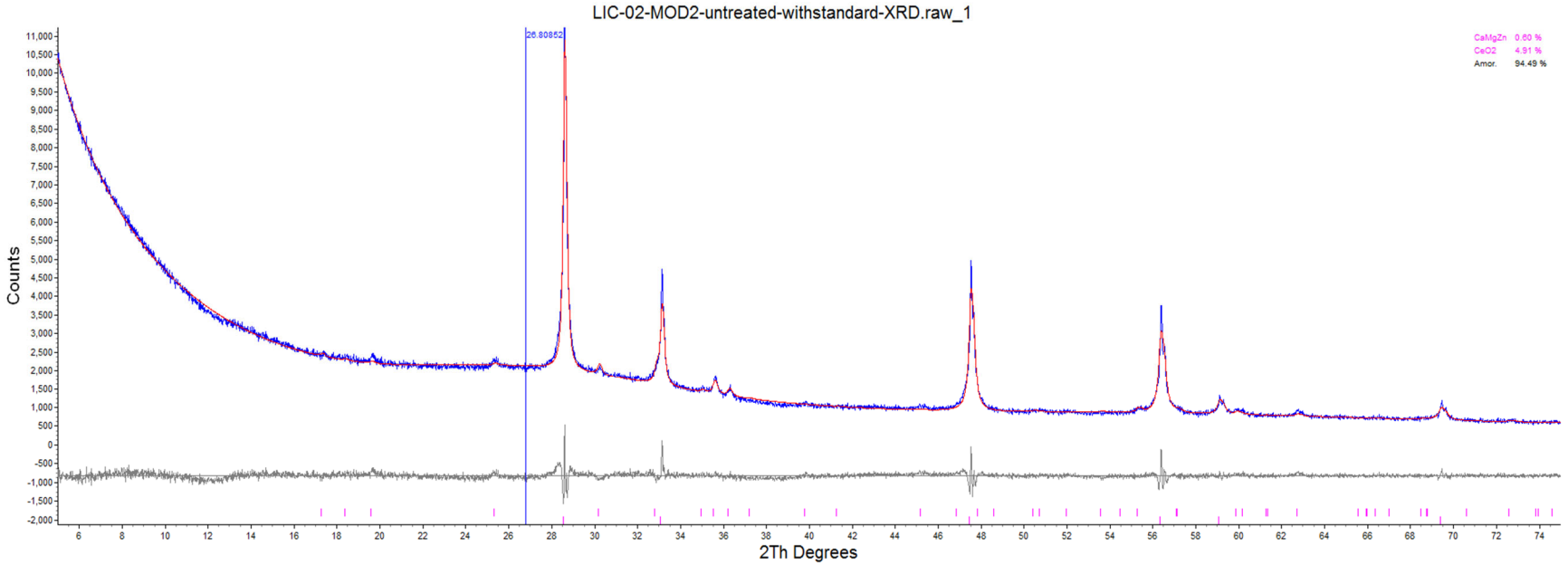

Figure D.7. XRD data for LIC-02-MOD2 final melt.

Table D.7. XRD data for LIC-02-MOD2 final melt.

Phase Name	Wt% of Spike	Wt% in Spiked Sample	Wt% in Original Sample
CaMgZn	0	0.60	0.64
CeO_2	4.91	4.91	0

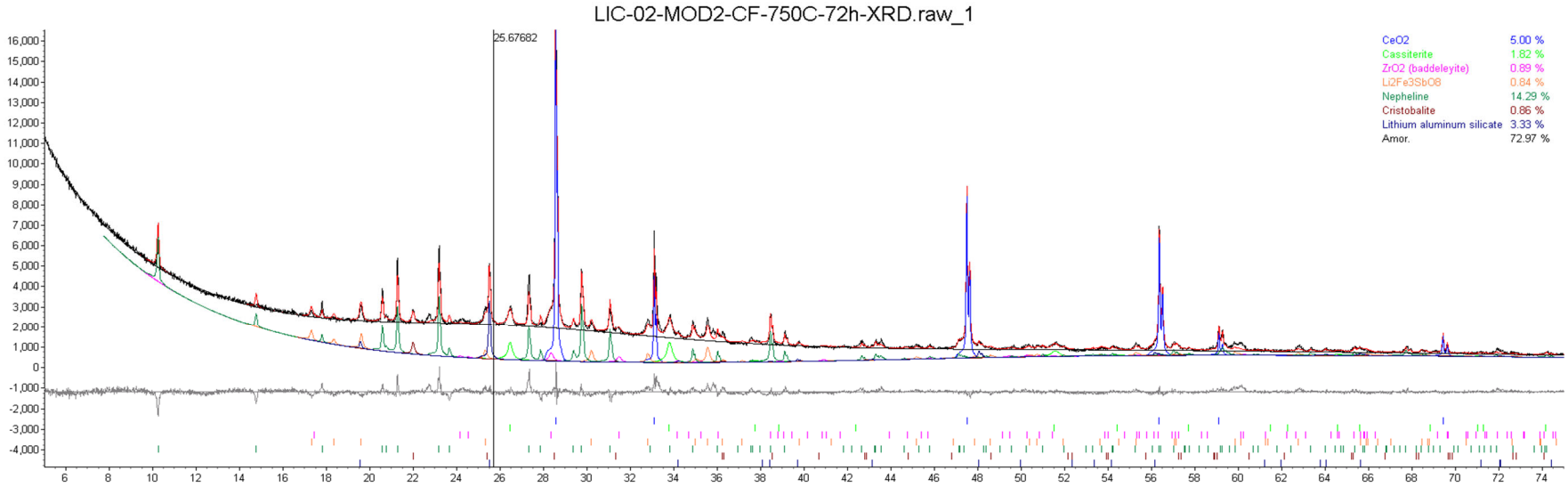

Figure D.8. XRD data for LIC-02-MOD2-750C-72hr.

Table D.8. XRD data for LIC-02-MOD2-750C-72hr.

Phase Name	Wt% of Spike	Wt% in Spiked Sample	Wt% in Original Sample
CeO_2	5.00	5.00	0.00
Cassiterite	0	1.82	1.91
ZrO_2 (baddeleyite)	0	0.89	0.94
$Li_2Fe_3SbO_8$	0	0.84	0.89
Nepheline	0	14.29	15.04
Cristobalite	0	0.86	0.91
Lithium aluminum silicate	0	3.33	3.51

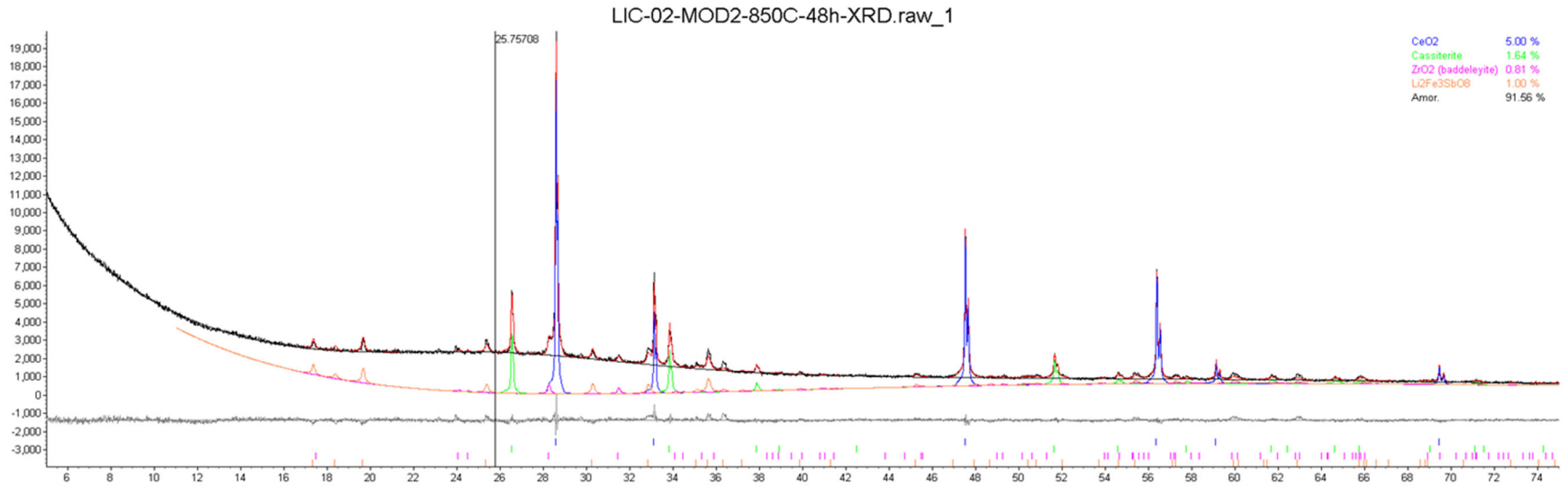

Figure D.9. XRD data for LIC-02-MOD2-850C-48hr.

Table D.9. XRD data for LIC-02-MOD2-850C-48hr.

Phase Name	Wt% of Spike	Wt% in Spiked Sample	Wt% in Original Sample
CeO_2	5.00	5.00	0.00
Cassiterite	0.00	1.64	1.72
ZrO_2 (baddeleyite)	0.00	0.81	0.85
$Li_2Fe_3SbO_8$	0.00	1.00	1.05

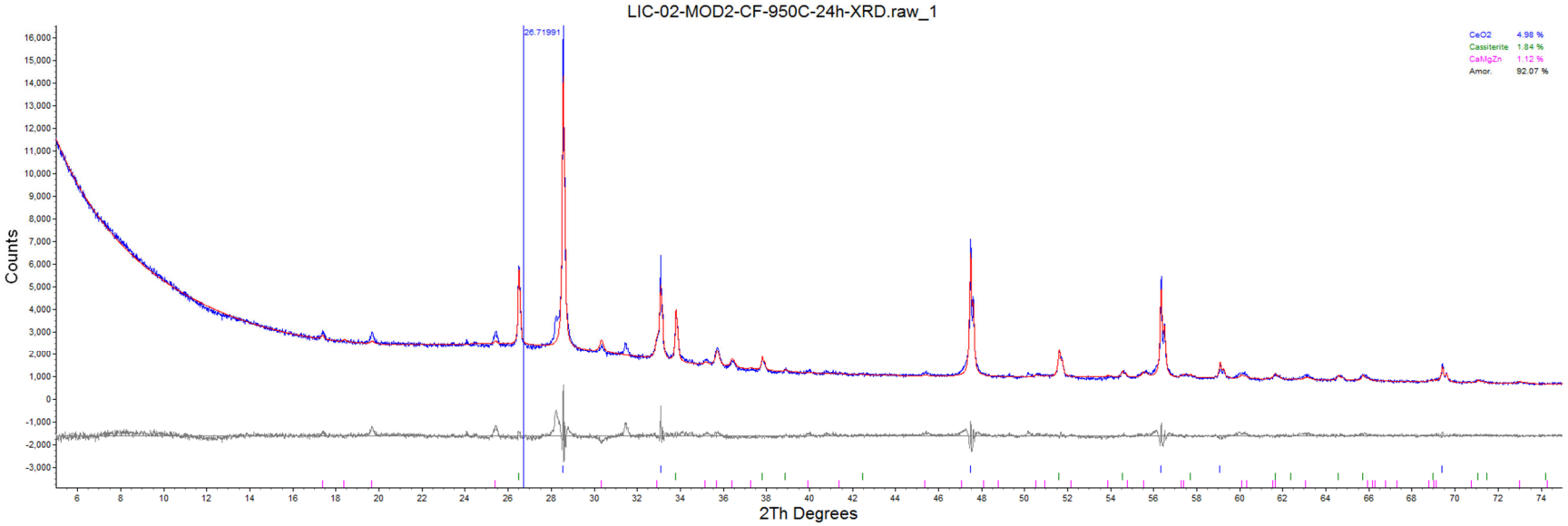

Figure D.10. XRD data for LIC-02-MOD2 -950C-24hr.

Table D.10. XRD data for LIC-02-MOD2 -950C-24hr.

Phase Name	Wt% of Spike	Wt% in Spiked Sample	Wt% in Original Sample
CeO_2	4.98	4.98	0.00
Cassiterite	0.00	1.76	1.85
ZrO_2 (baddeleyite)	0.00	1.48	1.56
$Li_2Fe_3SbO_8$	0.00	0.84	0.89

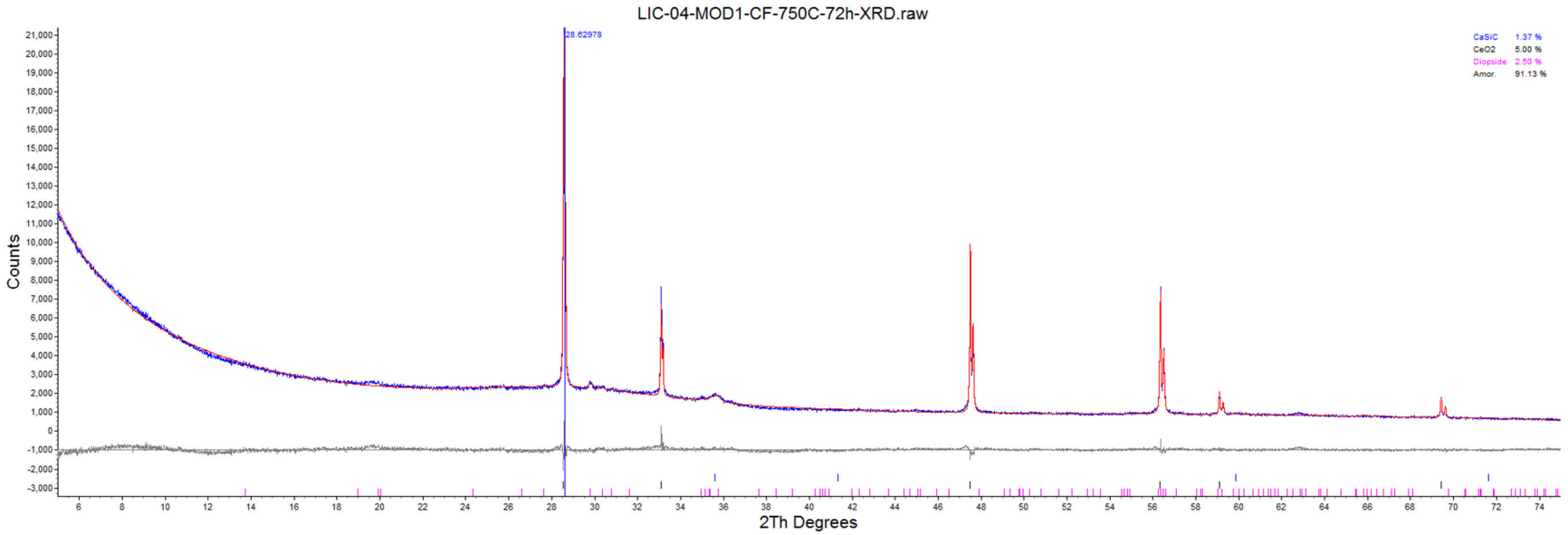

Figure D.11. XRD data for LIC-04-MOD1-750C-72h.

Table D.11. XRD data for LIC-04-MOD1-750C-72h.

Phase Name	Wt% of Spike	Wt% in Spiked Sample	Wt% in Original Sample
CeO_2	5.00	5.00	0.00
$Li_2Fe_3SbO_8$	0.00	0.65	0.69
Diopside	0.00	2.26	2.38

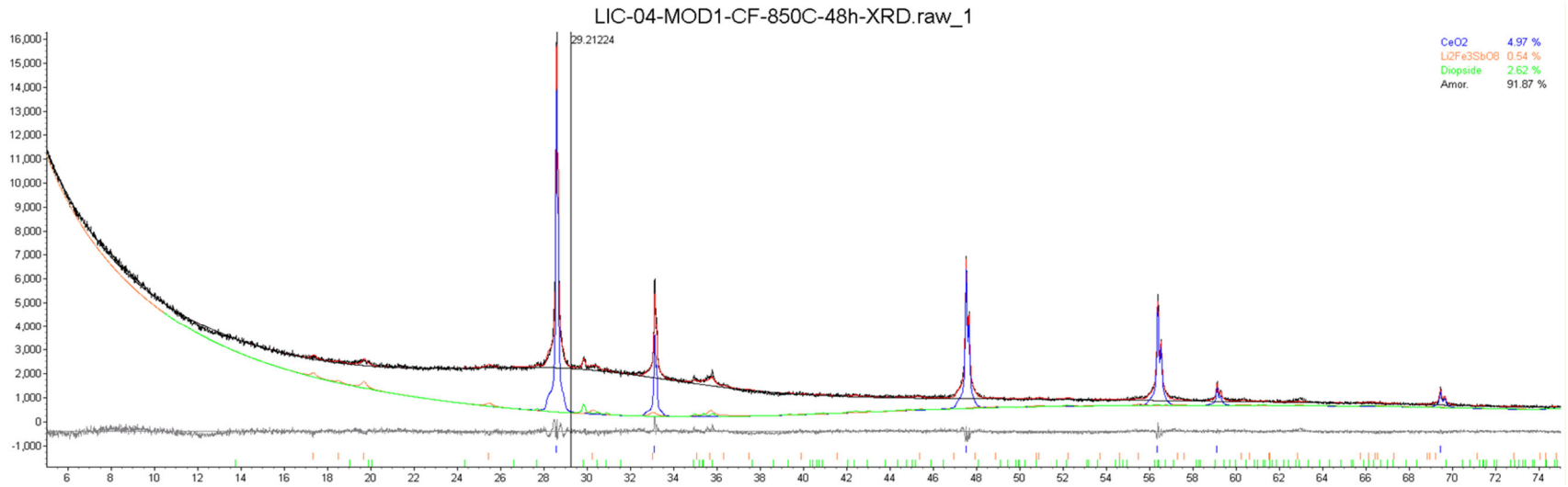

Figure D.12. XRD data for LIC-04-MOD1-850C-48h.

Table D.12. XRD data for LIC-04-MOD1-850C-48h.

Phase Name	Wt% of Spike	Wt% in Spiked Sample	Wt% in Original Sample
CeO_2	4.97	4.97	0.00
$Li_2Fe_3SbO_8$	0.00	0.54	0.57
Diopside	0.00	2.62	2.75

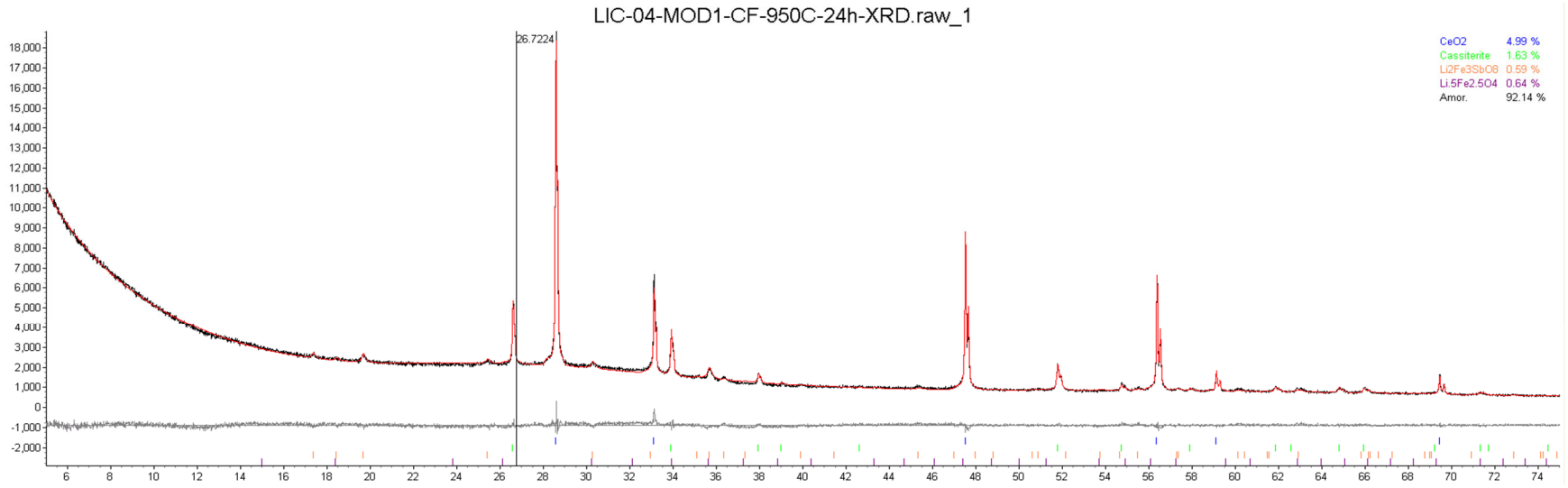

Figure D.13. XRD data for LIC-04-MOD1-950C-48h.

Table D.13. XRD data for LIC-04-MOD1-950C-48h.

Phase Name	Wt% of Spike	Wt% in Spiked Sample	Wt% in Original Sample
CeO_2	4.99	4.99	0.00
Cassiterite	0.00	1.63	1.72
$Li_2Fe_3SbO_8$	0.00	0.60	0.63
$Li_{0.5}Fe_{2.5}O_4$	0.00	0.64	0.67

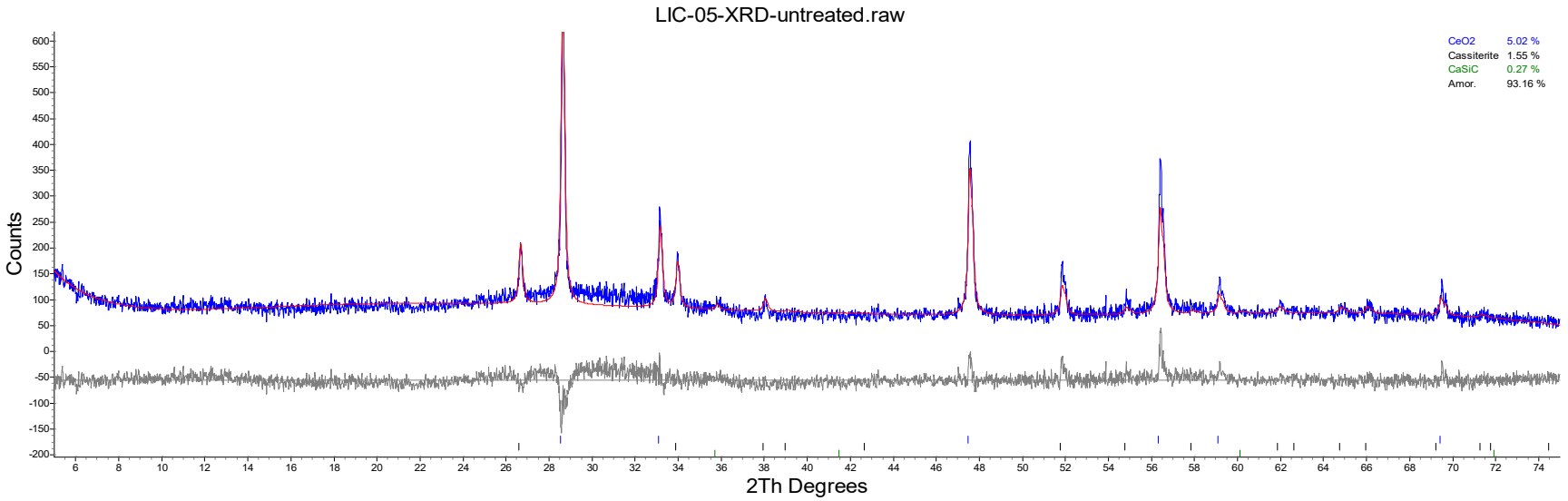

Figure D.14. XRD data for LIC-05 final melt.

Table D.14. XRD data for LIC-05 final melt.

Phase Name	Wt% of Spike	Wt% in Spiked Sample	Wt% in Original Sample
CeO_2	5.02	5.02	0
Cassiterite	0	1.55	1.63
CaSiC	0	0.27	0.29

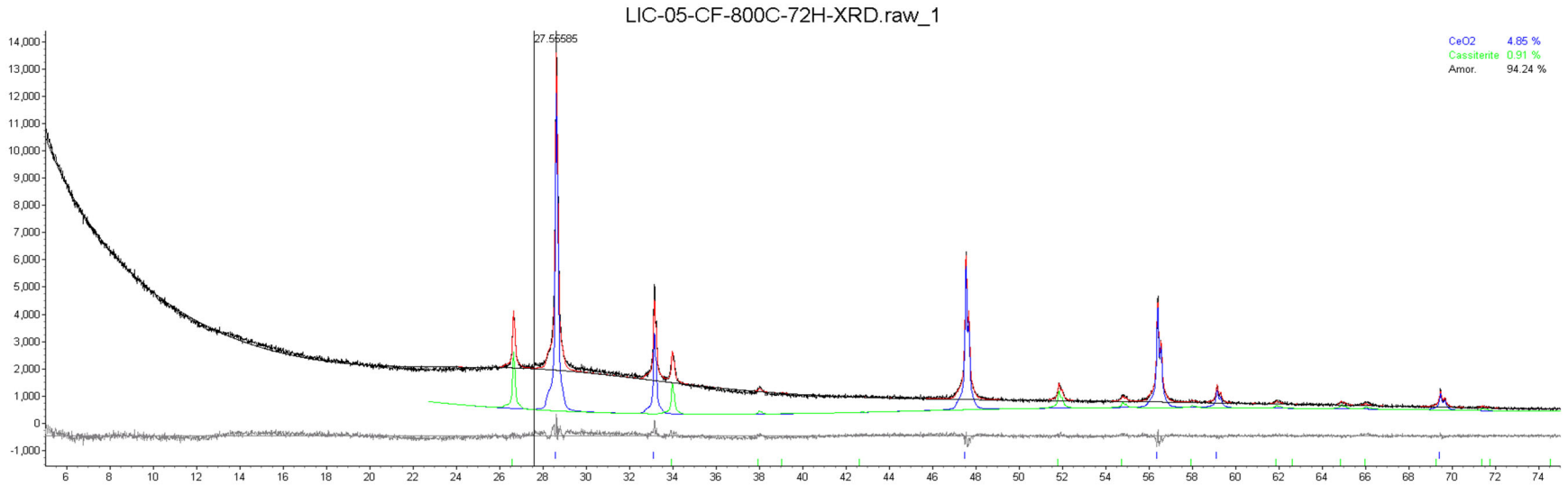

Figure D.15. XRD data for LIC-05-CF-800C-72h.

Table D.15. XRD data for LIC-05-CF-800C-72h.

Phase Name	Wt% of Spike	Wt% in Spiked Sample	Wt% in Original Sample
CeO_2	4.85	4.85	0.00
Cassiterite	0.00	0.91	0.95

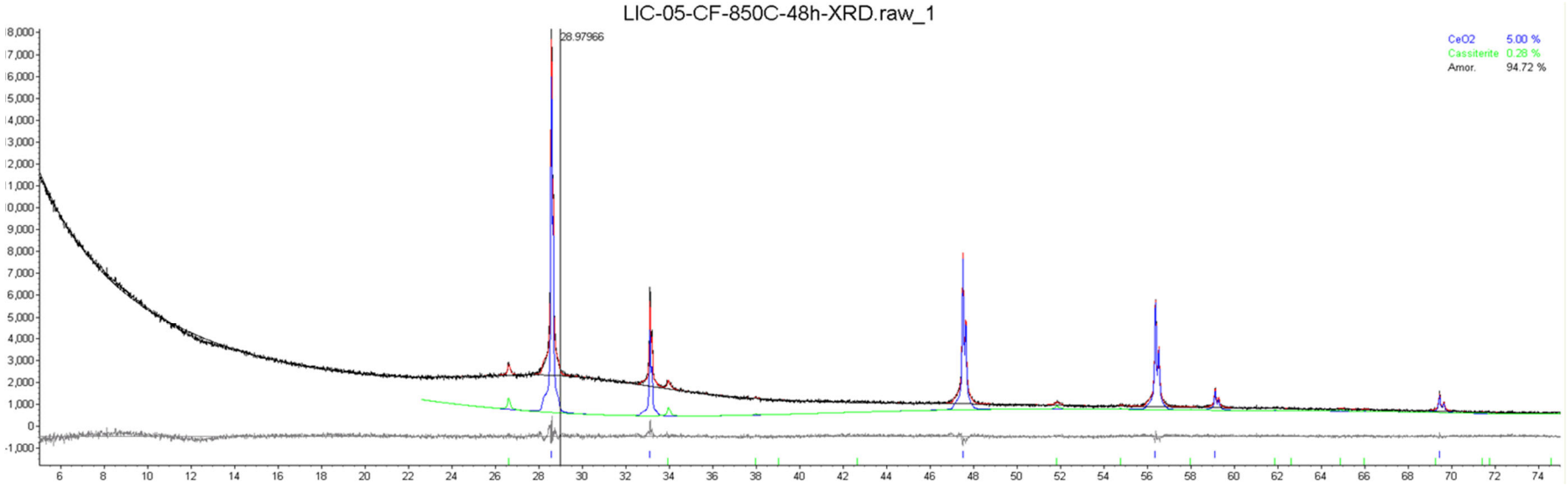

Figure D.16. XRD data for LIC-05-CF-850C-48h.

Table D.16. XRD data for LIC-05-CF-850C-48h.

Phase Name	Wt% of Spike	Wt% in Spiked Sample	Wt% in Original Sample
CeO_2	5.00	5.00	0.00
Cassiterite	0.00	0.28	0.30

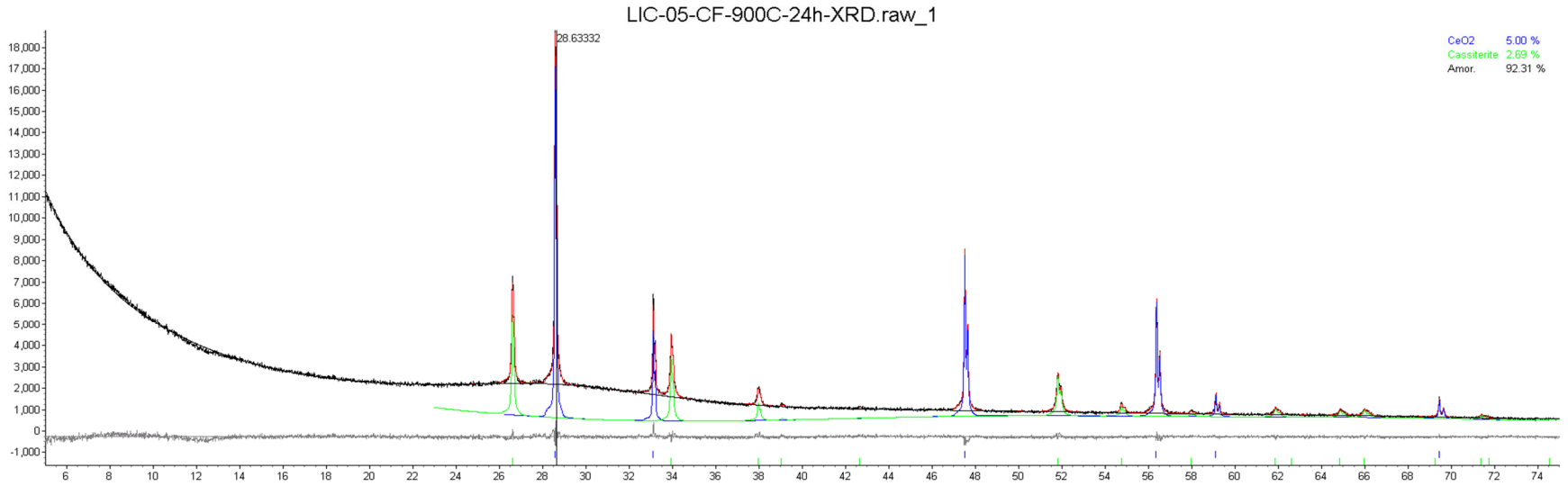

Figure D.17. XRD data for LIC-05-900C-24h.

Table D.17. XRD data for LIC-05-900C-24h.

Phase Name	Wt% of Spike	Wt% in Spiked Sample	Wt% in Original Sample
CeO_2	5.00	5.00	0.00
Cassiterite	0.00	2.69	2.83

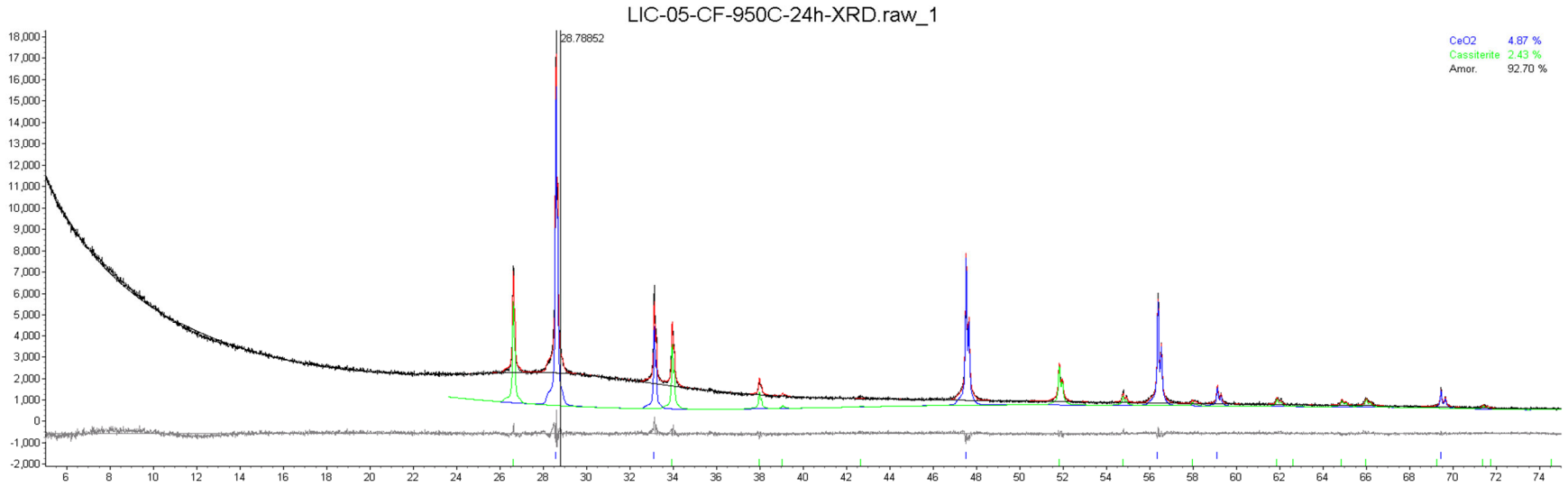

Figure D.18. XRD data for LIC-05-CF-950C-24h.

Table D.18. XRD data for LIC-05-CF-950C-24h.

Phase Name	Wt% of Spike	Wt% in Spiked Sample	Wt% in Original Sample
CeO_2	4.87	4.87	0.00
Cassiterite	0.00	2.43	2.55

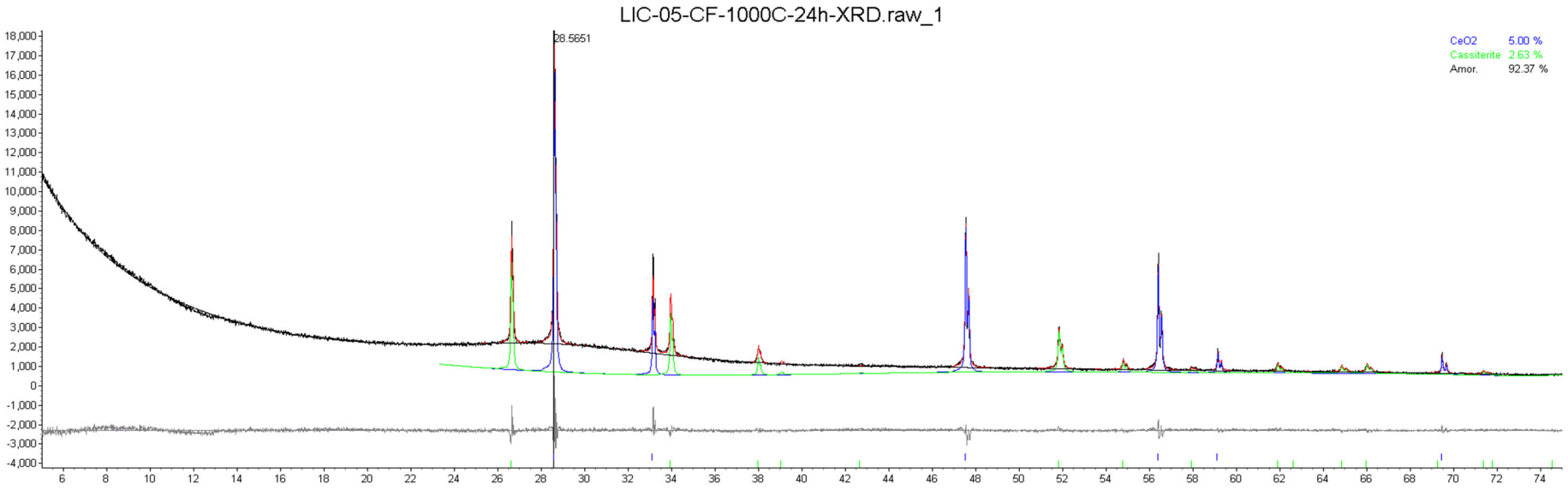

Figure D.19. XRD data for LIC-05-1000C-24h.

Table D.19. XRD data for LIC-05-1000C-24h.

Phase Name	Wt% of Spike	Wt% in Spiked Sample	Wt% in Original Sample
CeO_2	5.00	5.00	0.00
Cassiterite	0.00	2.63	2.77

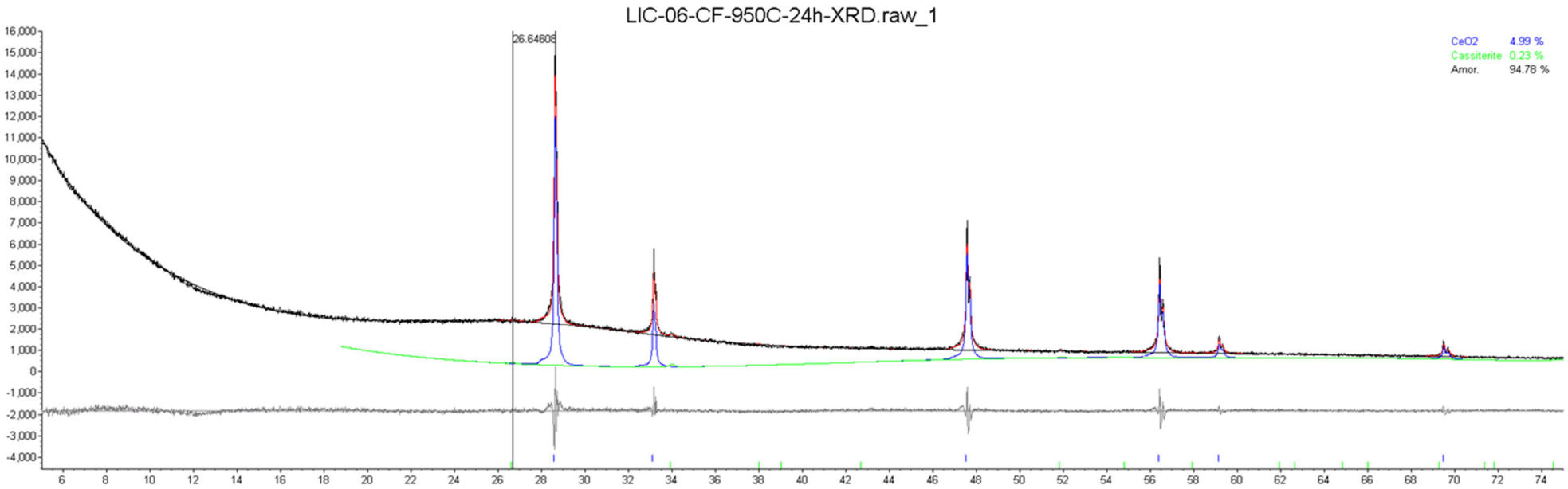

Figure D.20. XRD data for LIC-06-CF-950C-24h.

Table D.20. XRD data for LIC-06-CF-950C-24h.

Phase Name	Wt% of Spike	Wt% in Spiked Sample	Wt% in Original Sample
CeO_2	4.99	4.99	0.00
Cassiterite	0.00	0.23	0.24

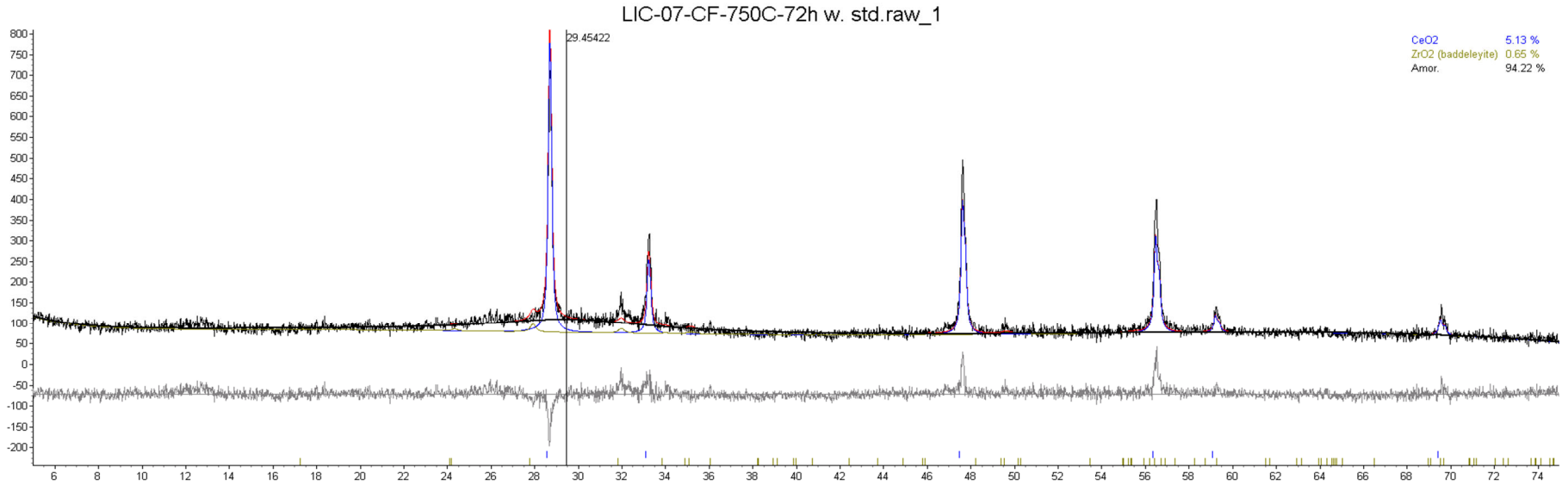

Figure D.21. XRD data for LIC-07-CF-750C-72h.

Table D.21. XRD data for LIC-07-CF-750C-72h.

Phase Name	Wt% of Spike	Wt% in Spiked Sample	Wt% in Original Sample
CeO_2	5.13	5.13	0.00
ZrO_2 (baddeleyite)	0.00	0.65	0.68

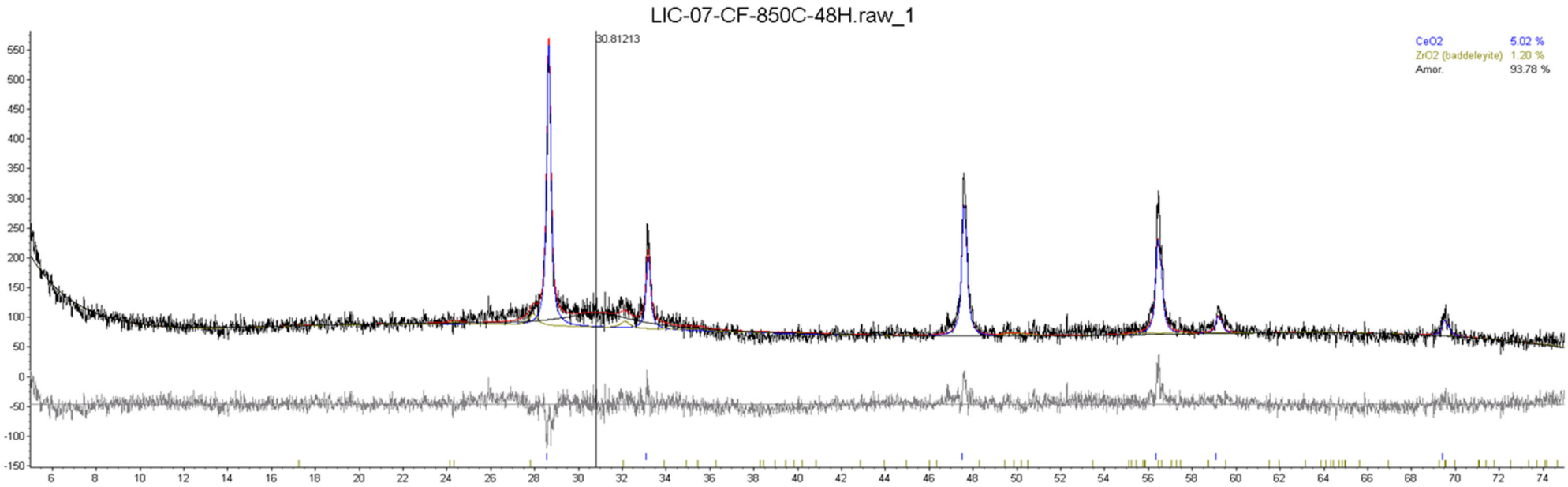

Figure D.22. XRD data for LIC-07-850C-48h.

Table D.22. XRD data for LIC-07-850C-48h.

Phase Name	Wt% of Spiked	Wt% in Spiked Sample	Wt% in Original Sample
CeO_2	5.02	5.02	0.00
ZrO_2 (baddeleyite)	0.00	1.20	1.27

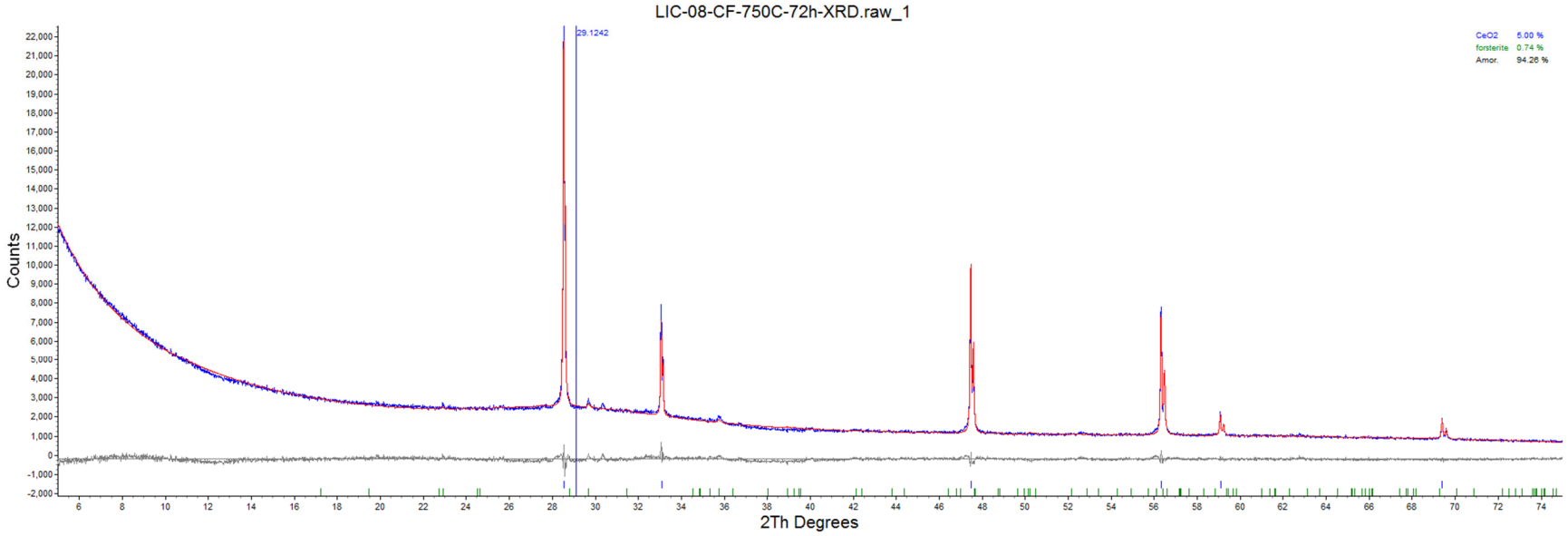

Figure D.23. XRD data for LIC-08-CF-750C-72h.

Table D.23. XRD data for LIC-08-CF-750C-72h.

Phase Name	Wt% of Spike	Wt% in Spiked Sample	Wt% in Original Sample
CeO_2	5.00	5.00	0.00
Forsterite	0.00	1.20	1.26
Diopside	0.00	3.19	3.35

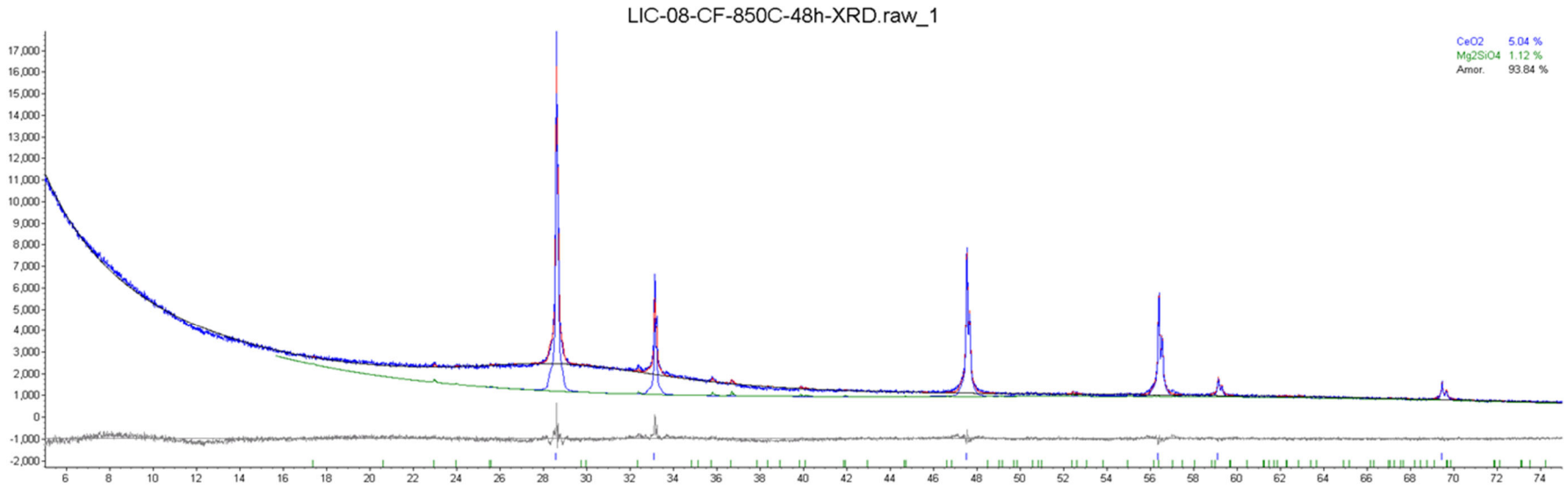

Figure D.24. XRD data for LIC-08-CF-850C-48h.

Table D.24. XRD data for LIC-08-CF-850C-48h.

Phase Name	Wt% of Spike	Wt% in Spiked Sample	Wt% in Original Sample
CeO_2	5.04	5.04	0.00
Forsterite	0.00	1.12	1.18

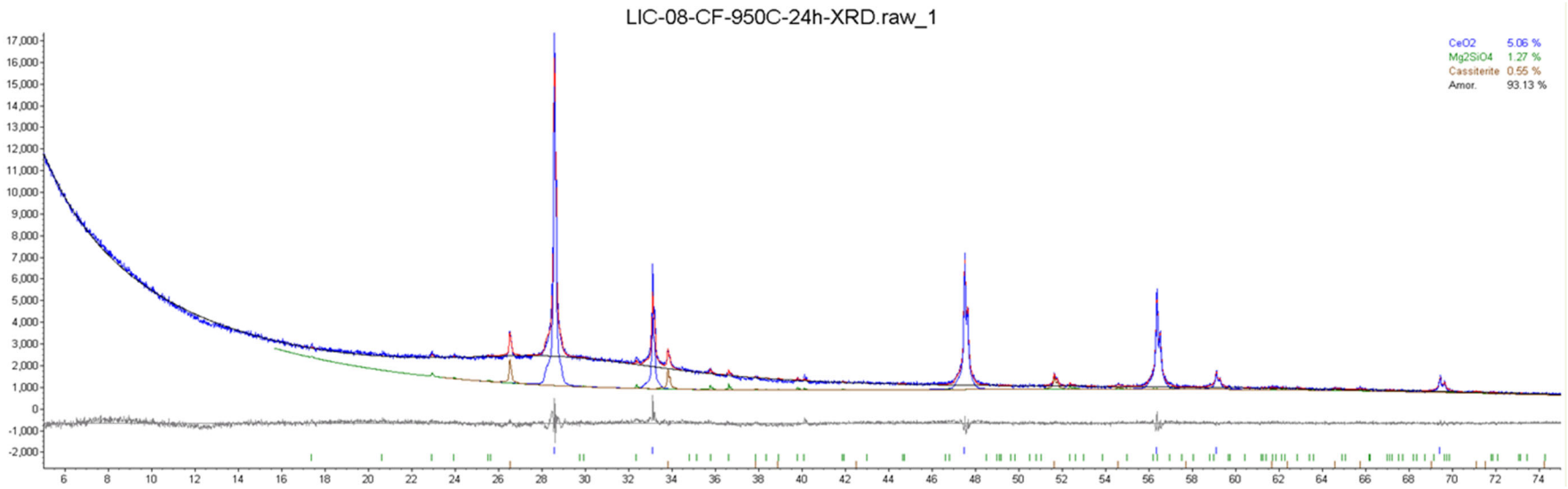

Figure D.25. XRD data for LIC-08-CF-950C-24h.

Table D.25. XRD data for LIC-08-CF-950C-24h.

Phase Name	Wt% of Spike	Wt% in Spiked Sample	Wt% in Original Sample
CeO_2	5.06	5.06	0.00
Forsterite	0.00	1.27	1.33
Cassiterite	0.00	0.55	0.58

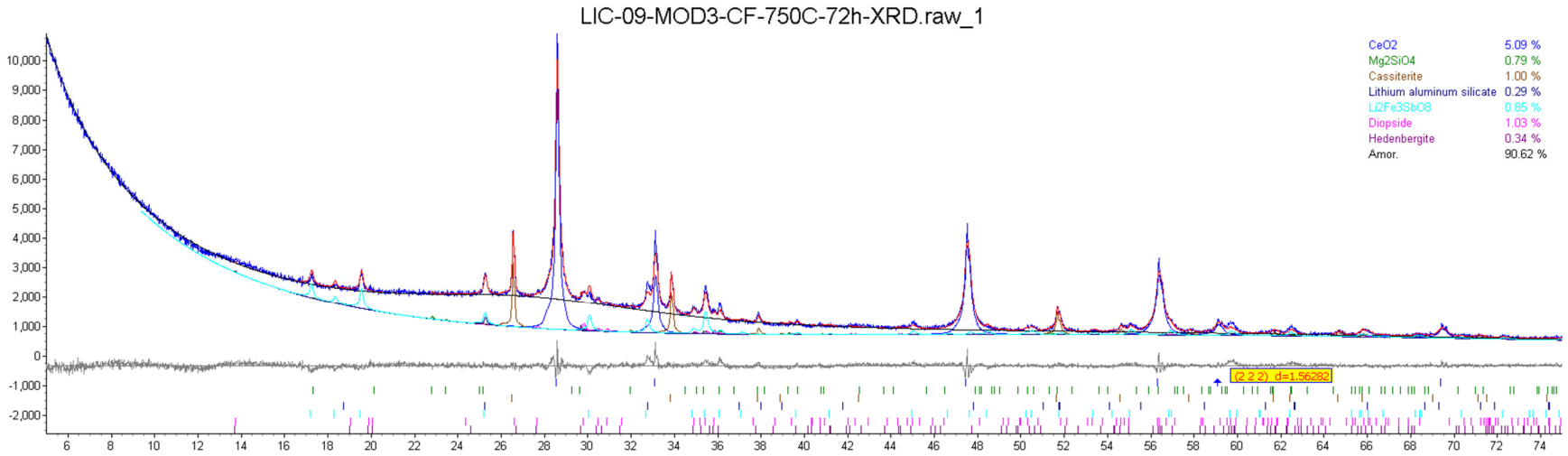

Figure D.26. XRD data for LIC-09-MOD3-CF-750C-72h.

Table D.26. XRD data for LIC-09-MOD3-CF-750C-72h.

Phase Name	Wt% of Spike	Wt% in Spiked Sample	Wt% in Original Sample
CeO_2	5.09	5.09	0.00
Forsterite	0.00	0.79	0.84
Cassiterite	0.00	1.00	1.05
Diopside	0.00	1.03	1.08
Hedenbergite	0.00	0.34	0.36
Lithium aluminum silicate	0.00	0.29	0.31
$Li_2Fe_3SbO_8$	0.00	0.85	0.89

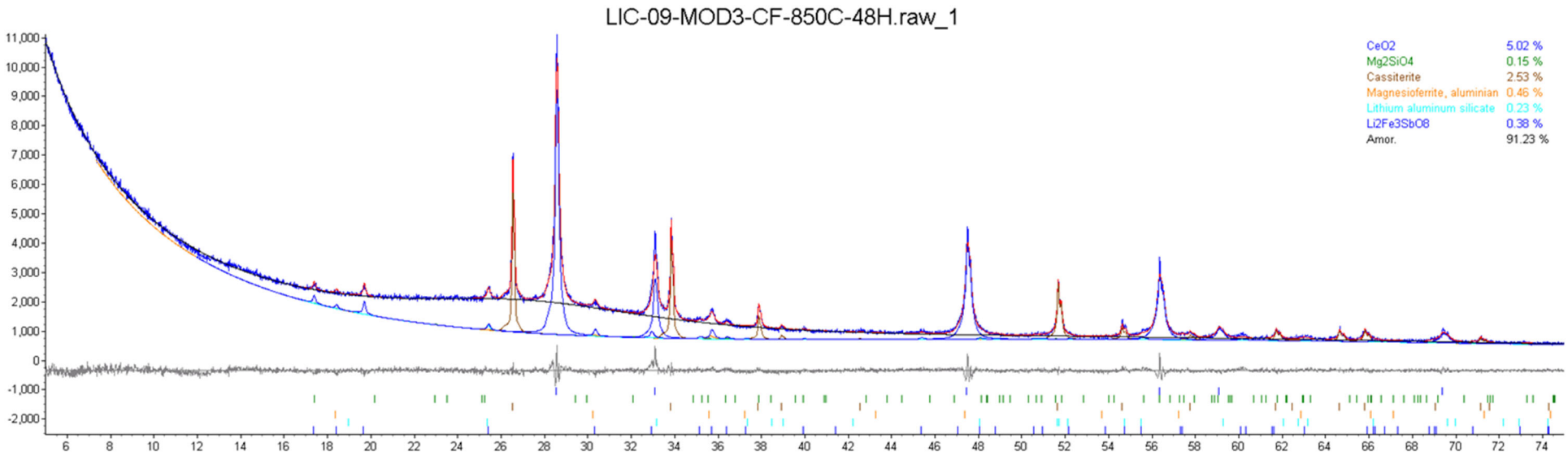

Figure D.27. XRD data for LIC-09-MOD3-CF-850C-48h.

Table D.27. XRD data for LIC-09-MOD3-CF-850C-48h.

Phase Name	Wt% of Spike	Wt% in Spiked Sample	Wt% in Original Sample
CeO_2	5.02	5.02	0.00
Forsterite	0.00	0.15	0.16
Cassiterite	0.00	2.53	2.66
Magnesioferrite, aluminian	0.00	0.46	0.48
Lithium aluminum silicate	0.00	0.23	0.25
$Li_2Fe_3SbO_8$	0.00	0.38	0.40

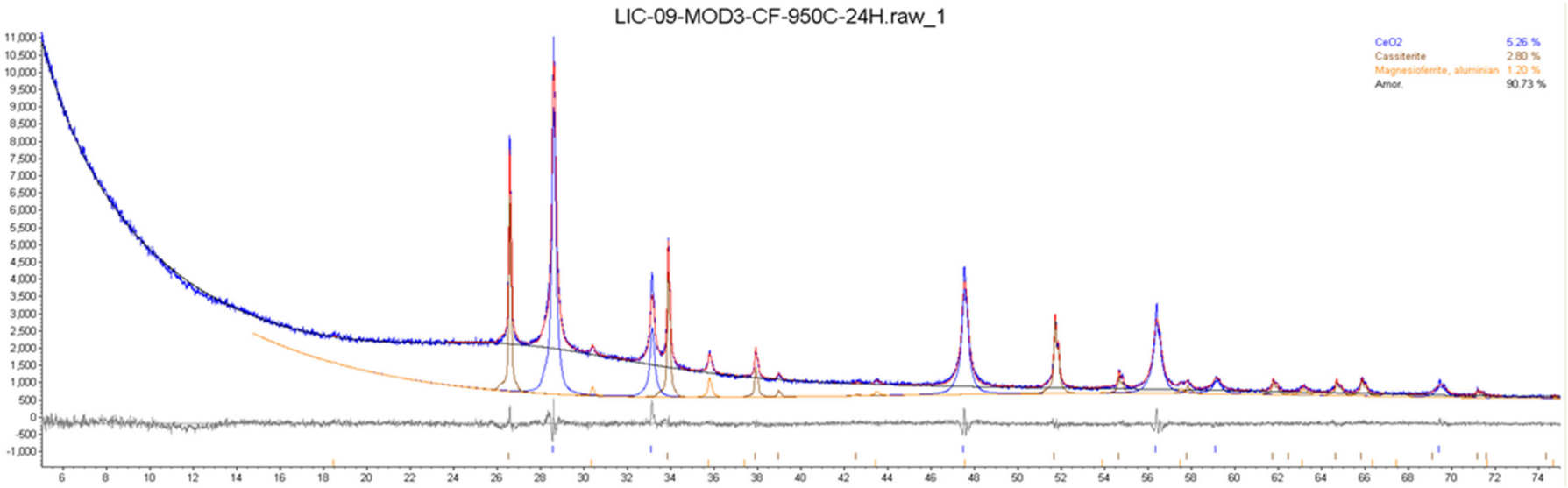

Figure D.28. XRD data for LIC-09-MOD3-CF-950C-24h.

Table D.28. XRD data for LIC-09-MOD3-CF-950C-24h.

Phase Name	Wt% of Spike	Wt% in Spiked Sample	Wt% in Original Sample
CeO_2	5.26	5.26	0.00
Cassiterite	0.00	2.80	2.96
Magnesioferrite, aluminian	0.00	1.20	1.27

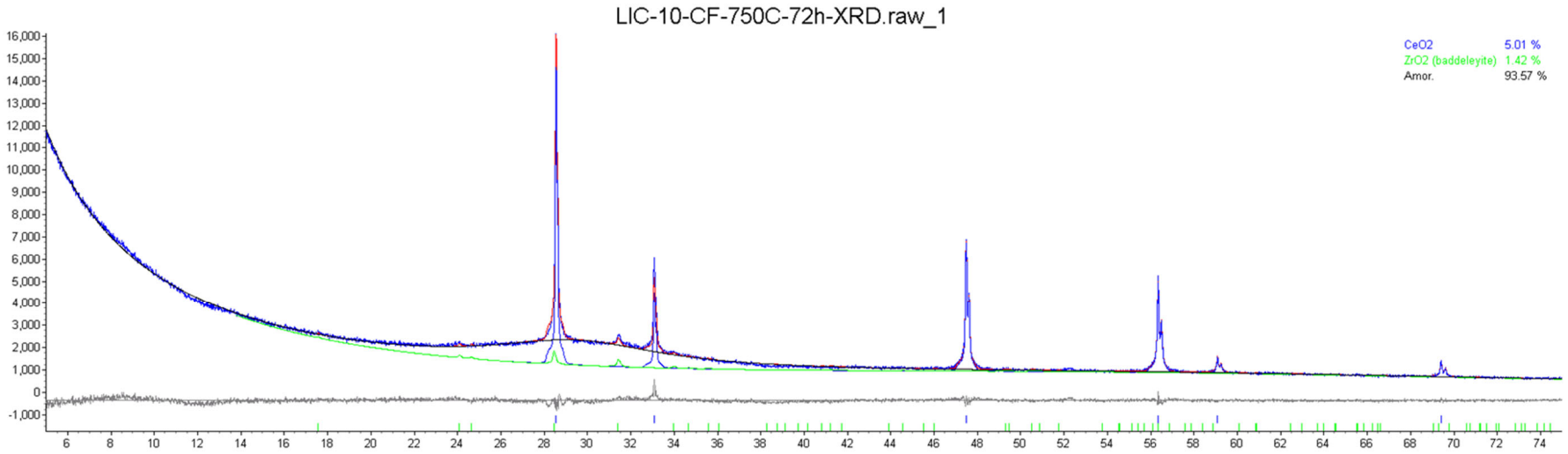

Figure D.29. XRD data for LIC-10-CF-750C-72h.

Table D.29. XRD data for LIC-10-CF-750C-72h.

Phase Name	Wt% of Spiked	Wt% in Spiked Sample	Wt% in Original Sample
CeO_2	5.01	5.01	0.00
ZrO_2 (baddeleyite)	0.00	1.42	1.50

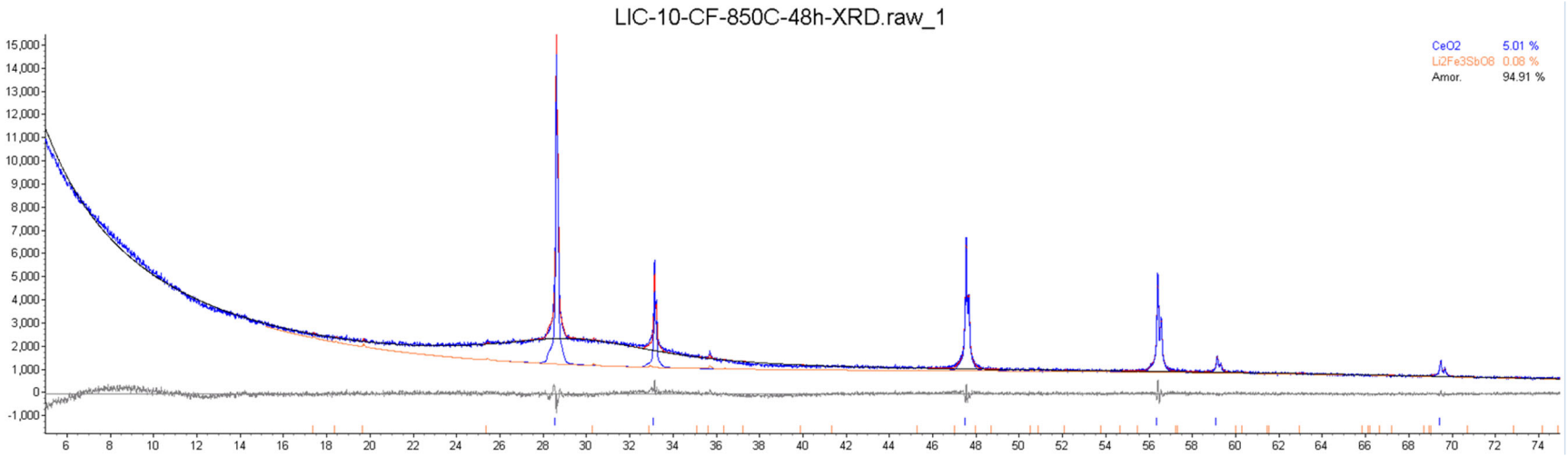

Figure D.30. XRD data for LIC-10-CF-850C-48h.

Table D.30. XRD data for LIC-10-CF-850C-48h.

Phase Name	Wt% of Spike	Wt% in Spiked Sample	Wt% in Original Sample
CeO_2	5.01	5.01	0.00
$Li_2Fe_3SbO_8$	0.00	0.08	0.09

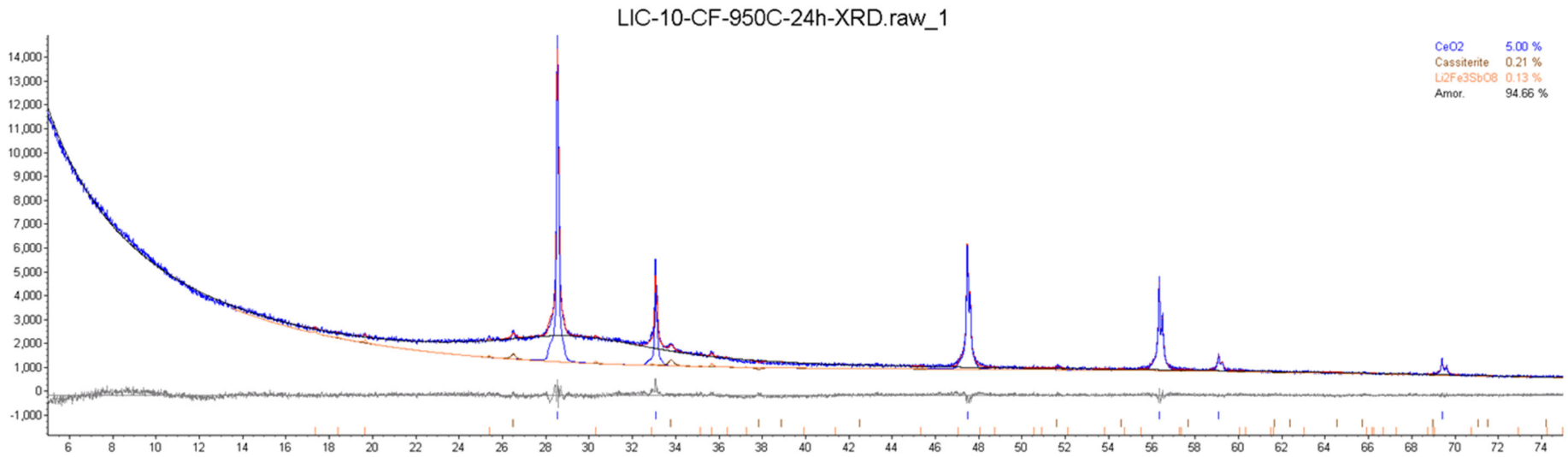

Figure D.31. XRD data for LIC-10-CF-950C-24h.

Table D.31. XRD data for LIC-10-CF-950C-24h.

Phase Name	Wt% of Spiked	Wt% in Spiked Sample	Wt% in Original Sample
CeO_2	5.00	5.00	0.00
Cassiterite	0.00	0.21	0.22
$Li_2Fe_3SbO_8$	0.00	0.13	0.13

Pacific Northwest National Laboratory

902 Battelle Boulevard
P.O. Box 999
Richland, WA 99354
1-888-375-PNNL (7665)

www.pnnl.gov